DOE/NV/0003590-06

Project 57 Air Monitoring Report: January 1 through December 31, 2016

Prepared by

Steve A. Mizell, George Nikolich, Craig Shadel, Greg McCurdy, and Julianne J. Miller

Submitted to

U.S. Department of Energy
Environmental Management Nevada Program
Las Vegas, Nevada

November 2017

Publication No. 45280

Nevada System of Higher Education

Available for sale to the public from:

U.S. Department of Commerce
National Technical Information Service
5301 Shawnee Rd.
Alexandria, VA 22312
Phone: 800.553.6847
Fax: 703.605.6900
Email: orders@ntis.gov
Online ordering: http://www.osti.gov/ordering.htm

Available electronically at http://www.osti.gov/bridge

Available for a processing fee to the U.S. Department of Energy and its contractors, in paper, from:

U.S. Department of Energy
Office of Scientific and Technical Information
P.O. Box 62
Oak Ridge, TN 37831-0062
Phone: 865.576.8401
Fax: 865.576.5728
Email: reports@adonis.osti.gov

DOE/NV/0003590-06

Project 57 Air Monitoring Report: January 1 through December 31, 2016

Prepared by

Steve A. Mizell, George Nikolich, Craig Shadel, Greg McCurdy,
and Julianne J. Miller

Desert Research Institute
Nevada System of Higher Education

Publication No. 45280

Submitted to

U.S. Department of Energy
Environmental Management Nevada Program
Las Vegas, Nevada

November 2017

The work upon which this report is based was supported by the U.S. Department of Energy under Contract #DE-NA0003590 and Contract #DE-NA0000939. Approved for public release; further dissemination unlimited.

THIS PAGE INTENTIONALLY LEFT BLANK

EXECUTIVE SUMMARY

On April 24, 1957, the Atomic Energy Commission (AEC, now the Department of Energy [DOE]) conducted the Project 57 safety experiment in western Emigrant Valley northeast of the Nevada National Security Site (NNSS, formerly the Nevada Test Site) on lands withdrawn by the Department of Defense (DOD) for the Nevada Test and Training Range (NTTR). The test was undertaken to develop (1) a means of estimating plutonium distribution resulting from a non-nuclear detonation; (2) biomedical evaluation techniques for use in plutonium-laden environments; (3) methods of surface decontamination; and (4) instruments and field procedures for prompt estimation of alpha contamination (Shreve, 1958). Although the test did not result in the fission of nuclear materials, it did disseminate plutonium across the land surface. Following the experiment, the AEC fenced the contaminated area and returned control of the surrounding land to the DOD. Various radiological surveys were performed in the area and in 2007, the DOE expanded the demarked Contamination Area (CA) by posting signs 200 to 400 ft (60 to 120 m) outside of the original fence.

Plutonium in soil attaches preferentially to smaller particles (Tamura, 1985; Friesen, 1992; Murarik *et al*., 1992; and Misra *et al*., 1993). Therefore, redistribution of soil particles by wind (dust) and water are the mechanisms most likely to transport plutonium beyond the boundary of the Project 57 CA. Monitoring was implemented in 2011 by Desert Research Institute (DRI) to determine if radionuclide contamination was detectable in samples of airborne dust and to characterize meteorological and environmental parameters that influence dust transport. The collected data also allow comparisons between radiological conditions at the Project 57 monitoring stations and conditions observed at Community Environmental Monitoring Program (CEMP) stations around the NTTR that are operated by DRI for the DOE. Initially, two monitoring stations consisting of radiological, meteorological, and dust sampling equipment were installed near the southeast and northeast corners of the CA. In January 2015, the original monitoring stations were dismantled and moved farther to the west along the CA boundary. This move was made to place the monitoring stations downwind of ground zero and the High Contamination Area (HCA) during the dominant northerly and southerly winds.

Samples of particles suspended in the air are collected every two weeks and submitted for laboratory assessments of gross alpha and gross beta radioactivity, and for determinations of gamma-emitting radionuclides. The mean gross alpha concentrations at monitoring stations P57-3 and P57-4 are approximately 1.5 times and approximately 2.3 times, respectively, the mean gross alpha concentrations at the surrounding CEMP stations. The minimum gross alpha concentrations reported for the Project 57 stations are in the range of the minimum values observed at the CEMP stations. However, maximum gross alpha concentrations are greater than the maximum concentrations observed at the surrounding CEMP stations. Gamma spectroscopy analyses identified only naturally occurring radionuclides.

During each quarter in calendar year (CY) 2015 and CY2016, two samples from each of the monitoring stations were selected from the regular biweekly samples for alpha spectrometery analysis. Three of the eight CY2015 samples from P57-4 had plutonium-238 (Pu-238) detections above the minimum detectable concentration (MDC). None of the CY2015 samples from P57-3 produced Pu-238 detections above the MDC. Three samples from P57-3 and nine from P57-4 produced plutonium-239/240 (Pu-239/240) detections above the MDC. None of the CY2016 samples from P57-3 or P57-4 produced Pu-238 detections above the MDC. Six samples from P57-4 produced Pu-239/240 detections above the MDC. None of the CY2016 samples from P57-3 produced Pu-239/240 detections above the MDC.

Soil material is also transported by saltation, which is a wind driven phenomena that bounces sand-sized soil particles that are too heavy to be suspended in air across the land surface. Samples of particles transported by saltation were collected downwind and upwind of the CA at both monitoring stations. The mass of collected material was slightly greater in traps facing the southerly winds. Although there is the suggestion of a trend for net migration of saltation material from south to north, this is contrary to previously observed conditions. The current and previous observations indicate that the net migration by saltation is dependent on wind conditions during the evaluation period and must be assessed over a substantial period of observation. Radiological analyses of the saltation samples show that the smaller particle size faction (<63 µm) generally produced the highest activity levels of americium-241 (Am-241), Pu-238, and Pu-239/240. In general, the isotope activity levels decreased as the particle size increased. These results are consistent with the expectation that the greatest potential for transport of radiological contamination is with the smaller particles.

Thermoluminescent dosimeters (TLDs) indicated that the average annual external radioactivity dose at the monitoring stations is higher than the dose determined at the surrounding CEMP stations (NSTec, 2016), but approximately half of the estimated national average dose received by the general public from exposure to natural sources. The TLDs at the Project 57 monitoring stations are exposed to both natural sources (terrestrial and cosmic) and radioactive releases from the Project 57 CA.

Winds in excess of approximately 15 mph (24.1 km/hr) begin to generate dust movement by saltation or suspension in the air as determined by the monitoring instruments. Saltated particles, PM_{10} (i.e., inhalable dust), and $PM_{2.5}$ (i.e., fine particulate dust) exhibit an approximately exponential increase with increasing wind speed. The greatest concentrations of dust occur for winds exceeding 20 mph (32.2 km/hr). When the wind/dust analysis is performed for winds separated into the dominant northerly and southerly wind directions, it is evident that the southerly winds generate the higher PM_{10} concentrations and have the dominate influence on the PM10 concentration determined for all wind speeds when all wind directions are evaluated together. During the reporting period, winds in excess of 20 mph (32.2 km/hr) occurred approximately two percent of the time. Although winds sufficient to generate dust occur at the Project 57 site, they are infrequent and of short duration.

A preliminary assessment of individual wind events suggests that dust generation in response to specific wind conditions is highly variable. Wind speeds that would be expected to generate noticeable dust may not do so in every instance. Additionally, saltation transport in response to wind conditions was less common than expected. These variations are likely because of the influence of meteorological and environmental parameters other than wind. The potential influence of factors such as soil moisture content, humidity, wind event duration, and time intervals between wind events have not yet been fully assessed.

CONTENTS

LIST OF FIGURES

LIST OF TABLES

LIST OF ACRONYMS

AEC	Atomic Energy Commission
Am-241	americium-241
Be-7	beryllium-7
BSNE	Big Spring Number Eight
CA	Contamination Area
CAS	Corrective Action Site
CAU	Corrective Action Unit
CEMP	Community Environmental Monitoring Program
cfm	cubic feet per minute
cps	counts per second
CY	calendar year
DOD	U.S. Department of Defense
DOE	U.S. Department of Energy
DRI	Desert Research Institute
ft	feet
g	grams
in	inch
K-40	potassium-40
km/hr	kilometers per hour
lpm	liters per minute
MDA	minimum detectable activity
MDC	minimum detectable concentration
µCi/ml	microcurie per milliliter

$\mu g/m^3$	microgram per cubic meter
mi	miles
µm	micrometers
mph	miles per hour
mR	millirem
NAFR	Nellis Air Force Range
NFO	Nevada Field Office
NNSA	National Nuclear Security Administration
NNSS	Nevada National Security Site
NSTec	National Security Technologies
NTTR	Nevada Test and Training Range
P57-1	Project 57 monitoring station 1
P57-2	Project 57 monitoring station 2
P57-3	Project 57 monitoring station 3
P57-4	Project 57 monitoring station 4
Pb-210	lead-210
$PM_{2.5}$	particulate matter with an aerodynamic diameter less than 2.5 µm
PM_{10}	particulate matter with an aerodynamic diameter less than 10 µm
Pu-238	plutonium 238
Pu-239/240	plutonium 239/+240
Pu-241	plutonium 241
RCT	radiological control technician
RMA	Radiological Material Area
TLD	thermoluminescent dosimeter

THIS PAGE INTENTIONALLY LEFT BLANK

INTRODUCTION

During the late 1950s, the Atomic Energy Commission (AEC) (now the U.S. Department of Energy [DOE]) conducted a series of safety experiments to determine if a nuclear device subjected to a large conventional explosives detonation would result in a nuclear yield. The AEC obtained temporary use of a large portion of western Emigrant Valley from the U.S. Department of Defense (DOD) for one of these experiments: Project 57. Following the Project 57 safety experiment, the AEC fenced the contaminated area and returned control of the surrounding land to the DOD.

Emigrant Valley is part of the Nevada Test and Training Range (NTTR, formerly the Nellis Air Force Range [NAFR]). For safety and security reasons, access to the NTTR is controlled through the use of both physical (i.e., fences) and administrative (e.g., signs and postings) controls. Therefore, the public cannot access the Project 57 site and there are no known human receptors that routinely access the site.

Project 57 was detonated on April 24, 1957, in Emigrant Valley approximately 13 mi (21 km) northeast of the north end of Yucca Flat (Figure 1). This test was undertaken to develop: (1) a means of estimating immediate distribution and long-term redistribution of plutonium dispersed during a non-nuclear detonation; (2) biomedical evaluation techniques for use in likely plutonium-laden environments; (3) methods of decontamination of ground areas, pavements, and building materials; and (4) alpha survey instruments and field monitoring procedures to promptly estimate contaminant deposition (Shreve, 1958). Data collection stations were distributed on a variable-scale rectangular grid pattern that extended approximately 9.5 mi (15.3 km) north of the ground zero detonation point and encompassed a total of approximately 64.5 mi^2 (167 km^2). Although the test did not result in the fission of nuclear materials, it did disseminate plutonium across the ground surface.

Various radiological surveys have been performed in the area since Project 57 was conducted. The original fence constructed by the AEC to control access to Project 57 (Figure 2) delineated the initial Contamination Area (CA) and was located based on radioactivity surveys performed shortly after the Project 57 test was conducted. The distribution of americium-241 (Am-241) in the area was determined in a 1997 flyover (written communication from Navarro to Desert Research Institute [DRI], 2010) and showed Am-241 concentrations ranging from as much as 70,000 counts per second (cps) at ground zero to background values (<70 cps). This survey documented Am-241 concentrations on the ground surface beyond the east side CA fence at levels of up to 150 cps. In 2007, the DOE expanded the CA by posting "Contamination Area" signs 200 to 400 ft (60 to 120 m) beyond of the original fence, which formed a new, concentric CA boundary. Americium-241 concentrations in the range of 70 to 150 cps are observed in the 1997 airborne survey data to extend beyond the east side of the new CA boundary (Figure 2).

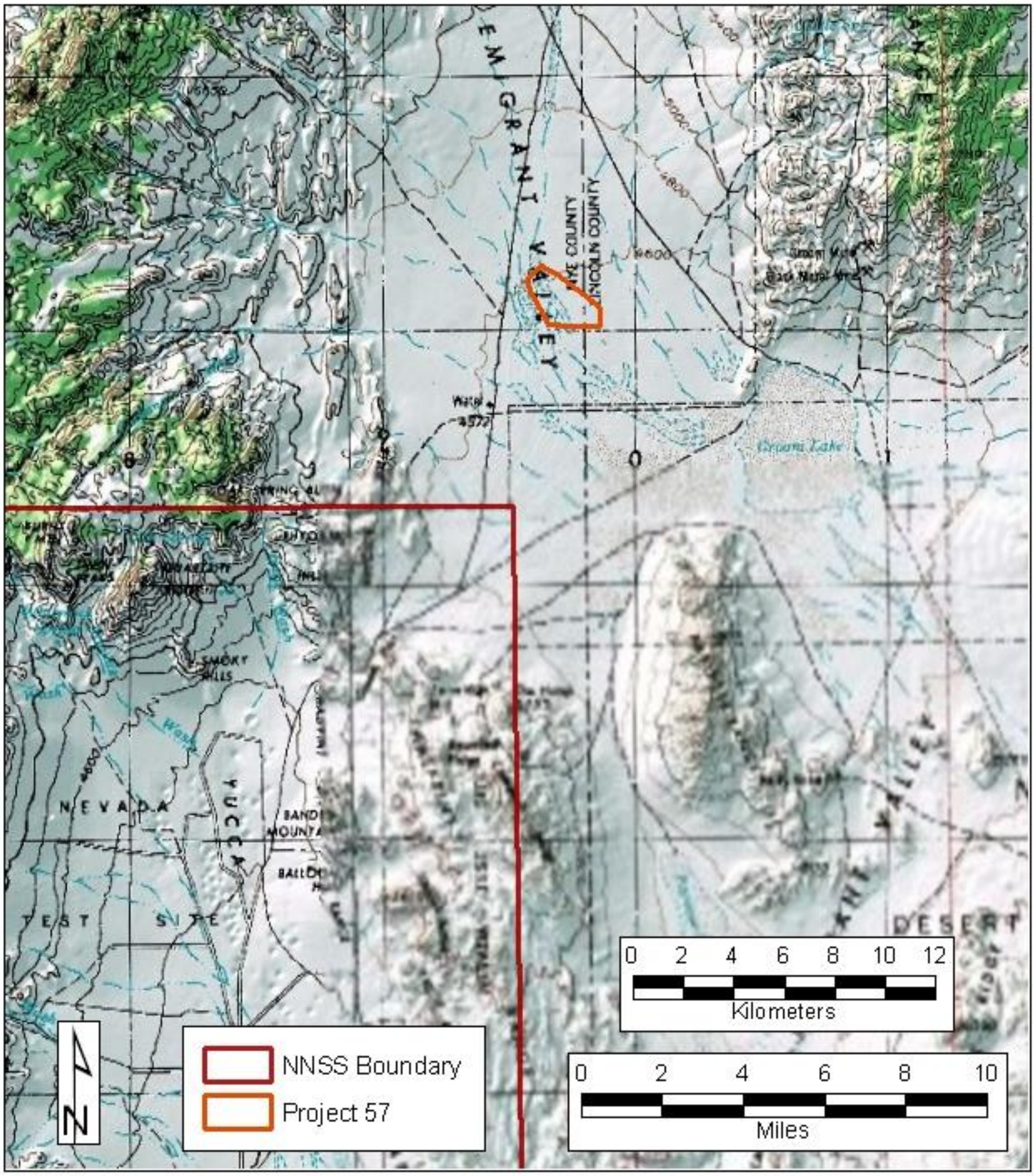

Figure 1. Project 57, outlined in orange, is beyond the north east corner of the Nevada National Security Site on the Nevada Test and Training Range at the Lincoln/Nye County border in western Emigrant Valley.

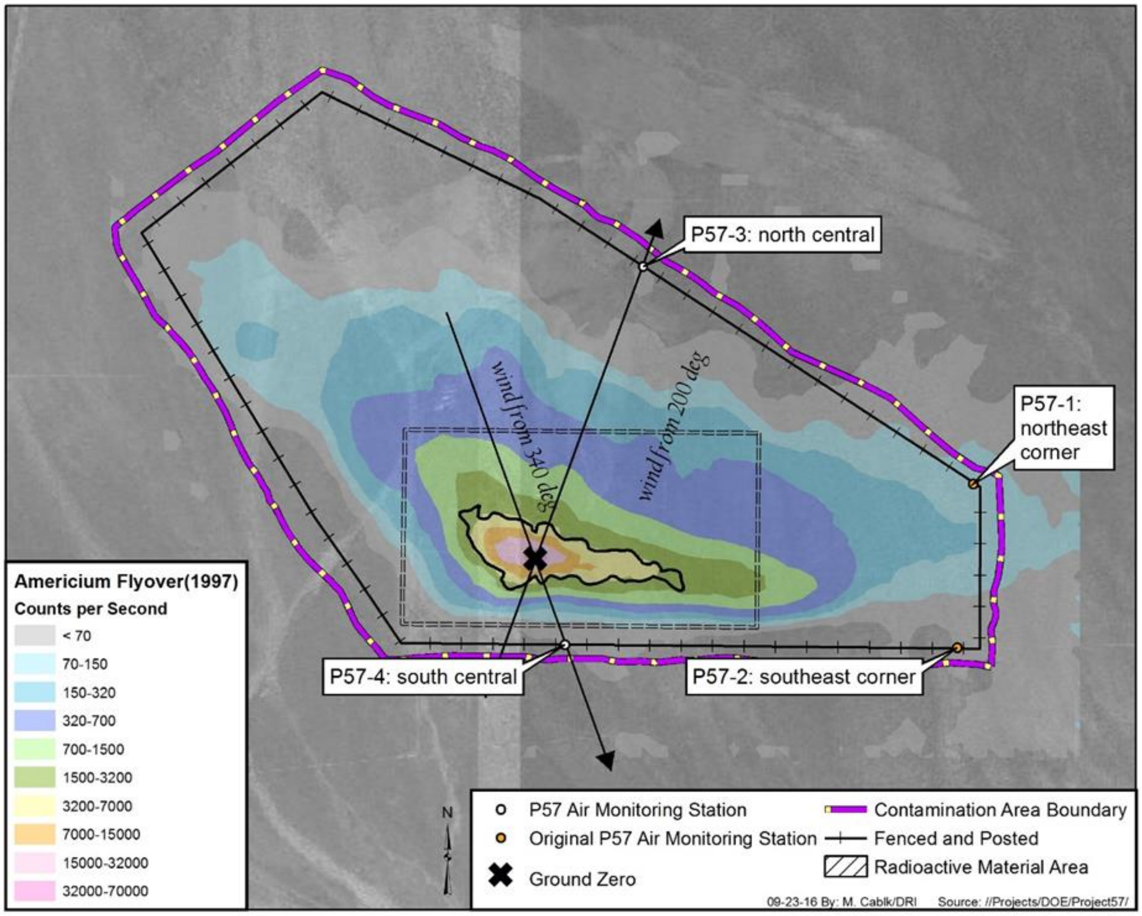

Figure 2. Locations of the original monitoring stations (P57-1 and P57-2) and those downwind of ground zero (P57-3 and P57-4) are shown in relation to the Am-241 concentrations measured during the 1997 flyover survey (from Navarro [2010]) and the original and 2007 Contamination Area (CA) boundaries.

The DOE, National Nuclear Security Administration, Nevada Field Office (NNSA/NFO) is currently working to achieve regulatory closure of radionuclide-contaminated soil sites under its purview. With respect to closure efforts, the Project 57 CA is designated Corrective Action Unit (CAU) 415, Project 57 No. 1 Plutonium Dispersion Site, which consists of one Corrective Action Site (CAS): NAFR-23-02, Pu Contaminated Soil. This CAS includes several facilities associated with Project 57 as well as the plutonium-contaminated soil.

In 2011, DRI constructed and deployed two environmental monitoring stations at Project 57 at the request of the NNSA/NFO. The data collected at these monitoring stations are used to assess the environmental and meteorological conditions and the associated potential for wind transport of radionuclide-contaminated soil from the Project 57 site. Preliminary assessments are performed and reported annually. These assessment are intended to provide site-specific information on meteorological conditions that result in airborne soil particle redistribution, as well as determine which, if any, of the radiological contaminants may be entrained with the soil particles and estimate their concentrations. Determining the potential for transport of radionuclide-contaminated soils will facilitate an appropriate closure design and post-closure monitoring program.

MONITORING STATION LOCATIONS AND CAPABILITIES

The Project 57 site is located near the center of the western sub-basin of Emigrant Valley. Soils in the area are dominated by fine particles that are subject to transport under moderate to strong winds. Tamura (1985), Friesen (1992), Murarik *et al.* (1992), and Misra *et al.* (1993) indicate that plutonium has a tendency to bind with fine soil particles. Therefore, the particles most likely to be transported by wind are also the particles most likely to be contaminated by radionuclides. Because plutonium is likely to reside in the upper few inches (or centimeters) of soil, soil erosion by wind can potentially lead to the mobilization and redistribution of radionuclide-contaminated soil. Additionally, inhaling airborne dust raised from an area of contaminated soil is the primary risk to humans.

There were no historical site-specific data describing wind direction, speed, or other climate parameters at the Project 57 site when the original monitoring stations were deployed. Regional wind data from the Community Environmental Monitoring Program (CEMP) (http://www.wrcc.dri.edu/) and the Nevada National Security Site (NNSS) (NSTec, 2011b; Attachment A) indicate that southwest and northwest winds are predominant.

Two monitoring stations were installed at Project 57 (Figure 2) in 2011 to collect air quality, meteorological, and environmental data for a field-scale assessment of environmental conditions that could potentially affect the transport of contaminated soil from the site. The northeast location was selected to obtain downwind data along the southwest wind direction that is predominant during the spring, summer, and fall. The southeast location was selected to obtain downwind information for the northwest winds that are common during the winter. Both stations were positioned to maximize wind fetch across the fenced CA as the winds passed over the monitoring stations. These locations were selected in an effort to maximize the fetch over the CA as winds approached the monitoring stations.

The northeast monitoring station (P57-1) was installed on April 20, 2011, at a temporary location outside of the northeast corner of the current CA boundary (Figure 2). National Security Technologies (NSTec) radiological control technicians (RCTs) surveyed two corridors from the current CA boundary to the former CA boundary at the fence and determined that the corridors could be downgraded to Radioactive Material Areas (RMAs). Radioactive Material Areas can be accessed by Radiological Worker II-trained personnel without RCT support. On August 11, 2011, P57-1 was reinstalled within the RMA at the fence line on the northeast side of the CA. The southeast monitoring station (P57-2) was installed on the southern RMA corridor at the fence boundary on November 18, 2011. Table 1 lists the coordinates and elevations of both monitoring stations. Figures 3 and 4 show the P57-1 and P57-2 monitoring stations, respectively, as deployed at the fence boundary.

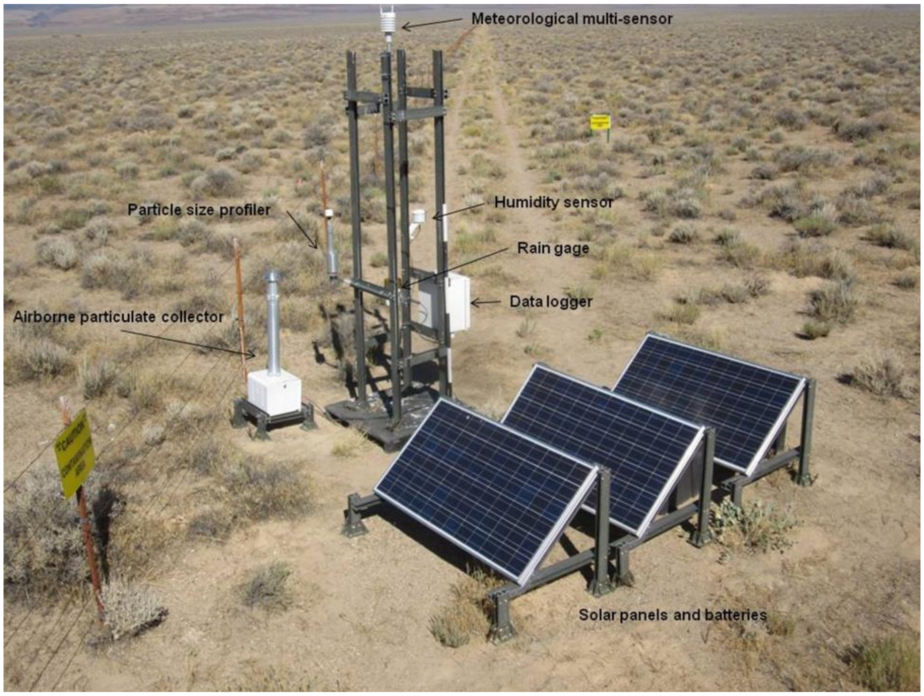

Figure 3. Project 57 monitoring station #1 (P57-1) was installed at the northeast corner of the Project 57 fenced boundary in August 2011. The associated saltation sensor (not pictured) was installed in January 2012.

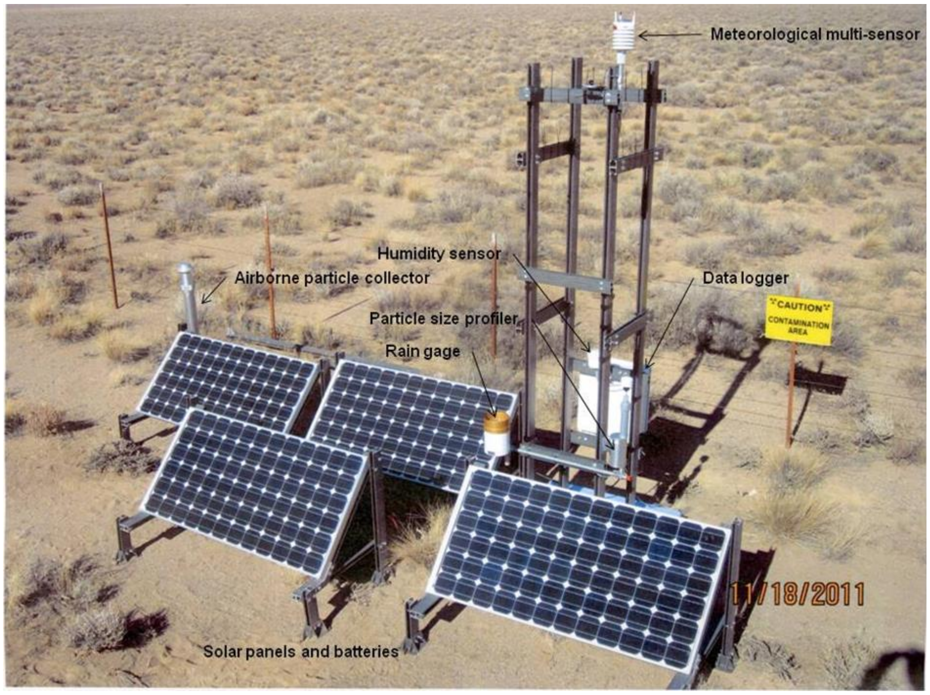

Figure 4. Project 57 monitoring station #2 (P57-2) was installed at the southeast corner of the Project 57 fence boundary in November 2011. The associated saltation sensor (not pictured) was installed in December 2011.

Table 1. Project 57 meteorological stations are located in Emigrant Valley, Nevada, at the coordinates and elevations given.

Meteorological Station	Latitude	Longitude	Elevation (ft [m])
P57-1	37º 19’ 19”	115º 53’ 20”	4,590 (1,399)
P57-2	37º 18’ 53”	115º 53’ 21”	4,575 (1,394)
P57-3	37º 19’ 47”	115º 54’ 5”	4,618 (1,408)
P57-4	37º 18’ 57”	115º 54’ 17”	4,586 (1,398)

Meteorological data collected from the P57-1 and P57-2 stations provided site-specific wind direction information. These data indicated that the dominant winds passing over the monitoring stations were not traversing the Project 57 ground zero. The site-specific data were used to select new monitoring locations, which are directly downwind of the Project 57 ground zero during the predominant southwest and northwest winds. Stations P57-1 and P57-2 were decommissioned and the equipment was relocated to establish new monitoring stations, P57-3 and P57-4, on January 7, 2015, at locations directly downwind of ground zero when winds were blowing in the predominant directions. This report reviews and analyzes data collected from the P57-3 and P57-4 stations for calendar year (CY) 2016. The following description of monitoring equipment and the equipment operation applies to the both the original stations (P57-1 and P57-2) and the current stations (P57-3 and P57-4).

The fundamental design of these stations is similar to that used in the CEMP (DeSilva, 2004; NSTec, 2011a). The equipment deployed provides data on radiological, meteorological, and environmental conditions. Table 2 lists the parameters measured. The Quality Assurance Program (Appendix G) is also patterned after that used by the CEMP. All equipment models and manufactures are listed in Appendix H.

Met One™ particle size profilers (Model 212) are deployed to determine suspended dust concentrations. Air is drawn through the Met One™ at a constant rate of one liter per minute (lpm) (0.04 ft^3/min) (Met One, 2007). An internal near-infrared laser diode is directed through the sample air flow. When an airborne particle intersects the laser beam, the light is scattered in proportion to the particle cross section area. The scattered light is collected on a photo diode, which converts the light signal to a pulse with a voltage proportional to the particle size. Output from the photo diode is analyzed to determine the number of particles. The particle counts are distributed into eight bins defined by particle size. The particle counts reported for each size bin are used to determine the concentration of particulate matter with an aerodynamic diameter ≤10 µm (PM_{10}) and particulate matter with an aerodynamic diameter ≤2.5 µm ($PM_{2.5}$). The Met One™ instruments are retrieved annually and submitted for recalibration to ensure accurate particle count and size estimates.

Continuous flow, low-volume air samplers manufactured by Hi-Q Environmental Products Company are used to collect suspended particulate matter at each station. Air is drawn through the sampler at a flow rate of approximately 2 ft^3/min (57 lpm) per minute. Suspended dust particles are collected on 4-in (10-cm) diameter glass-fiber filters

(Hi-Q, 2016). The sample filters are retrieved every two weeks and are submitted to the Radioanalytical Services Laboratory at the University of Nevada, Las Vegas. The Radioanalytical Services Laboratory performs gross alpha, gross beta, and gamma spectroscopy analyses using a 24-hour counting procedure. Gamma spectroscopy is performed to determine if Am-241, the daughter product of plutonium-241 (Pu-241), is present. If Am-241 is detected, then that sample is submitted to TestAmerica Laboratories, Inc., for alpha spectroscopy analysis to determine the quantity of plutonium isotopes present. Additionally, during each quarter of CY2016, the particulate matter sample that produced the highest gross alpha result and an additional, randomly selected sample were submitted to TestAmerica for alpha spectroscopy analysis. The TestAmerica procedure uses a six-hour counting period. These samples are provide a record of plutonium isotope concentrations and are used to compare suspended particulate matter and saltated particulate matter.

Table 2. Radiological, meteorological, and environmental sensors deployed at the Project 57 air monitoring stations. Dates refer to the first occurrence of data collection for the specified parameter.

Instrument/Measurement[1]	**P57-1**	**P57-2**	**P57-3**	**P57-4**	**Data Collection Interval**
Wind speed	8/11/2011	11/18/2011	1/7/2015	1/7/2015	3 seconds
Wind direction	8/11/2011	11/18/2011	1/7/2015	1/7/2015	3 seconds
Precipitation	8/11/2011	11/18/2011	1/7/2015	1/7/2015	3 seconds
Temperature	8/11/2011	11/18/2011	1/7/2015	1/7/2015	3 seconds
Relative humidity	8/11/2011	11/18/2011	1/7/2015	1/7/2015	3 seconds
Solar radiation	not installed	11/18/2011	1/7/2015	1/7/2015	3 seconds
Barometric pressure	8/11/2011	11/18/2011	1/7/2015	1/7/2015	3 seconds
Soil temperature	8/11/2011	11/18/2011	1/7/2015	1/7/2015	3 seconds
Soil moisture content	8/11/2011	11/18/2011	1/7/2015	1/7/2015	3 seconds
Airborne particle size profiler	8/11/2011	11/18/2011	1/7/2015	1/7/2015	1 minute
Saltation sensor	1/09/2012	1/09/2012	1/7/2015	1/7/2015	3 seconds
Datalogger	8/11/2011	11/18/2011	1/7/2015	1/7/2015	Monthly
Airborne particle collector	8/11/2011	11/18/2011	1/7/2015	1/7/2015	Biweekly
Thermoluminescent dosimeters	1/09/2012	1/09/2012	1/7/2015	1/7/2015	Quarterly
BSNE saltation sand traps	4/14/2014	4/14/2014	1/7/2015	1/7/2015	Seasonal[2]

[1] See Appendix H for instrument make, model, and manufacturer.

[2] The original data collection interval for the Big Spring Number Eight (BSNE) saltation sand traps was approximately annual. A seasonal collection cycle has been implemented to coordinate with seasonal wind patterns.

On April 14, 2014, DRI installed Big Spring Number Eight (BSNE) saltation sand traps to collect dust and soil transported by saltation at the Project 57 monitoring stations. The BSNE saltation sand traps are isokinetic wind aspirated samplers (Figure 5) that collect a large portion of the airborne sand that enters the opening regardless of wind speed. Three replicate BSNE saltation sand traps, each with two collectors, were installed along the fence line at each of the Project 57 monitoring stations. The inlet height is set at 6 in (15 cm) to collect the maximum amount of erodible soil material. The two collectors are installed so that one is pointed toward the CA to collect material downwind of the CA. The other collector is pointed in the opposite direction to collect material upwind of the CA. The BSNE saltation sand traps allow for a radiological assessment of soil material transported near the ground surface, an estimation of net movement of soil material to and from the contaminated area, and perhaps an assessment of the spatial variability in soil transport. Although previous BSNE traps have been collected approximately annually (Appendix D), the traps deployed on January 4, 2016, were retrieved on October 12, 2016, as a plan to sample seasonally predominant winds.

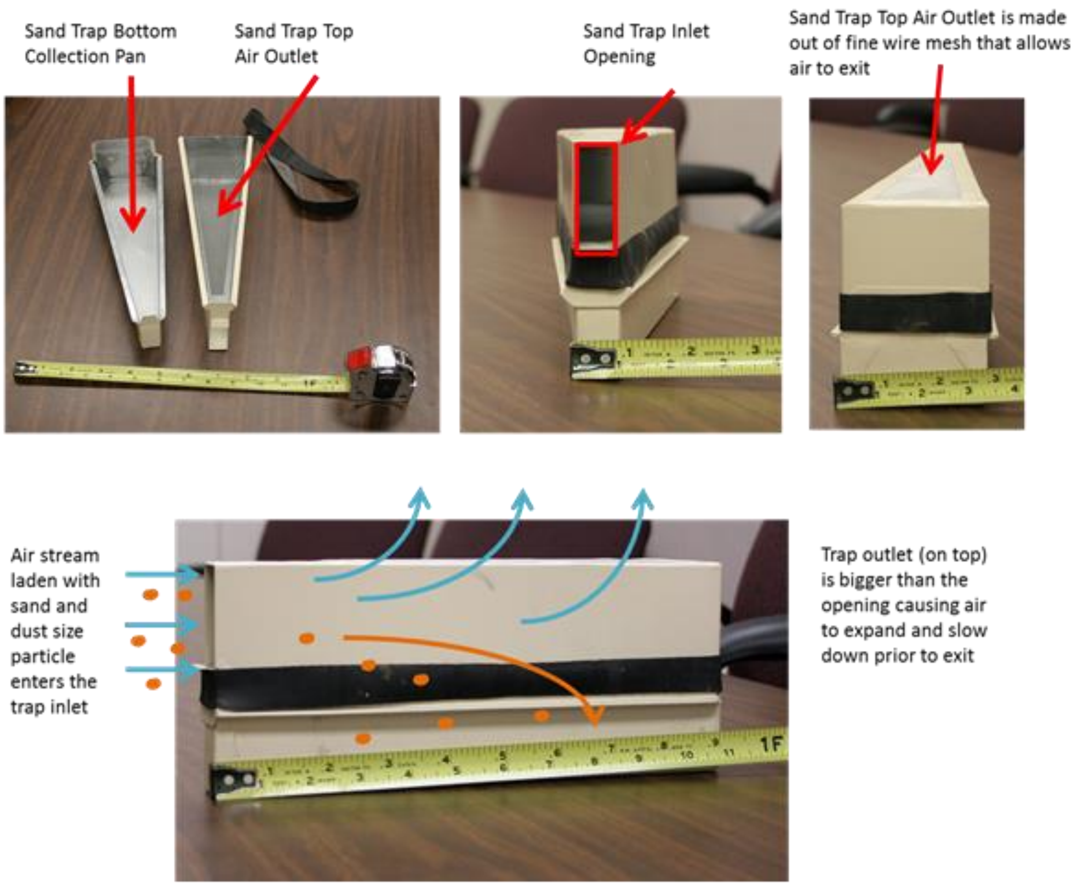

Figure 5. Sand and dust particles are carried into the BSNE Saltation Sand Trap by fast moving air. As the air slows down, momentum is lost and the particles settle on the bottom of the collection pan.

Suspension and transport of dust is controlled by local meteorological and other environmental conditions, such as wind speed and soil moisture content. Electronic sensors measure these parameters at the air monitoring stations every three seconds. The three-second measurements are averaged or totaled as appropriate. Both the 3-second observed and 10-minute summary values are stored on the on-site datalogger. The maximum and minimum values of each parameter observed during the 10 minute interval are also saved so that they can be used to evaluate data quality or be made available for future analysis. The dataloggers are downloaded during site visits once each month. The retrieved data are quality checked and archived by the Western Regional Climate Center for later interpretation.

Thermoluminescent dosimeters (TLDs) were installed at both stations in November 2011. They are collected on a quarterly basis for laboratory analysis. Saltation sensors, which are used to measure the occurrence and frequency of soil particle transport by saltation, were installed at the P57-2 and P57-1 stations in December 2011 and early January 2012, respectively.

All instrumentation and operational parameters were transferred from P57-1 and P57-2 to stations P57-3 and P57-4, respectively, when the original stations were decommissioned and the new stations were established.

OBSERVED METEOROLOGICAL AND ENVIRONMENTAL CONDITIONS

Meteorological and environmental sensors (Table 2) operated continuously and a complete record of observations was collected at P57-3 and P57-4 during the reporting period: January 1, 2016, through December 31, 2016, with two exceptions. The Met One™ suspended particle size profiler failed to operate at P57-3 between January 1, 2016, and July 20, 2016. Therefore, approximately six months of data are available from that instrument. Additionally, the Sensit™ saltation particle counter at P57-4 failed between January 1, 2016, and October 11, 2016. Therefore, approximately three months of data are available from that instrument. Tables 3 and 4 show monthly average/total values, as appropriate, of the observed meteorological and environmental parameters for the year. Appendices A, B, and C show charts of the daily observations of these parameters.

Monthly average wind speed was less than 12 mph (19 km/hr) throughout the year; monthly average wind speeds were slightly higher at P57-3 than at P57-4. Monthly average wind directions varied from southwest to northwest (Tables 3 and 4). Winds from the north-northwest were the most common, occurring late fall through late spring; winds from the southwest were most common during the summer (Figures A-3 and A-12). Average monthly air temperature ranged from 34 ^{o}F (1.1 ^{o}C) in December to 78 ^{o}F (25.6 ^{o}C) in July. Extreme air temperatures ranged from 6 ^{o}F (-14.4 ^{o}C) in February to 106 ^{o}F (41.1 ^{o}C) in July. The minimum relative humidity was two to three percent. Daily average air temperature follows the expected annual cycle (Figures A-1 and A-10). Over the reporting period, the seasonal variations in the daily average temperature ranged from approximately 25 ^{o}F (-3.9 ^{o}C) to 90 ^{o}F (32.2 ^{o}C) at both monitoring stations. Both stations are exposed to large diurnal temperature ranges with infrequent precipitation and seasonally directional winds. The general conditions observed are typical of a Great Basin Desert location.

Table 3. Monthly average or total meteorological and environmental observations at station P57-3 for CY2016.

		Date (mm-yy)											
		Jan-16	**Feb-16**	**Mar-16**	**Apr-16**	**May-16**	**Jun-16**	**Jul-16**	**Aug-16**	**Sep-16**	**Oct-16**	**Nov-16**	**Dec-16**
Solar Radiation (Ly)	Total	6,913	11,392	13,955	15,392	18,356	19,613	20,682	18,463	15,624	11,388	8,619	6,701
Mean Wind Speed (mph)	Ave.	7.73	11.46	8.54	9.26	8.61	8.36	8.10	7.07	7.78	7.55	6.60	9.23
Mean Wind Direction (Deg.)	Vector Ave.	346	347	320	332	329	214	203	213	314	229	350	358
Maximum Wind Gust (mph)	Max.	54.6	52.9	45.0	51.5	50.4	41.5	43.5	35.4	42.8	47.4	39.9	68.2
Average Air Temperature (Deg. F)	Ave.	34.84	40.52	47.21	53.30	60.19	76.75	78.54	75.35	66.61	56.89	43.22	34.24
	Ave. Daily Max.	47.53	55.88	63.22	68.53	75.37	93.67	96.11	93.73	84.45	73.41	63.12	49.46
	Max.	62.24	72.28	76.06	80.02	88.79	104.4	105.9	99.19	93.42	81.43	77.97	61.52
	Ave. Daily Min.	26.10	26.38	29.84	37.77	42.44	55.64	56.04	53.56	46.85	40.62	27.03	20.76
	Min.	15.37	7.38	22.48	30.64	30.00	42.58	46.58	44.68	36.34	32.76	10.92	12.78
Average Soil Temperature - 4 in (Deg. F)	Ave.	34.74	39.90	49.45	56.81	64.76	79.75	83.09	81.47	73.46	60.39	46.48	36.14
	Max.	45.98	56.21	66.13	73.04	87.53	97.66	99.18	97.29	91.90	76.28	65.64	49.32
	Min.	25.59	29.10	36.20	43.35	45.12	62.22	69.40	67.48	58.30	47.16	29.08	26.37
Average Relative Humidity (%)	Ave.	68.15	53.59	43.16	43.07	35.53	20.09	19.49	22.37	23.10	36.64	45.04	53.96
	Max.	100.0	99.10	99.20	97.80	97.60	93.40	92.30	90.00	91.30	97.90	97.80	100.0
	Min.	13.56	9.19	7.14	5.66	5.82	3.95	3.74	3.24	3.78	5.16	8.21	6.81
Barometric Pressure (in Hg)	Ave.	25.41	25.52	25.32	25.34	25.30	25.37	25.39	25.39	25.40	25.39	25.46	25.31
Precipitation (in)	Total	0.87	0.22	0.27	1.13	0.02	0.54	0.45	0.09	0.00	0.18	0.09	0.86

Table 4. Monthly average or total meteorological and environmental observations at station P57-4 for CY2015.

		Date (mm-yy)											
		Jan-15	**Feb-15**	**Mar-15**	**Apr-15**	**May-15**	**Jun-15**	**Jul-15**	**Aug-15**	**Sep-15**	**Oct-15**	**Nov-15**	**Dec-15**
Solar Radiation (Ly)	Total	6,885	11,113	14,201	15,924	19,021	20,187	21,426	19,254	16,120	11,815	8,828	6,922
Mean Wind Speed(mph)	Ave.	6.55	9.76	7.84	8.81	8.28	7.97	7.74	6.73	7.30	7.14	6.21	7.32
Mean Wind Direction (Deg.)	Vector Ave.	350	355	313	328	325	238	228	233	301	253	343	346
Maximum Wind Gust (mph)	Max.	34.7	42.1	43.8	48.5	49.5	37.0	43.2	38.2	42.3	44.9	38.8	34.2
Average Air Temperature (Deg. F)	Ave.	35.14	40.84	47.71	53.74	60.52	77.11	78.79	75.60	66.71	57.04	43.08	34.19
	Ave. Daily Max.	48.62	56.71	64.22	69.28	75.98	94.77	97.47	94.93	85.31	74.19	63.38	49.95
	Max.	63.93	71.89	74.25	81.43	89.76	103.8	106.6	100.0	94.44	81.81	77.07	61.29
	Ave. Daily Min.	25.58	25.57	29.60	37.14	42.02	54.96	55.27	53.10	45.50	39.54	25.72	19.93
	Min.	15.98	5.90	21.97	30.62	30.04	42.00	44.60	44.09	35.23	29.21	8.76	12.06
Average Soil Temperature – 4 in (Deg. F)	Ave.	34.44	41.20	52.16	60.37	68.29	84.16	87.61	84.63	74.95	61.35	46.11	35.50
	Max.	50.16	67.57	72.61	82.40	97.68	108.4	114.3	106.6	99.34	83.64	71.98	53.37
	Min.	21.74	29.70	33.80	42.65	43.59	60.93	65.61	63.77	54.30	43.54	22.78	21.70
Average Relative Humidity (%)	Ave.	69.75	56.12	44.19	44.63	38.09	21.87	21.57	24.64	25.07	38.67	46.94	55.50
	Max.	100.0	96.00	99.00	98.30	98.90	96.60	96.30	94.10	94.00	98.90	98.50	90.90
	Min.	15.44	8.65	6.67	5.09	5.74	2.93	2.76	2.04	2.73	4.48	8.56	6.66
Barometric Pressure (in Hg)	Ave.	25.42	25.55	25.35	25.37	25.33	25.42	25.43	25.43	25.44	25.42	25.48	25.43
Precipitation (in)	Total	0.95	0.44	0.19	0.97	0.12	0.52	0.51	0.12	0.00	0.30	0.13	1.10

Total precipitation for the reporting period was 4.72 in (119.9 mm) and 5.35 in (135.8 mm) at P57-3 and P57-4, respectively (Tables 3 and 4). No precipitation was observed during September. The four largest precipitation events produced daily rainfall amounts in excess of 0.35 in (8.9 mm) at both monitoring stations in January, May, June, and December (Figures A-2 and A-11). Other precipitation events typically produced less than 0.25 in (6.4 mm). Precipitation events were more common between January and May, and least common in August and September. Maximum monthly precipitation occurred in April at P57-3 and in December at P57-4 (Table 5). Maximum daily precipitation occurred in June at P57-3 but in December at P57-4. Maximum hourly and 10-minute precipitation occurred at both stations in April and June, respectively. Station P57-4 appears to receive slightly more precipitation than station P57-3 throughout the year.

Soil temperature and soil moisture are also collected at the P57 stations. Like the average daily air temperature, the average daily soil temperature exhibits an annual seasonal pattern (Figure B-1 and B-3). The soil temperature is typically warmer at P57-4 than at P57-3, especially during the spring and summer. During CY2016, soil moisture was between approximately 6 percent and 20 percent of soil volume at P57-3 (Figure B-2) and between 10 percent and 27 percent at P57-4 (Figure B-4). Generally, soil moisture at P57-4 appears to be slightly higher and is slower to drop than at P57-3.

Peak wind speeds reached approximately 68 mph (109.4 km/hr) at P57-3 and 50 mph (80 km/hr) at P57-4 during 2016. The peak wind speed of 48 mph (77 km/hr) observed at P57-4 was measured in April and November. Wind rose diagrams for all 10-minute average wind conditions observed during 2016 (Figures 6, A-7, and A-16) indicate that winds were predominantly from the north to northwest and secondarily from the south to southwest at both Project 57 monitoring stations.

To evaluate seasonal differences in wind conditions, wind roses were constructed for spring/summer (March 1 to August 31) winds (Figures A-8 and A-17) and fall/winter (September 1 to February 28) winds (Figures A-9 and A-18). The seasonal winds came from the same predominant directions identified for all winds. However, winds from the south to southwest appear somewhat more common during the summer, whereas winds from the northeast to northwest were more common during the winter.

Table 5. Precipitation extremes observed during calendar year 2016.

Station	Minimum Monthly (in)	Maximum Monthly (in)	Maximum Daily (in)	Maximum Hourly (in)	Maximum 10-min (in)
P57-3	0.00 September 2016	1.13 April 2016	0.52 June 11, 2016	0.28 April 29, 2016 2300h	0.11 June 11, 2016 0300h
P57-4	0.00 September 2016	1.10 December 2016	0.58 December 23, 2016	0.25 April 29, 2016 2300h	0.12 June 11, 2016 0300h

Generally, wind speeds must exceed 15 mph (24 km/hr) to produce dust by saltation or suspension (see discussions in the section on dust transport that follows). At the Project 57 stations, wind speed exceeded 15 mph (24 km/hr) approximately 13 percent of the time at P57-3 and 9 percent of the time at P57-4. Wind roses for winds in excess of 15 mph (24 km/hr) (Figure 6) show the same dominant directions seen in the analysis of all winds. Two dominant wind directions account for 96.9 percent of all winds over 15 mph (24 km/hr) at P57-3, and 97.9 percent of all winds over 15 mph (24 km/hr) at P57-4. The dominance of these wind directions are equivalent to conditions observed in CY2015 (Mizell *et al.*, 2017). At P57-3, winds from the northeast-to-northwest quadrant are most common, they occurred approximately 53.5 percent of the time, whereas the south-to-southwest winds occurred approximately 43.4 percent of the time. At P57-4, the two dominant wind directions are slightly more balanced. Winds from the northeast to northwest occurred approximately 50.4 percent of the time, whereas winds from the south to southwest occurred approximately 47.5 percent of the time (Figures 6, 7, A-3, and A-12).

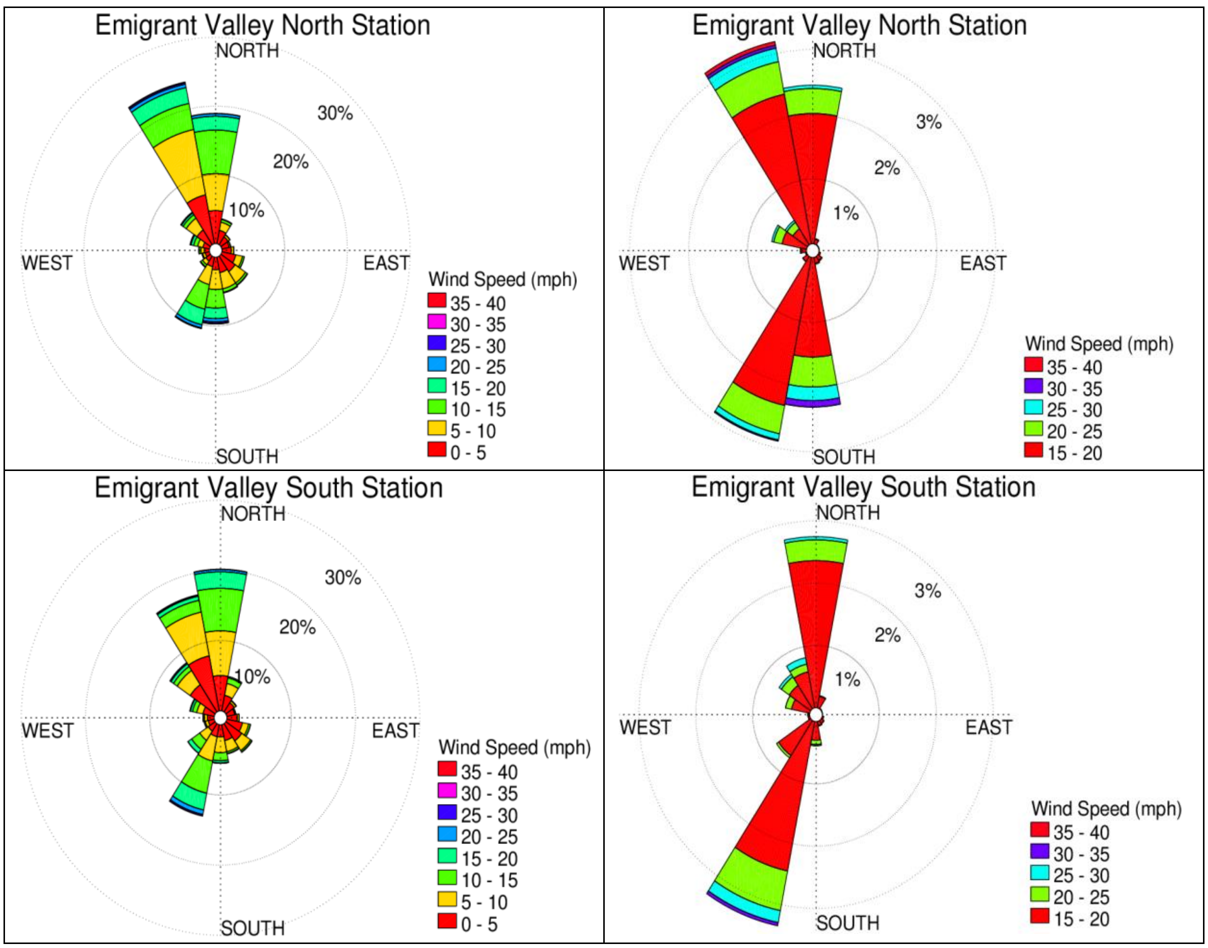

Figure 6. Wind roses for Project 57 monitoring stations P57-3 (top row) and P57-4 (bottom row) for January 1 through December 31, 2016. The left column represents all wind speeds and the right column represents only wind speeds in excess of 15 mph (24 km/hr).

The wind direction data were assigned to bins representing 10-degree direction intervals and bin counts were expressed as percentage of all observations. Figure 7 shows the wind direction frequency distribution for the wind direction bins. This chart shows that south-southwest winds are defined as being from 170 degrees to 260 degrees, and that winds from the northeast to northwest are from 300 degrees to 60 degrees. An analysis of dust transport conditions associated with these two predominant wind directions was performed to determine if there are major differences.

The wind roses (Figure 6) and wind direction frequency distribution (Figure 7) show that northerly winds are somewhat more frequent than southerly winds. Wind direction frequency observed during CY2016 indicates a slight increase in the frequency of southerly winds accompanied by a reduction in northerly winds when compared with the CY2015 observations (Mizell *et al.*, 2017). This shift appears to be more pronounced at P57-4.

Both sites are exposed to large diurnal temperature ranges with infrequent precipitation events and seasonally directional winds, which is typical of a Great Basin Desert location. A comparison of the data from both stations shows only minor differences in temperature, precipitation, humidity, and barometric pressure. Wind patterns distinctly show two dominant directions. Soil temperature and moisture show strong similarities to meteorological patterns.

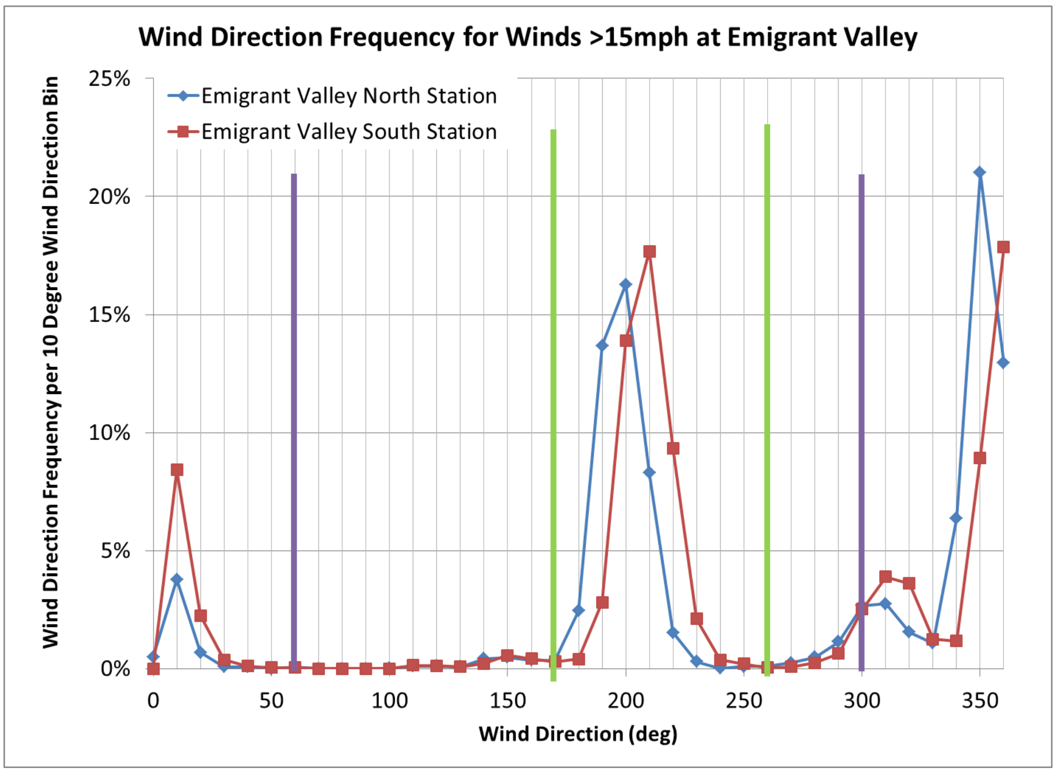

Figure 7. Wind direction frequency for 10-minute average wind speeds in excess of 15 mph (24 km/hr) at the Project 57 monitoring stations. The wind direction data were assigned to bins representing 10-degree direction intervals and bin counts expressed as percentage of all observations. In later analyses the southerly winds (bounded by the green lines) and northerly winds (bounded by the purple lines) were separated for comparison.

OBSERVATIONS OF SOIL/DUST TRANSPORT BY WIND

Soil movement initiated by wind forces is characterized as either surface creep, saltation, or suspension (Figure 8). Surface creep is a process by which particles are rolled across the ground surface by wind and impacts from saltating particles. Particles moved by creep are generally over 500 µm (0.02 in) in aerodynamic diameter and are too heavy to be lifted into the air. Saltation is the mechanism by which soil particles in the range of 50 µm (0.002 in) to 500 µm (0.02 in) are transported. These particles are dislodged and carried a small distance in the air before falling back to the ground. Their transport paths usually follow a parabolic trajectory, so the particles essentially bounce across the ground surface. The amount of time the particles are in the air and the distances they travel are functions of wind speed and particle mass. Saltation is important because the impact of saltated particles may push creep particles and dislodge smaller particles that are ejected into the air where they are transported via suspension. Suspended particles are usually smaller than 50 µm (0.002 in). Particles less than 20 µm (0.0008 in) in diameter can be entrained in the air by wind or from impact with saltation-sized particles. Once these particles are suspended in the air, they can be transported over extremely long distances. Fine particles, which are particles with an aerodynamic diameter <10 µm (0.0004 in) (PM_{10}), are small enough to be inhaled by humans and are called respirable suspended particles. At the Project 57 monitoring stations, suspended particles are counted using the Met One™ Ambient Particulate Profiler Model 212 and saltated particles are counted using the Sensit H11-LIN™.

The Sensit™ sensor impact area is made of piezoelectric material that wraps completely around the vertically oriented instrument. The sensor registers impacts from all directions and converts them to electrical impulses. The impact surface is centered 4 in (10 cm) above the ground surface based on the recommendation of the manufacturer (http://www.sensit.com/images/Tech_Note_5.pdf, accessed December 7, 2015). Particle counts are summed over 10-minute intervals and stored on the station datalogger. Currently, the saltation sensors are located near the meteorological towers at each station in areas that are free of vegetation and recent disturbances, which might interfere with their operation.

Because raindrop impact dislodges and ejects soil particles into the air, counts on the saltation sensors sometimes register during precipitation events. This phenomenon does not result in the same type of particle trajectory or dust emission associated with the wind-driven saltation described above. Raindrops can also be carried by wind and hit the saltation sensor and register as false saltation counts. The saltation sensor cannot distinguish between

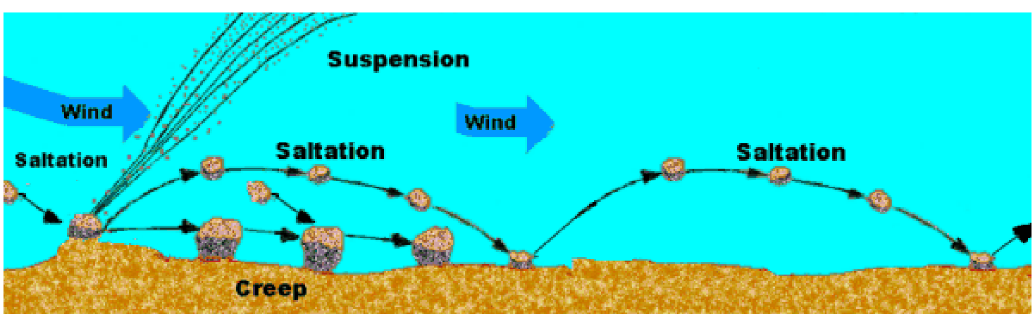

Figure 8. Illustration of the saltation process. (The Weather Doctor, http://www.islandnet.com/~see/weather/elements/dustwind.htm, accessed December 7, 2015.)

raindrop or soil particle impacts. Therefore, even though rain plays an important role in soil mechanics in desert environments, counting periods that are coincident with precipitation are removed from the data set to ensure that the analyses focus on wind driven saltation.

Suspended particles are counted using a Met One™. The Met One™ detects and records the suspended particle count in eight different size groups that range from 0.5 µm (0.00002 in) to 10 µm (0.00039 in) in diameter. These particle counts are used to calculate PM_{10} and $PM_{2.5}$ concentrations. Particle counts are reported every minute and the average for each 10-minute interval is recorded in the datalogger. The Met One™ instruments are mounted so that the air inlet of the instrument is between 4.9 ft (1.5 m) and 5.6 ft (1.7 m) from the ground, which is the respirable zone for most adults.

Dust Transport by Saltation

Saltation-related particle counts are strongly dependent on wind speed. The relationship between wind speed and saltation particle counts was investigated by determining the average number of particle counts/10-minute interval for sustained wind speeds categorized in 5-mph (8-km/hr) wind speed classes (Table 6 and Figure 9) after removing those intervals influenced by rainfall. The Sensit™ saltation sensor at P57-3 was operational throughout CY2016. However, the Sensit™ at P57-4 was not operating during the first three quarters of CY2016. Therefore, the data summaries presented in Table 6 and Figure 9 for P57-4 represent only data collected between October 11, 2016, and December 31, 2016.

Table 6. Average saltation particle counts by wind speed class at Project 57 monitoring stations.

Wind Speed Class (mph)	Duration (hours)	Average Wind Speed (mph)	Average Particle Counts (count/10-min)
P57-3			
0 – 5	3026.00	3.52	0.003
5 – 10	2857.50	6.97	0.068
10 – 15	1581.83	12.32	0.025
15 – 20	826.00	17.04	0.255
20 – 25	188.00	21.97	0.074
25 – 30	56.50	26.89	1.646
30 – 35	14.50	31.86	0.931
Total	8550.33	--	--
P57-4*			
0 – 5	2190.83	3.50	0.017
5 – 10	1450.00	6.96	0.006
10 – 15	846.33	12.22	0.107
15 – 20	353.83	16.91	0.012
20 – 25	45.17	21.74	0.218
25 – 30	6.67	26.63	4.800
30 – 35	--	--	--
Total	4892.83	--	--

* Because of Sensit™ failure saltation counts reflect the time from October 11, 2016, to December 31, 2016.

Saltation particle counts are generally low at wind speeds below 25 mph (40 km/hr) (Table 6, Figure 9). The saltation particle counts increase sharply for sustained wind speeds between 25 mph (40 km/hr) and 30 mph. At P57-3, the particle counts drop off just as sharply for wind speeds above 30 mph (48 km/hr). The drop off in saltation particle counts at the highest observed wind speeds suggests that the available supply of particles suitable for saltation transport is limited and that winds in the 25 mph (40 km/hr) to 30 mph (48 km/hr) range are sufficient to move the available materials. During CY2016, saltation particle counts were collected for more than 8,550 hours and winds in excess of 25 mph (40 km/hr) were measured for approximately 71 hours, which is less than one percent of the year. At P57-4, winds in excess of 25 mph (40 km/hr) were recorded for a total of 6.67 hours during the time saltation particle counts were recorded, which is approximately 0.14 percent of the time. Although the higher wind speeds are critical to the transport of soil material by saltation, the occurrence of higher wind speeds is relatively infrequent. Because these winds are infrequent, they are not statistically significant nor sufficient to formulate a predictive model for saltation transport associated with sustained winds in excess of 25 mph (40 km/hr).

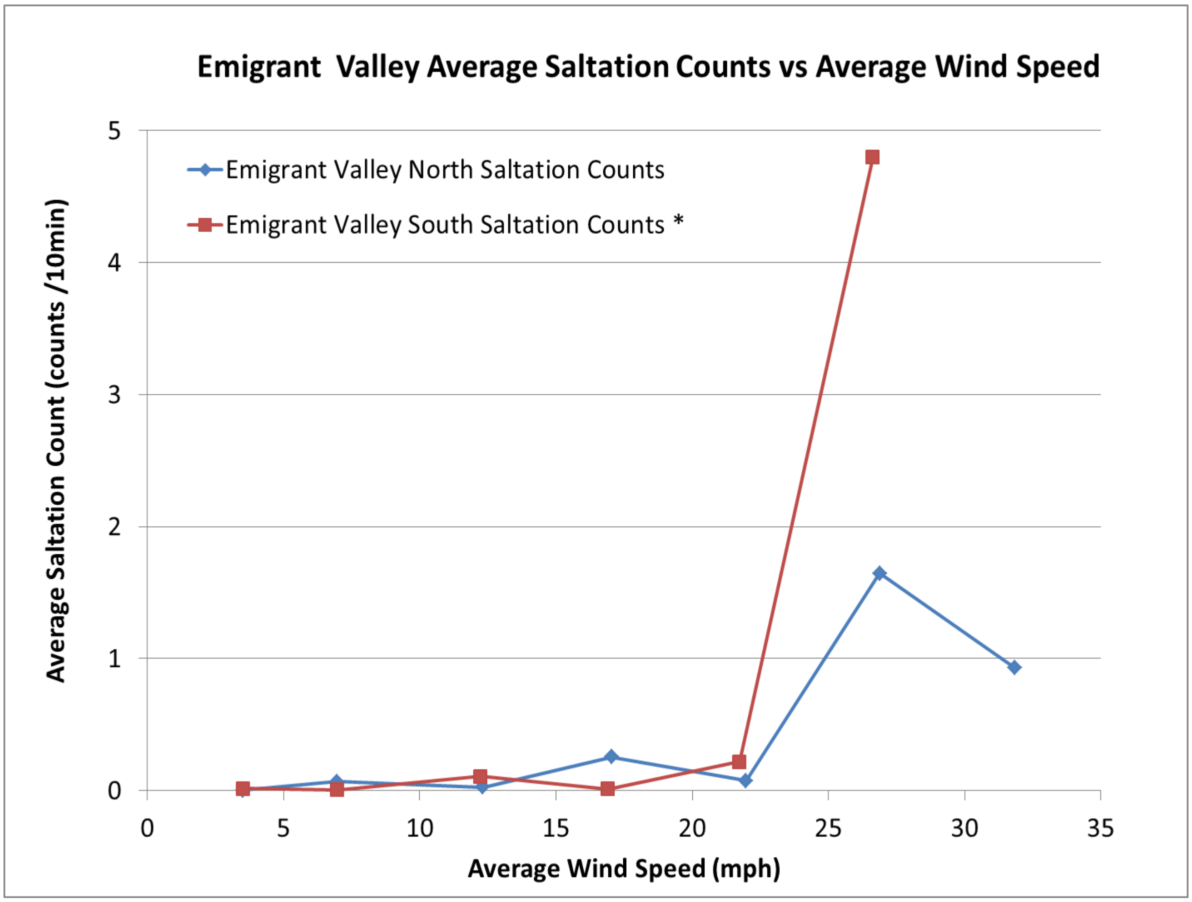

Figure 9. Average saltation counts for Emigrant Valley North (P57-3) and South (P57-4) stations. The saltation counts generally increase exponentially as the wind speed increases. Note that saltation data for P57-4 are available only for June 1, 2016, thorugh December 31, 2016, because of instrument failure.

Dust Transport by Suspension

Table 7 summarizes wind speed and the corresponding PM_{10} concentration by wind-speed class for Emigrant Valley monitoring stations. The wind speed at both stations was below 15 mph (24 km/hr) approximately 90 percent of the time and the corresponding average PM_{10} concentrations are below 25 µg/m^3 (2.5 × 10^{-8} oz/ft^3). Consequently, the wind speed was above 15 mph (24 km/hr) only 10 percent of the time. Although PM_{10} concentrations generally increase as wind speed increases, the PM_{10} concentrations remained fairly low until winds exceeded approximately 25 mph (40 km/hr); this happened less than 0.5 percent of the time during CY2016. The PM_{10} concentrations increased with increasing wind speed and exceeded 172 µg/m^3 for winds between 25 mph (40 km/hr) and 30 mph (48 km/hr) at P57-3 and 314 µg/m^3 (3.1 × 10^{-7} oz/ft^3) for wind speeds between 30 mph (48 km/hr) and 35 mph (56 km/hr) at PM-4. However, high wind speeds and high PM_{10} events were relatively rare and generally lasted for only short periods of time. Wind speeds exceeded 30 mph (48 km/hr) only 0.022 percent (<1 hr) of the time at P57-3 between July 18, 2016, and December 31, 2016; PM_{10} data were not available at P57-3 between January 1, 2016, and July 18, 2016. Wind speed exceeded 30 mph (48 km/hr) only 0.057 percent (<5 hr) of the time at P57-4 for the twelve month period covered in this report.

Light winds (0 to 5 mph [0 to 8 km/hr]) were most common at P57-4 and moderate winds (5 to 10 mph [8 to 16 km/hr]) were most common at P57-3 (Figure 10). Wind speeds in excess of 15 mph (24 km/hr) occurred less than four percent of the time and wind speeds in excess of 20 mph (32 km/hr) occurred less than one percent of the time (Table 7).

The average PM_{10} concentrations at P57-3 and P57-4 increase more rapidly than the wind speed (Figure 11). As expected, the two monitoring stations show very similar trends. Values for average PM_{10} concentrations are nearly identical for wind speeds below 25 mph (40 km/hr) (Table 7). For wind speeds over 25 mph (40 km/hr) the PM_{10} shows a non-linear increase and concentration for high wind speeds that exceed 250 µg/m^3 (2.5 × 10^{-7} oz/ft^3). At station P57-3, winds in the 30 mph (48 km/hr) to 35 mph (56 km/hr) range occur for only about 0.8 hours (45 minutes) during the period when PM_{10} concentration data are available. The lack of these high wind speeds during the time of year when dust data are available may result in the reduced dust concentration at the highest wind speeds. The lower graph in Figure 11 is plotted on a log scale to highlight the rapid rise in PM_{10} concentration for wind speeds over 20 mph (32 km/hr). Although the PM_{10} concentration increased approximately exponentially at high wind speeds, this does not imply that large volumes of soil material were moving. The wind speeds necessary to generate the higher PM_{10} concentrations occurred less than approximately two percent of the time, which limits the net soil transport.

Because saltating particles are likely to dislodge and eject smaller particles from the soil surface, the relationship between saltation particle counts and PM_{10} concentrations is important. In addition to PM_{10} transported from upwind locations, some PM_{10} is generated locally because of saltation. A correlation analysis was performed to investigate this relationship. A strong correlation between high saltation values and high PM_{10} values would indicate that strong winds are driving the saltation activity, which in turn contributes to fine dust emissions. Figure 12 shows the correlation between saltation counts and PM_{10} concentration at P57-3. At this station, there is a linear correlation between saltation counts and PM_{10} concentration. However, the slope of the relationship shown is controlled entirely by the saltation counts and PM_{10} at the highest wind speed.

Table 7. Summary of wind and PM_{10} data for Project 57 stations P57-3 and P57-4 during the period from January 1, 2016, to December 31, 2016. Note that PM_{10} data for P57-3 were not available for the period January 1, 2016, through July 18, 2016.

Wind Speed Class (mph)	**Duration (hours)**	**Frequency (%)**	**Cumulative Frequency (%)**	**Average Wind Speed (mph)**	**PM_{10} (μg/m^3)**
P57-3					
0 – 5	1530.50	41.144%	41.144%	3.54	23.65
5 – 10	1241.50	33.375%	74.519%	6.86	22.98
10 – 15	599.00	16.103%	90.622%	12.24	24.71
15 – 20	287.83	7.738%	98.360%	17.06	28.11
20 – 25	51.00	1.371%	99.731%	21.66	56.44
25 – 30	9.17	0.246%	99.978%	26.76	172.54
30 – 35	0.83	0.022%	100.000%	31.32	67.09
Total	3719.83	--	--	--	--
P57-4					
0 – 5	3,407.83	39.886%	39.886%	3.53	11.50
5 – 10	2,696.33	31.559%	71.445%	7.03	10.80
10 – 15	1,609.83	18.842%	90.287%	12.26	14.81
15 – 20	655.33	7.670%	97.958%	16.96	19.04
20 – 25	133.67	1.564%	99.522%	21.60	47.41
25 – 30	36.00	0.421%	99.943%	26.87	121.06
30 – 35	4.83	0.057%	100.000%	30.84	314.69
Total	8543.83	--	--	--	--

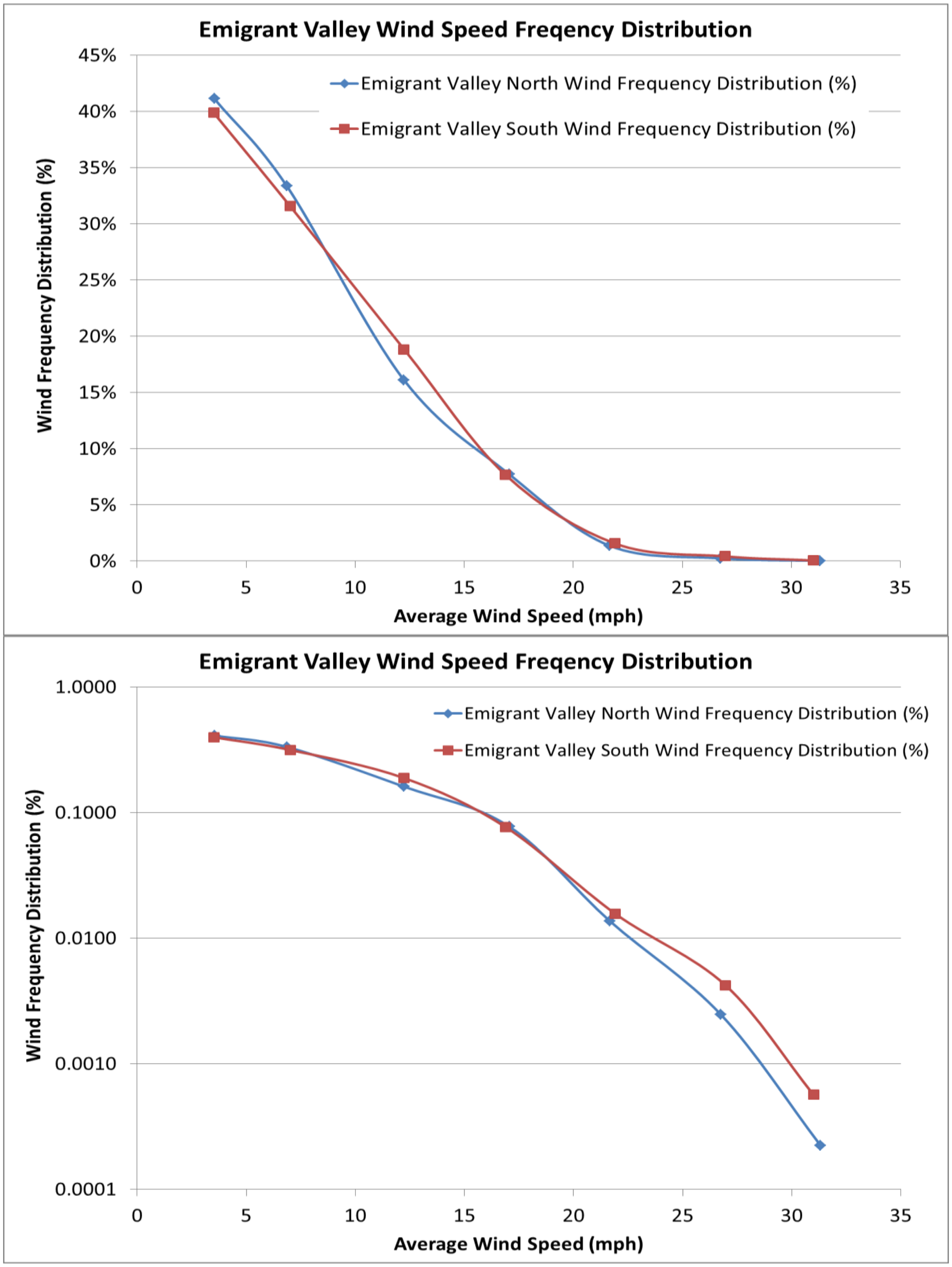

Figure 10. Wind speed frequency by wind class for Project 57 monitoring stations during the period of January 2016 through December 2016. A logarithmic scale is used on the y-axis in the lower graph to give a better sense of the dynamic range and low frequency of high winds. The north station is P57-3; the south station is P57-4.

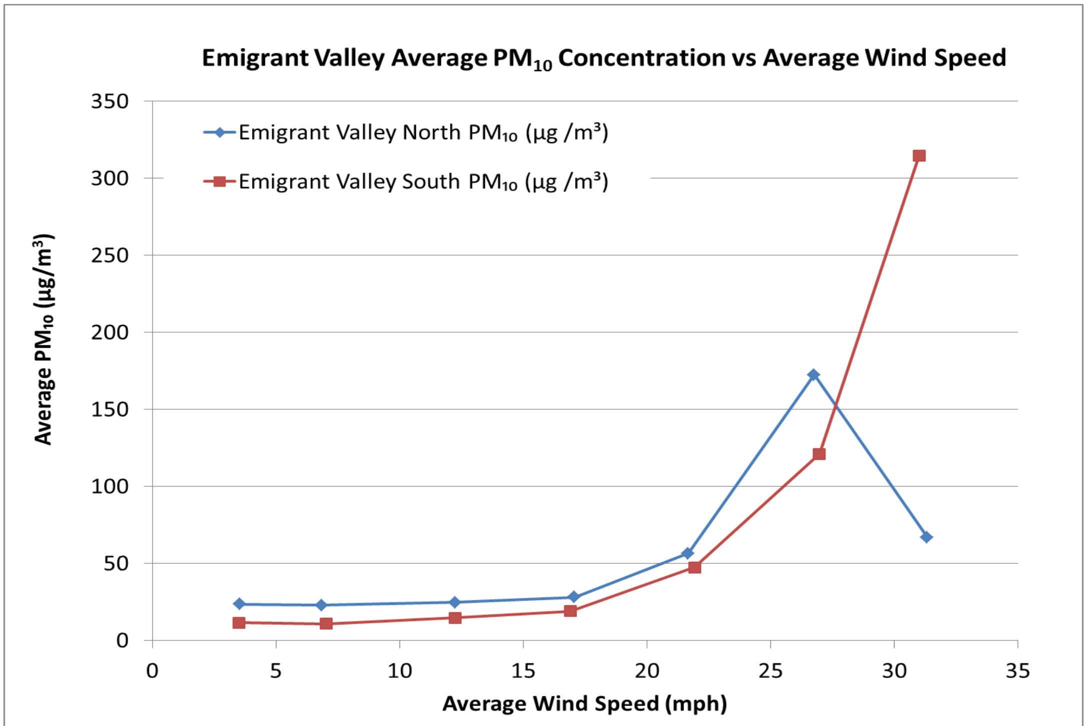

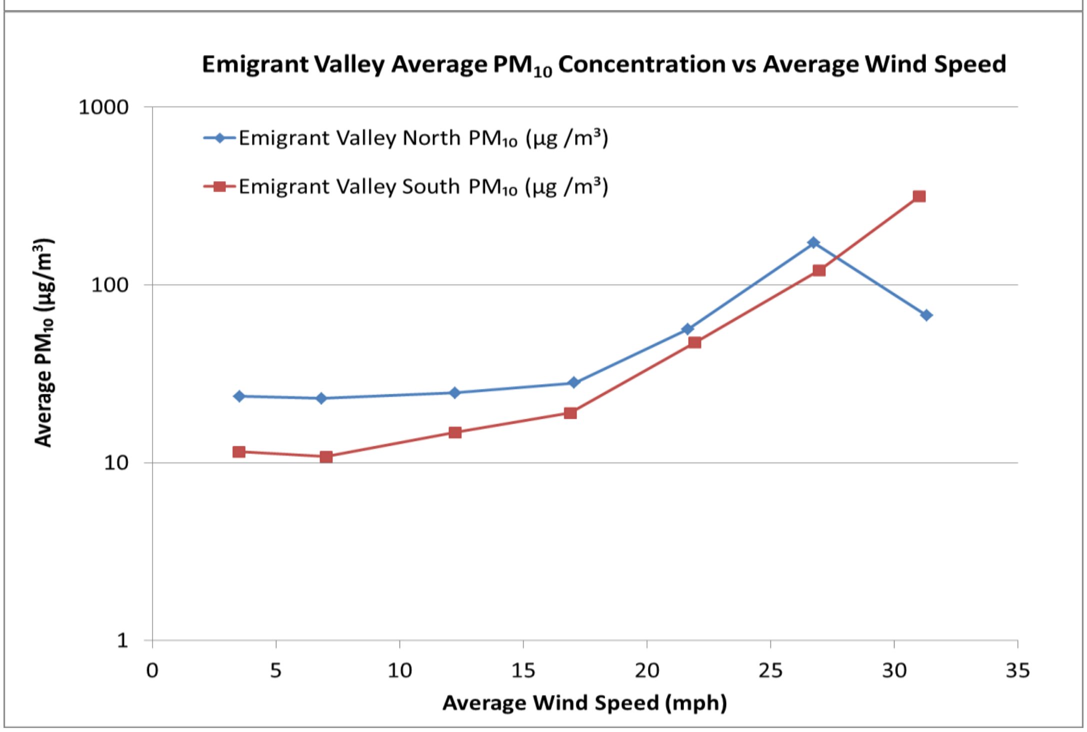

Figure 11. PM_{10} trends as a function of wind speed for P57-3 (north) and P57-4 (south). A logarithmic y-axis is used in the lower graph to illustrate the wide dynamic range of PM_{10} concentrations. Note that PM_{10} data are available for P57-3 from July 18, 2016, through December 31, 2016.

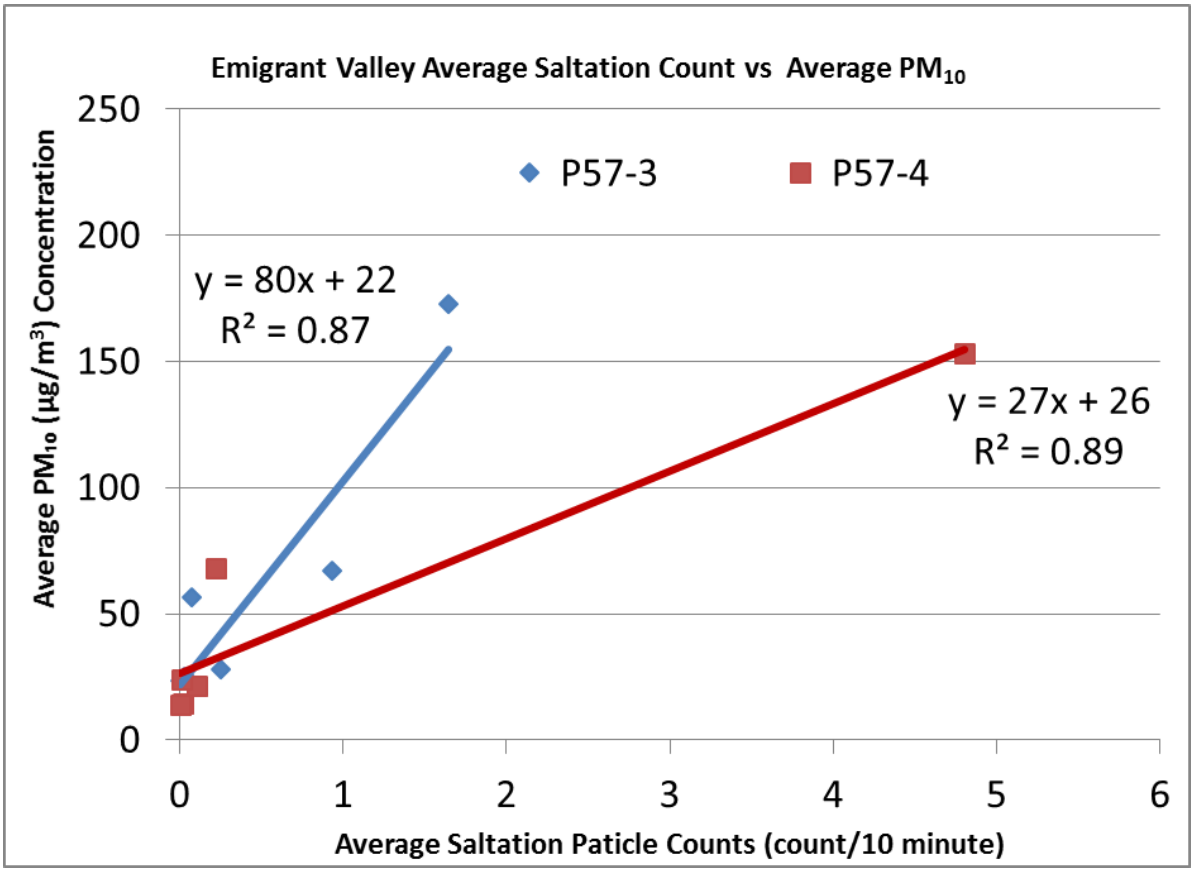

Figure 12. Regression of 2016 PM_{10} concentration and saltation counts for wind speed class shows a linear relationship that is controlled by the values observed for the highest wind speeds. Note P57-3 is the north station and P57-4 is the south station.

Comparison of PM_{10} Concentrtions During the Predominant Northerly and Southerly Winds

Figure 7 shows that winds over 15 mph (24 km/hr) were predominantly from the northwest to northeast and from the south to southwest. Because there are two major wind directions, it is important to determine if one direction or the other is likely to produce more dust transport. Table 8 summarizes the wind frequency and average PM_{10} concentration for all wind directions, for northwest-to-northeast winds, and for south-to-southwest winds at P57-3. However, because the Met One™ was not operating during the first half of the year, the data in Table 8 reflect only the period of July 18, 2016, through December 31, 2016. Table 9 provides similar data for the entire year at P57-4. Figure 13 provides a visual summary of the relationship between average wind speed and PM_{10} dust concentrations for the average and dominant wind directions at each of the monitoring stations. Because the dust data from the P57-3 and P57-4 monitoring stations represent different periods of the year, it is not appropriate to make direct comparisons between them. However, some general observations can be drawn. In 2016, dust concentrations during south-to-southwest winds were higher than concentrations during northwest-to-northeast winds. This is a reversal of conditions observed in 2015 when the larger dust concentrations were associated with winds from the northwest to northeast. This reversal appears to be because the PM_{10} dust concentrations associated with the northwest to northeast winds were lower in 2016 than in 2015 although north winds were of similar magnitude during both years.

Table 8. Summary of wind and PM_{10} data for all winds and for the two predominant wind directions at station P57-3. Note that PM_{10} data for P57-3 were not available for the period of January 1, 2016, through July 18, 2016.

Wind Speed Class (mph)	Duration (hours)	Frequency (%)	Cumulative Frequency (%)	Average Wind Speed (mph)	PM_{10} (µg/m^3)
P57-3 All Winds					
0 – 5	1530.50	41.144	41.144	3.54	23.65
5 – 10	1241.50	33.375	74.519	6.86	22.98
10 – 15	599.00	16.103	90.622	12.24	24.71
15 – 20	287.83	7.738	98.360	17.06	28.11
20 – 25	51.00	1.371	99.731	21.66	56.44
25 – 30	9.17	0.246	99.978	26.76	172.54
30 – 35	0.83	0.022	100.000	31.32	67.09
Total	3719.83	--	--	--	--
P57-3 Northwest-to-northeast Winds					
0 – 5	823.00	43.112	43.112	3.73	28.58
5 – 10	676.33	35.429	78.540	6.63	23.11
10 – 15	272.83	14.292	92.832	12.19	8.97
15 – 20	115.33	6.042	98.874	17.11	20.72
20 – 25	19.83	1.039	99.913	21.26	37.66
25 – 30	1.67	0.087	100.000	26.95	218.05
30 – 35	--	--	--	--	--
Total	1909.00	--	--	--	--
P57-3 South-to-southwest Winds					
0 – 5	264.00	24.796	24.796	3.36	17.69
5 – 10	317.17	29.790	54.587	7.38	27.09
10 – 15	276.83	26.002	80.589	12.40	42.39
15 – 20	168.33	15.811	96.399	17.02	32.32
20 – 25	30.00	2.818	99.217	21.89	67.49
25 – 30	7.50	0.704	99.922	26.71	162.43
30 – 35	0.83	0.078	100.000	31.32	67.09
Total	1064.67	--	--	--	--

Table 9. Summary of wind and PM_{10} data for all winds and for the two predominant wind directions at station P57-4.

Wind Speed Class (mph)	Duration (hours)	Frequency (%)	Cumulative Frequency (%)	Average Wind Speed (mph)	PM_{10} (μg/m^3)
		P57-4 All Winds			
0 – 5	3,407.83	39.886	39.886	3.53	11.50
5 – 10	2,696.33	31.559	71.445	7.03	10.80
10 – 15	1,609.83	18.842	90.287	12.26	14.81
15 – 20	655.33	7.670	97.958	16.96	19.04
20 – 25	133.67	1.564	99.522	21.60	47.41
25 – 30	36.00	0.421	99.943	26.87	121.06
30 – 35	4.83	0.057	100.000	30.84	314.69
Total	8543.83	--	--	--	--
		P57-4 Northwest-to-northeast Winds			
0 – 5	1927.50	40.494	40.494	3.69	11.94
5 – 10	1560.00	32.773	73.267	6.90	8.11
10 – 15	856.17	17.987	91.254	12.22	6.10
15 – 20	335.83	7.055	98.309	16.86	12.11
20 – 25	63.50	1.334	99.643	21.84	30.36
25 – 30	17.00	0.357	100.000	26.74	71.37
30 – 35	--	--	--	--	--
Total	4760.00	--	--	--	--
		P57-4 South-to-southwest Winds			
0 – 5	544.83	23.457	23.457	3.51	12.15
5 – 10	724.00	31.171	54.628	7.31	16.21
10 – 15	661.00	28.459	83.087	12.31	26.85
15 – 20	302.00	13.002	96.089	16.99	25.71
20 – 25	67.00	2.885	98.974	21.57	60.55
25 – 30	19.00	0.818	99.792	27.60	165.52
30 – 35	4.83	0.208	100.000	30.32	314.69
Total	2322.67	--	--	--	--

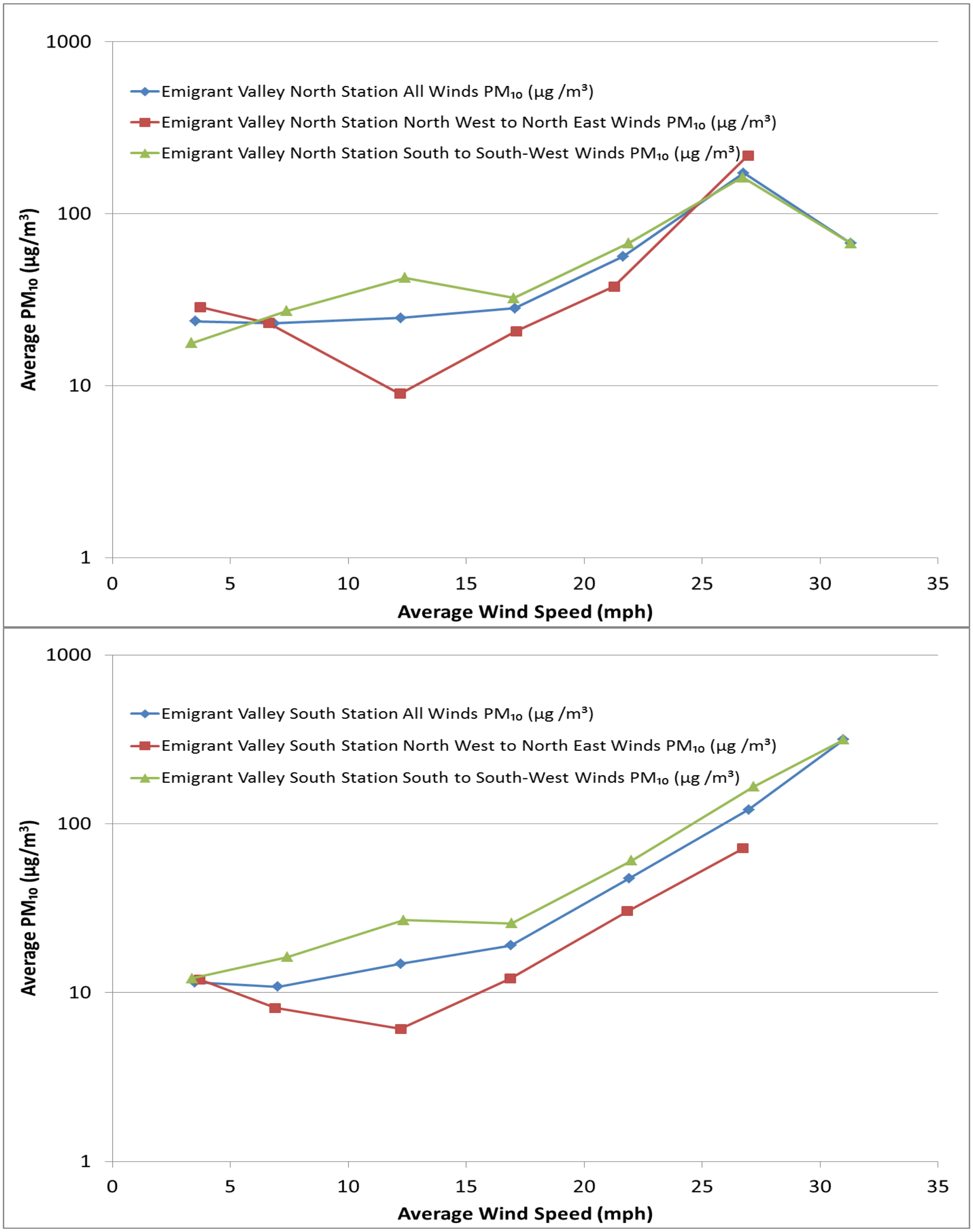

Figure 13. Average PM_{10} concentrations for 5 mph (8 km/hr) wind speed intervals at P57-3 (the north station, top) and P57-4 (the south station, bottom) for winds from all directions and for winds from the two predominant wind directions. Note that dust concentration data at P57-3 were only collected between July 18, 2016, and December 31, 2016.

Dust Source Proximity Analysis

Wind is the driving mechanism for transport of dust, soil, and potentially contaminated material, but the difficulty in data analysis is to decouple and identify dust generated locally from the Project 57 site versus dust transport from the surrounding areas that exhibit the same or similar dust emission potential. Native, undistributed desert areas in the arid southwest U.S. are well-known to emit dust under strong winds. The ratio of PM_{10} to $PM_{2.5}$ concentrations is used to determine the dust contribution between near and far sources at the Project 57 monitoring stations. The smaller size $PM_{2.5}$ particles have a considerably lower settling velocity. Therefore, they have a longer residence time in the atmosphere, which results in longer transport distances. Under normal atmospheric conditions, the PM_{10} concentration is four to eight times higher than the $PM_{2.5}$ concentration. However, this ratio can be exceeded when there are local resuspension sources and windy conditions. The ratio between PM_{10} and $PM_{2.5}$ can be used to make a qualitative assessment of near versus far dust sources relative to the observation location. Higher PM_{10} to $PM_{2.5}$ ratios indicate aerosol closer to the source area.

The $PM_{2.5}$ concentration as a function of average wind speed class is shown in Figure 14 and exhibits a trend similar to the trend of PM_{10} concentration shown in Figure 11. Figure 15 shows the ratio between PM_{10} and $PM_{2.5}$ for increasing wind speed classes. The $PM_{2.5}$ mass concentrations at both P57-3 and P57-4 are approximately four to seven times less than the PM_{10} concentrations for winds below 20 mph (32 km/hr). As wind speeds increase from 20 mph to 35 mph, the ratio of the PM_{10} to $PM_{2.5}$ increases to nine or ten. The increase in the ratio of PM_{10} to $PM_{2.5}$ as wind speeds exceed 20 mph (32 km/hr) corresponds closely to the increase in saltation counts as wind speeds exceed 20 mph (32 km/hr) to 25 mph (40 km/hr) (Table 6, Figure 9). When soil particles moving by saltation bounce across the soil surface, they dislodge other soil particles resulting in a significant increase in both $PM_{2.5}$ and PM_{10} concentrations. The increase in PM_{10} is greater than the increase in $PM_{2.5}$, which suggests that these stronger winds are raising dust from the local area. The offset between the two curves is because of the slight difference in how Met One™ instruments are calibrated and the differences in the time period when the Met One™ profilers were operating at the two stations.

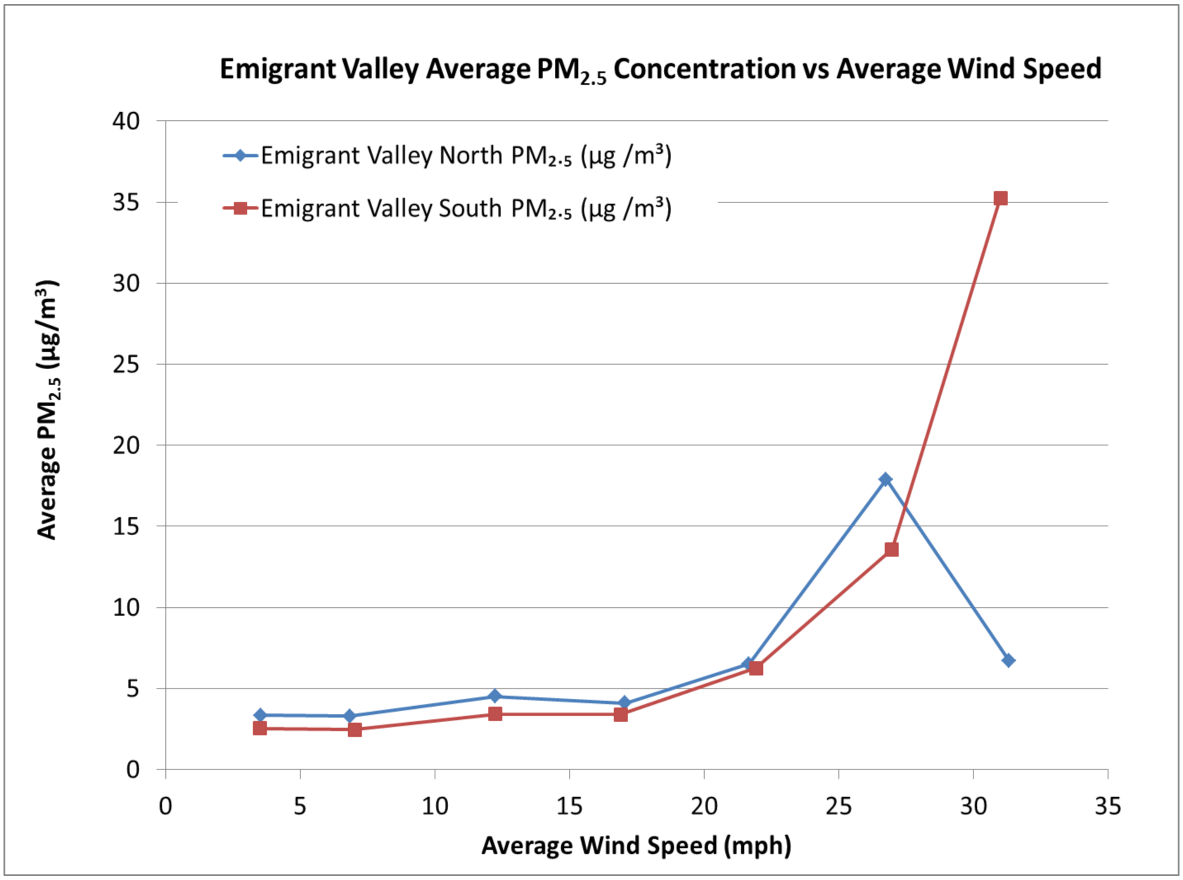

Figure 14. $PM_{2.5}$ trends as a function of wind speed for the P57-3 (north station) and P57-4 (south station) monitoring stations at Project 57 for CY2016.

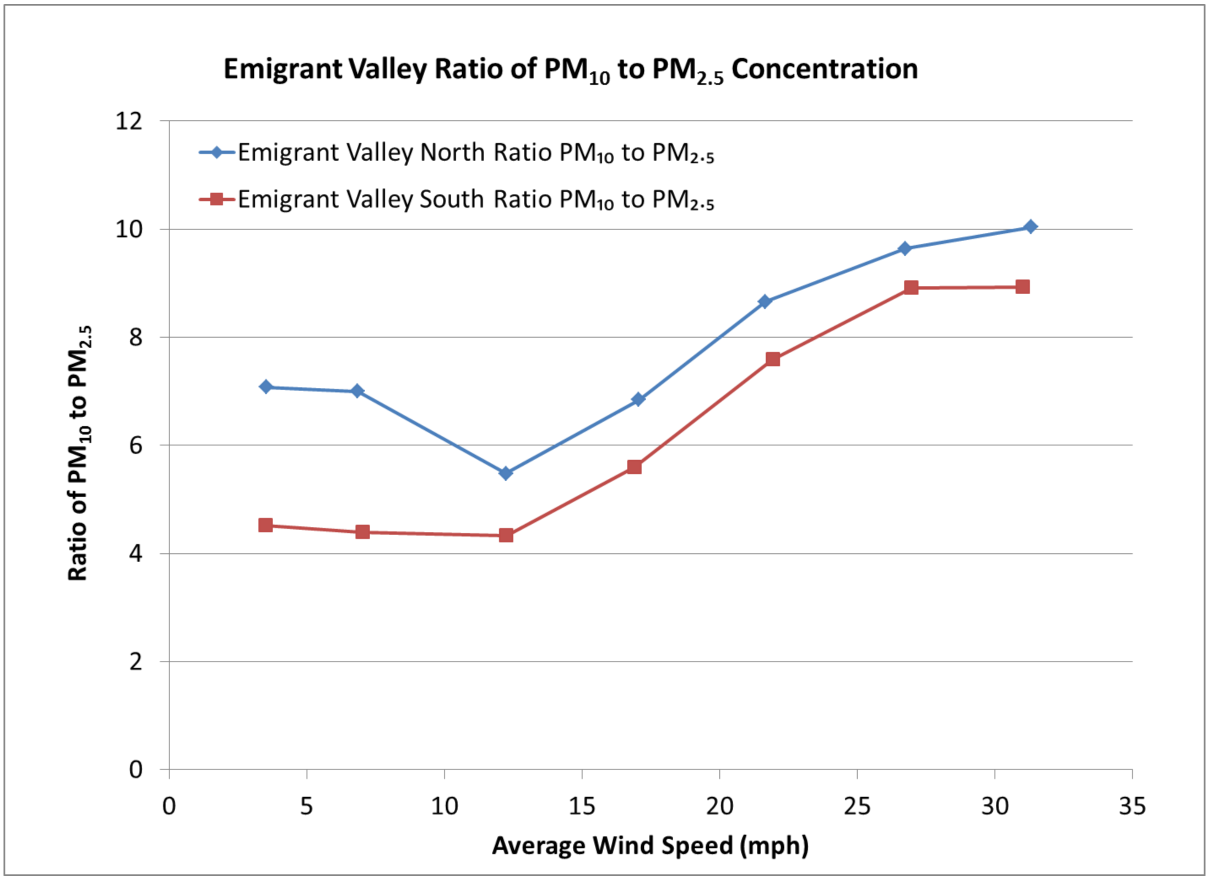

Figure 15. Ratio of PM_{10} to $PM_{2.5}$ trends as a function of wind speed for Project 57 monitoring stations P57-3 (north stattion) and P57-4 (south station) for CY2016.

MAJOR SUSPENSION AND SALTATION DUST TRANSPORT EPISODES

Most dust transport occurs during high-wind events that are usually short in duration. During CY2016, eight significant wind/dust events were identified based on elevated PM_{10} concentrations. Table 10 summarizes the wind and dust conditions associated with these notable wind episodes. Appendix Figures E-1 through E-8 show the wind speed and PM_{10} concentration and saltation counts observed during these wind episodes. Four of the wind and dust events occurred during the summer season (March through August) and four occurred during the winter season (September through February). The strongest winds usually occur in the spring (between March and May), but during 2016, winds were also fairly strong throughout the summer, which resulted in significant transport during the middle and later parts of the year. The number of summer dust transport events appears to result from very low soil moisture and low humidity, which permitted dust that had not been incorporated in the soil crust to be resuspended and transported. Overall, PM_{10} concentrations and saltation counts during 2016 were lower than in 2015 (Mizell *et al.*, 2017), which were most likely because of more frequent light rains that provided some soil moisture but did not cause significant soil crust disturbance.

Table 10. Description of wind and dust conditions during selected high-wind episodes observed during CY2016.

Date	Wind Speed (mph)	Wind Direction	PM_{10} (µg/m^3)	Saltation (#/10 min)	Figure	Comments
Apr 22, 2016	15 to 48	Southeast	560	0	E-1	Average 10-minute wind speed was near 30 mph for approximately 6 hours. Peak 10-minute wind speeds were above 30 mph for approximately 11.5 hours. Maximum gust during storm was 48.5 mph. PM_{10} concentration was above 100 µg/m^3 throughout the storm and peaked at approximately 556 µg/m^3. No saltation activity indicates the dust source was not local.
May 20, 2016	15 to 50	Southwest	280	0	E-2	Average 10-minute wind speed increased steadily from 15 mph to 31 mph between 0700h and 1300h. Peak 10-minute wind speed, 49.5 mph, was recorded at approximately 1320h. Maximum PM_{10} concentrations 286 µg/m^3 was recorded at time of peak wind gust. PM_{10} decreased sharply wind speed declined after 1330h. The high wind speeds generated only moderate PM_{10} concentrations indicating a dust supply limitation perhaps the result of light rain events early in the month.
June 28, 2016	15 to 37	Not available	780	0	E-3	Average 10-minute wind speeds were between 15 mph and 25 mph. Peak 10-minute wind speeds were between 15 mph and 37 mph. The PM_{10} dust event lasted approximately 30 minutes during which dust concentration went from 75 µg/m^3 to 1208 µg/m^3. The lack of saltation dust indicates that little, if any, local dust is transported. This pattern is common during the summer when air and soil are dry and there is a buildup of dust deposition on the ground and plants. This dust deposit is easily removed after the wind speed threshold for transport is exceeded.
July 30, 2016	15 to 34	South and southwest	1200	0	E-4	Average 10-minute wind speeds were less than 15 mph throughout the dust event. Peak 10-minute wind speeds ranged from 15 mph to 25 mph during the majority of the dust event and peaked at 34 mph later. PM_{10} concentration peaked at approximately 1200 µg/m^3 at approximately 1000h during average 10-minute wind speeds of approximately 15 mph and peak 10-minute wind speeds of 20 mph to 25 mph. the dust concentration remained high for several hours under relatively light winds.

Table 10. Description of wind and dust conditions during selected high-wind episodes observed during the reporting period (continued).

Date	Wind Speed (mph)	Wind Direction	PM_{10} ($\mu g/m^3$)	Saltation (#/10 min)	Figure	Comments
Sept 13, 2016	15 to 42	Southwest	472	0	E-5	Average 10-minute wind speed increased rapidly from approximately 10 mph to 21 mph; it remained above 20 mph for approximately 3 hours and 25 minutes. Peak 10-minute winds rose quickly to more than 30 mph and remained near 30 mph for approximately 3.5 hours. The PM_{10} dust peaked at 472 $\mu g/m^3$ event and remained elevated for approximately 1 hr. The short duration of high dust concentrations suggests that the available dust supply was limited.
October 30, 2016	15 to 45	Southeast to southwest	104	65	E-6	Average 10-minute wind speeds ranged from 15 mph to 29 mph and remained above 20 mph from 0915h to 1615h. Peak 10-minute wind speeds ranged from 15 mph to 45 mph and remained above 30 mph from 0915h to 1615h. PM_{10} began to rise as average wind speeds exceeded 15 mph and remained above 50 $\mu g/m^3$ for approximately 1.5 hours. Saltation particle counts rose in conjunction with the maximum observed wind speed. The maximum saltation count and maximum PM_{10} concentration occurred concurrently with the maximum average 10-minute and peak 10-minute wind speeds. Fluctuations in dust PM_{10} and saltation counts were dictated by changes in wind speed demonstrating locally sourced dust material. This dust event is notable for the saltation particle counts in conjunction with low PM_{10} concentration. Light rain on October 29 may have caused the fine dust particles to hold together resulting in movement by saltation rather than suspension.
Nov 8, 2016	15 to 19	Not available	341	16	E-7	Average 10-minute wind speed consistent at approximately 12 mph for approximately 4.5 hours. Peak 10-minute wind speeds were approximately consistent at approximately 17 mph for approximately the same time period. At 1300h, there was a 20 minute spike in saltation particle counts and in PM_{10} concentration; the PM_{10} concentration peaked at 341 $\mu g/m^3$.
Nov 16, 2016	15 to 38	Southwest shifting to northwest	412	0	E-8	Average 10-minute wind speeds ranged between 15 mph and 25 mph. Peak 10-minute wind speeds ranged between 20 mph and 38 mph. PM_{10} concentration occurred in two spikes: 251 $\mu g/m^3$ at 1600h and 412 $\mu g/m^3$ at 1905h. PM_{10} peaks were associated with the change in wind direction. Strong winds earlier during the day may have weakened the soil crust allowing the afternoon wind in conjunction with the direction change to cause the PM_{10} concentration to rise.

RADIOLOGICAL ASSESSMENT OF AIRBORNE PARTICULATE MATTER

Airborne dust particles are collected using Hi-Q™ air samplers located at each of the monitoring stations. These collectors draw ambient air through a 4-in (10-cm) diameter, glass-fiber filter (pore size 0.3 µm [0.00001 in]) at a rate of 2 cubic feet per minute (cfm) (56.6 lpm). The collector is designed to maintain a constant flow rate as dust accumulates on the filter. The total volume of air passed through the filter and the total hours of operation are recorded when the filters are collected. The deployed filters are collected and replaced with new filters every two weeks. Filters are weighed before and after deployment to determine the mass of the particles collected. Filters are submitted to the Radiological Services Laboratory at the University of Nevada, Las Vegas, for gross alpha, gross beta, and gamma spectroscopy assessment. Additionally, selected filters are submitted to TestAmerica Laboratories, Inc., for alpha spectroscopy analysis.

During the operational period covered in this report, sample filters were deployed for approximately 14-day periods from December 22, 2015, through December 20, 2016. At P57-3, a total of only 21 samples were collected because 5 samples were lost because of air sampler failures from June 21, 2016, to August 2, 2016, and September 12, 2016, to October 11, 2016. At P57-4, a total of 26 samples of airborne particulate matter were collected.

Gross Alpha, Gross Beta, and Gamma Spectroscopy Results

The gross alpha and gross beta observations for the reporting period are summarized in Tables 11 and 12, respectively. Table 13 gives the CY2016 gross alpha and gross beta concentrations reported for CEMP stations surrounding the northern ranges of the NTTR (NSTec, 2016). Sampling procedures at the Project 57 and CEMP stations are similar, which allow general comparisons to be made for the region.

Table 11. Gross alpha results for Project 57 sampling stations during CY2016.

Sampling Location	Number of Samples	Concentration (× 10^{-15} µCi/ml [3.7 × 10^{-5} Bq/m^3])			
		Mean	Standard Deviation	Minimum	Maximum
P57-3	21	2.10	1.12	0.35	5.25
P57-4	26	3.21	2.10	0.68	8.09

NOTES: Bq = Becquerel; m^3 = cubic meter; µCi/ml = microcurie per milliliter.

Table 12. Gross beta results for Project 57 sampling stations during CY2016.

Sampling Location	Number of Samples	Concentration (× 10^{-14} µCi/ml [3.7 ×10^{-4} Bq/m^3])			
		Mean	Standard Deviation	Minimum	Maximum
P57-3	22	1.72	0.66	1.02	3.96
P57-4	26	1.75	0.54	0.97	3.66

NOTES: Bq = Becquerel; m^3 = cubic meter; µCi/ml = microcurie per milliliter.

Table 13. Mean annual gross alpha and gross beta concentrations for CY2016 reported at CEMP stations that surround the Tonopah Test Range.

Sampling Location	Gross alpha (× 10^{-15} µCi/ml)			Gross beta (× 10^{-14} µCi/mL)		
	Mean	Minimum	Maximum	Mean	Minimum	Maximum
Alamo	1.80	0.73	3.97	2.02	1.13	3.53
Beatty	1.19	0.51	2.43	1.80	1.13	3.28
Goldfield	1.13	0.56	2.44	1.73	1.10	2.98
Rachel	1.23	0.38	2.84	2.03	1.09	3.99
Sarcobatus Flat	1.90	0.57	4.88	1.97	1.22	3.57
Tonopah	1.02	0.44	1.82	1.64	1.12	3.20

The mean gross alpha concentration at P57-3 was approximately 1.5 times the mean gross alpha concentrations at the surrounding CEMP stations. The P57-4 mean gross alpha concentration was approximately 2.3 times the mean gross alpha concentration values at the surrounding CEMP stations. Minimum gross alpha concentrations reported for the Project 57 stations (Table 11) were in the range of minimum values observed at the CEMP stations (Table 13). However, the maximum gross alpha concentrations detected at the Project 57 stations were greater than the maximum concentrations observed at the surrounding CEMP stations. This is especially significant at P57-4, where six individual sample values exceeded the maximum value observed (Table 13, Sarcobatus Flat) at the surrounding CEMP stations. These results suggest that the Project 57 monitoring stations may be detecting gross alpha concentrations that reflect environmental conditions that are different from the conditions that influence gross alpha values at the surrounding CEMP stations. This difference may be due to the plutonium contamination of surficial soil at the Project 57 site or the different geologic materials in the vicinity of the monitoring stations.

Mean gross beta concentrations at the Project 57 stations were within the range of mean gross beta values observed at the CEMP stations. The minimum gross beta concentrations values for both P57-3 and P57-4 were slightly lower than the minimum values observed at the CEMP station, whereas the maximum values lie in the upper half of the range of gross beta values observed at the CEMP stations. These results suggest that the Project 57 monitoring stations are detecting gross beta concentrations that reflect environmental conditions similar to conditions at the surrounding CEMP stations.

Environmental monitoring at the NNSS includes collecting airborne particulate matter samples at 16 stations for gross alpha and gross beta concentration analyses (NSTec, 2016). For 2015 (results of the 2016 samples are not yet available), the mean annual gross alpha concentration values range from 1.96 × 10^{-15} µCi/ml to 3.19 × 10^{-15} µCi/ml and average 2.57 × 10^{-15} µCi/ml, and the mean annual gross beta concentration values range from 1.96 × 10^{-14} µCi/ml to 2.33 × 10^{-14} µCi/ml and average 2.15 × 10^{-14} µCi/ml (NSTec, 2016). The mean gross alpha concentration value for P57-3 was in the low end of values observed at the NNSS stations. The P57-4 value was at the high end of values observed at the NNSS stations. The mean gross beta concentration values for the both Project 57 stations are below the range of values observed for the 2015 NNSS samples. This comparison suggests that the gross alpha and gross beta observations from the Project 57 monitoring stations represent conditions similar to conditions that influence these measurements at the NNSS stations.

The naturally occurring radionuclides, beryllium-7 (Be-7), lead-210 (Pb-210), and potassium-40 (K-40) were detected in the particulate matter samples with varying frequency using gamma spectroscopy analyses (Table 14). Americium-241 was not detected by gamma spectroscopy in 2016 (as mentioned in the following section, it was detected in a sample from P57-4 during 2015). Americium-241 is an anthropogenic radionuclide that is not naturally occurring, and therefore may indicate the presence of Pu-241, which is a minor yet easily detected component of the material used for the Project 57 plutonium dispersal tests. When Am-241 is detected in any concentration using gamma spectroscopy, the sampling protocol stipulates that the sample be analyzed for Pu-238 and Pu-239/240.

Table 14. Gamma spectroscopy analyses of the airborne particle samples collected during CY2016 detected three radionuclides. All detected radionuclides are naturally occurring. The frequency of detection varied by radionuclide and location.

Radionuclide	**Number of samples showing detectable concentrations**	
	P57-3	**P57-4**
Beryllium (Be-7)	21	26
Lead-210 (Pb-210)	5	9
Potassium-40 (K-40)	4	0
Americium-241 (Am-241)	0	0

Alpha Spectrometry Results

During 2016, alpha spectroscopy analyses were performed to investigate the variation in ambient concentrations of the plutonium isotopes. Two sampling filters from each monitoring station were selected for each quarter of CY2015 and CY2016 and submitted to TestAmerica Laboratories, Inc. These quarterly samples included the sample with the highest gross alpha result plus one randomly selected sample from each of the Project 57 monitoring stations, resulting in a total of eight samples per station for each year.

Table 15 summarizes the results of the alpha spectroscopy analyses for plutonium-238 (Pu-238) and plutonium-239/240 (Pu-239/240) for CY2015. Plutonium-238 was detected only at station P57-4. Plutonium-239/240 was detected at both monitoring stations. The maximum value for Pu-238 at P57-4 was reported for a sample collected between April 13, 2015, and April 15, 2015; the short collection period was implemented to collect a sample associated with an observed dust storm (Mizell *et al.*, 2017). The maximum value for Pu-239/240 at P57-4 was determined on a sample retrieved on June 23, 2015. This sample produced an Am-241 detection during the gamma spectroscopy analysis and may have been associated with the passage of a dust devil (Mizell *et al.*, 2017).

Table 16 summarizes the results of alpha spectroscopy analysis for Pu-238 and Pu-239/240 for 2016. Plutonium-238 was not detected at either station P-57-3 or P-57-4. Plutonium-239/240 was only detected at station P-57-4.

Table 15. Project 57 alpha spectroscopy results for stations P-57-3 and P-57-4 for samples collected in 2015.

Location	Concentration (x10^{-16} µCi/ml [3.7 x 10^{-6} Bq/m^3])							
	Pu-238				Pu-239/240			
	Samples >MDC	Mean	Min	Max	Samples >MDC	Mean	Min	Max
P57-3	0	N/A	N/A	N/A	3	5.76 ± 8.61	0.56	15.70
P57-4	3	3.10 ±3.94	0.73	7.65	9	53.37 ±108.9	1.04	339.0

N/A = not applicable, no samples >MDC
MDC = minimum detectable concentration;
MDC Pu-238 = 0.68 ± 0.15 µCi/ml x 10^{-16}; MDC Pu-239/240 = 0.40 ± 0.15 µCi/ml x 10^{-16}

Table 16. Project 57 alpha spectroscopy results for stations P-57-3 and P-57-4 for samples collected in 2016.

Location	Concentration (x10^{-16} µCi/ml [3.7 x 10^{-6} Bq/m^3])							
	Pu-238				Pu-239/240			
	Samples >MDC	Mean	Min	Max	Samples >MDC	Mean	Min	Max
P57-3	0	N/A	N/A	N/A	0	N/A	N/A	N/A
P57-4	0	N/A	N/A	N/A	6	24.6 ±20.96	4.75	51.0

N/A = not applicable, no samples >MDC
MDC = minimum detectable concentration;
MDC Pu-238 = 4.92 ± 1.06 µCi/ml x 10^{-16}; MDC Pu-239/240 = 2.61 ± 0.73 µCi/ml x 10^{-16}

Thermoluminesence Detector Results

Two TLDs are deployed at each of the Project 57 monitoring stations to determine the radiation exposure external dose, whether from natural environmental sources or radiation transported from the Project 57 CA. The TLDs are collected and replaced quarterly. Tables 17 and 18 give the observed quarterly exposure external dose and the estimated equivalent annual external dose at the Project 57 monitoring stations. The estimated annual external doses at the P57-3 and P57-4 monitoring stations are 153.1 millirem (mR) and 157.6 mR, respectively. The millirem (0.001 rem) is a measure of the dose equivalence pertaining to the human body and takes into account both the absorbed energy and the biological effect on the body because of the different types of radiation.

Table 17. Annual radiological dose rate estimated from TLDs deployed at the P57-3 monitoring station.

Fiscal Year	Quarter	Days Deployed	Observed Dose (mR)	Estimated Daily External Dose (mR)	Estimated Annual External Dose (mR)
2016	1	91	39	0.4286	153.1
			45	0.4945	
	2	92	33	0.3587	
			35	0.3804	
	3	90	38	0.4222	
			38	0.4222	
	4	91	40	0.4286	
			39	0.4176	

Table 18. Annual radiological dose rate estimated from TLDs deployed at the P57-4 monitoring station.

Fiscal Year	Quarter	Days Deployed	Observed Dose (mR)	Estimated Daily External Dose (mR)	Estimated Annual External Dose (mR)
2016	1	91	41	0.4505	157.6
			40	0.4396	
	2	92	36	0.3914	
			35	0.3804	
	3	90	40	0.4444	
			40	0.4444	
	4	91	42	0.4505	
			42	0.4505	

People are constantly exposed to radiation emitted by both natural environment and anthropogenic sources. Natural environmental sources include cosmic radiation, radiation emitted by the soil and geology of the Earth's surface, radiation ingested in food and water, and radiation from radon gas. The magnitude of natural radiation exposure varies from place to place, primarily because of differences in local geology and elevation. The general public is also exposed to anthropogenic sources of radiation associated with tobacco products, medical services, and consumer goods. The average annual radiation dose to the general public is estimated to be 620 mR (NRC, 2011), half of which is from natural sources and half of which is from anthropogenic sources (NRC, 2011). At the Project 57 monitoring stations, exposure to natural sources of radiation and any radiation transported from the CA is significantly less than (approximately half) the average annual dose experienced by the general public because of exposure to natural sources.

The estimated annual radiation doses at the Project 57 monitoring stations (153.1 mR and 157.6 mR, respectively; Tables 17 and 18) are slightly greater than the dose amounts reported for the CEMP stations surrounding the NTTR, which range from 116 mR at Alamo to 145 mR at Beatty, NV (Table 19). These differences are likely because of differences in local geology and elevation.

Table 19. Estimated annual radiological dose (mR) determined from TLDs deployed at CEMP stations surrounding the NTTR.

Station	CY2014	CY2015	CY2016
Alamo	119	119	116
Beatty	147	150	145
Goldfield	127	130	130
Rachel	134	131	126
Sarcobatus Flat	144	143	138
Tonopah	137	140	136

CY2016 SALTATION SAMPLE ANALYSES AND OBSERVATIONS

The BSNE saltation traps were installed at Project 57 to provide integrated mass samples of material transported by saltation in association with the dominant wind directions. Saltation is the mechanism by which soil particles in the range of 50 µm (0.002 in) to 500 µm (0.02 in) are transported. These particles are dislodged and carried a small distance in the air before falling to the ground. Their transport paths usually follow a parabolic trajectory, so the particles essentially bounce across the ground surface. The amount of time the particles are in the air and the distances they travel are functions of wind speed and particle mass. Saltation is important because the impact of saltated particles may push particles that creep or roll across the ground surface and may dislodge and eject smaller particles into the air where they may be transported as suspended material.

The saltation traps are deployed in pairs that are oriented to collect material transported by the predominant winds blowing across the CA and by winds coming from the opposing direction (Figure 16). This collection orientation facilitates estimates of the net flux of soil material transported to and from the CA by saltation. The design and installation of the BSNE samplers is described in the section titled Monitoring Station Locations and Capabilities. The original six BSNE saltation sand traps were installed at both monitoring stations P57-1 and P57-2 on April 14, 2014. Clean traps were deployed at P57-3 and P57-4 on March 3, 2015, shortly after these new stations were established. Saltation traps at P57-3 and P57-4 have been collected and replaced three times. The layout of saltation traps and the dates of deployment and collection are described in Appendix D. Results of particle size and radiological analyses of material collected in the traps deployed between January 4, 2016, and October 13, 2016, are presented below.

Figure 16. Typical installation of BSNE saltation traps. Photos for the Project 57 installations are not available, but this photograph taken at Clean Slate III (monitoring station 401) shows the type of installations used at Project 57. The BSNE saltation trap in the foreground is oriented with one opening facing the dominant wind direction coming across the fenced site to the right, and one facing away from the fenced area.

After traps are removed from the field, material collected in the three traps facing the same direction at each monitoring station are combined into a single sample for laboratory analysis. This ensures enough material is available for particle size and radiological analyses and results in one downwind sample at each monitoring station that collects material transported by wind blowing across the CA and one upwind sample that collects material transported by wind blowing toward the CA. Nikolich *et al.* (2016) describes extracting the saltation samples from the traps. Both the particle size and radiological analyses for the samples deployed between January 4, 2016, and October 13, 2016, were performed by the Southwest Research Institute in San Antonio, Texas, under contract to Navarro, which is the environmental remediation contractor at the NNSS. The Southwest Research Institute separated each sample into three size fractions: >250 µm (0.0098 in), 63 µm (0.0025 in) to 250 µm (0.0098 in), and <63 µm (0.0025 in). The mass of each size fraction for each sample was determined. Each size fraction was submitted for alpha spectrometry analysis to determine the concentrations of Am-241, Pu-238, and Pu-239/240.

Observations of Saltation Sample Mass

Figure 17 and Table D-5 (Appendix D) show the mass of material of each particle size fraction for the samples collected on October 13, 2016. Also included in Appendix D are the results for the saltation sample collections made in March 3, 2015, and January 4, 2016; these results were presented in Mizell *et al.* (2017). The results from the October 13, 2016, collection are the focus of the following discussion.

The downwind samples at both stations produced the largest sample mass, 4.766 g (0.010 lbs) at P57-3 and 3.483 g (0.008 lbs) at P57-4. The total mass of the saltation samples collected from P57-3 on October 13, 2016, was approximately equivalent to the mass of sample material collected on March 3, 2015, but 70 percent to 80 percent less than the mass collected on January 4, 2016. At P57-4 all three saltation sample collections (March 3, 2015; January 4, 2016; and October 13, 2016) produced approximately the same sample mass (Appendix D). The increased sample mass in the January 4, 2016, sample from P57-3 may have been because of dry soil conditions and poor vegetation development during the sample collection period. In all four samples collected on October 13, 2016, the 63 µm (0.0025 in) to 250 µm (0.0098 in) size fraction contained significantly greater mass of material than either the smaller or larger size fractions.

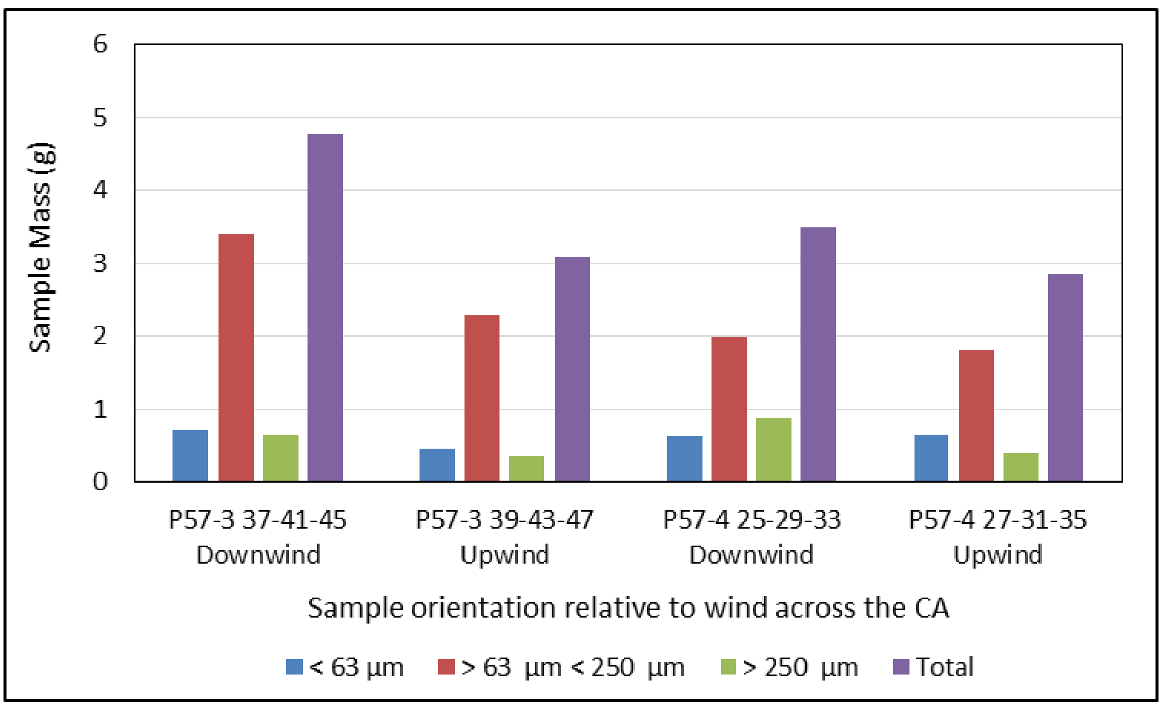

Figure 17. The 63 µm to 250 µm size fraction dominates the material collected in saltation traps deployed at the Project 57 monitoring stations between January 4, 2016, and October 13, 2016.

The total mass of the saltation samples from P57-3 was greater than the total mass of the saltation samples from P57-4. This is likely because a large area immediately west of station P57-3 consists of loose sandy soils that appear to have been disturbed at an unknown time in the past. Additionally, the vegetation in this area is not as large or dense as in other areas around the CA (Clifford, in review). This area of sandy soil and low vegetation density appears to extend to the southwest of P57-3, but the conditions have not been confirmed because the area southwest of P57-3 is inside the CA and not readily accessible. When saltation traps retrieved in October 2016 were analyzed, the traps oriented downwind of the CA collected greater sample mass than traps oriented upwind at both P57-3 and P57-4. The greater mass of saltation material has consistently been found in the downwind saltation samples at P57-4. But the saltation traps oriented downwind of the CA at P57-3 have not consistently collected the greatest mass of material (Figures 17, Tables D-1, D-3, and D-5).

Observations of Saltation Sample Radiological Analyses

Radionuclide results for the saltation samples are shown in Figure 18 and Table D-6. The Pu-238 result for the >250 µm (0.0098 in) size fraction in all four samples was below the minimum detectable activity (MDA). The Pu-238 result for the >63 µm (0.0025 in) to <250 µm (.00098 in) size fraction in the P57-4 upwind sample and the Am-241 result for the >250 µm (0.0098 in) size fraction were also below MDA. In each of the four samples, the <63 µm (0.0025 in) size fraction had the highest activity for each isotope with the exception of Pu-238 in the P57-3 upwind sample, which had a slightly higher activity level in the >63 µm (0.0025 in) to <250 µm (0.0098 in) size fraction. The difference between isotope activity levels in the upwind and downwind samples was inconsistent. The downwind sample for Am-241 at P57-4, Pu-238 at P57-3, and Pu-239/240 at P57-3 had higher activity levels than the associated upwind samples. However, the reverse was true for Am-241 at P57-3, Pu-238 at P57-4, and Pu-239/240 at P57-4, which had higher activity levels in the upwind samples.

Overall, these results from the October 13, 2016, samples are similar but not identical to results for the January 4, 2016, samples collected at the same monitoring stations (Mizell *et al.*, 2017). The <63 µm (0.0025 in) size fraction in the January 4, 2016, samples had higher activity levels than the two larger size fractions (Table D-4, Appendix D). The downwind samples collected on January 4, 2016, generally had higher activity levels than the upwind samples, but the results for the >63 µm (0.0025 in) to <250 µm (0.0098 in) size fraction at P57-3 were reversed.

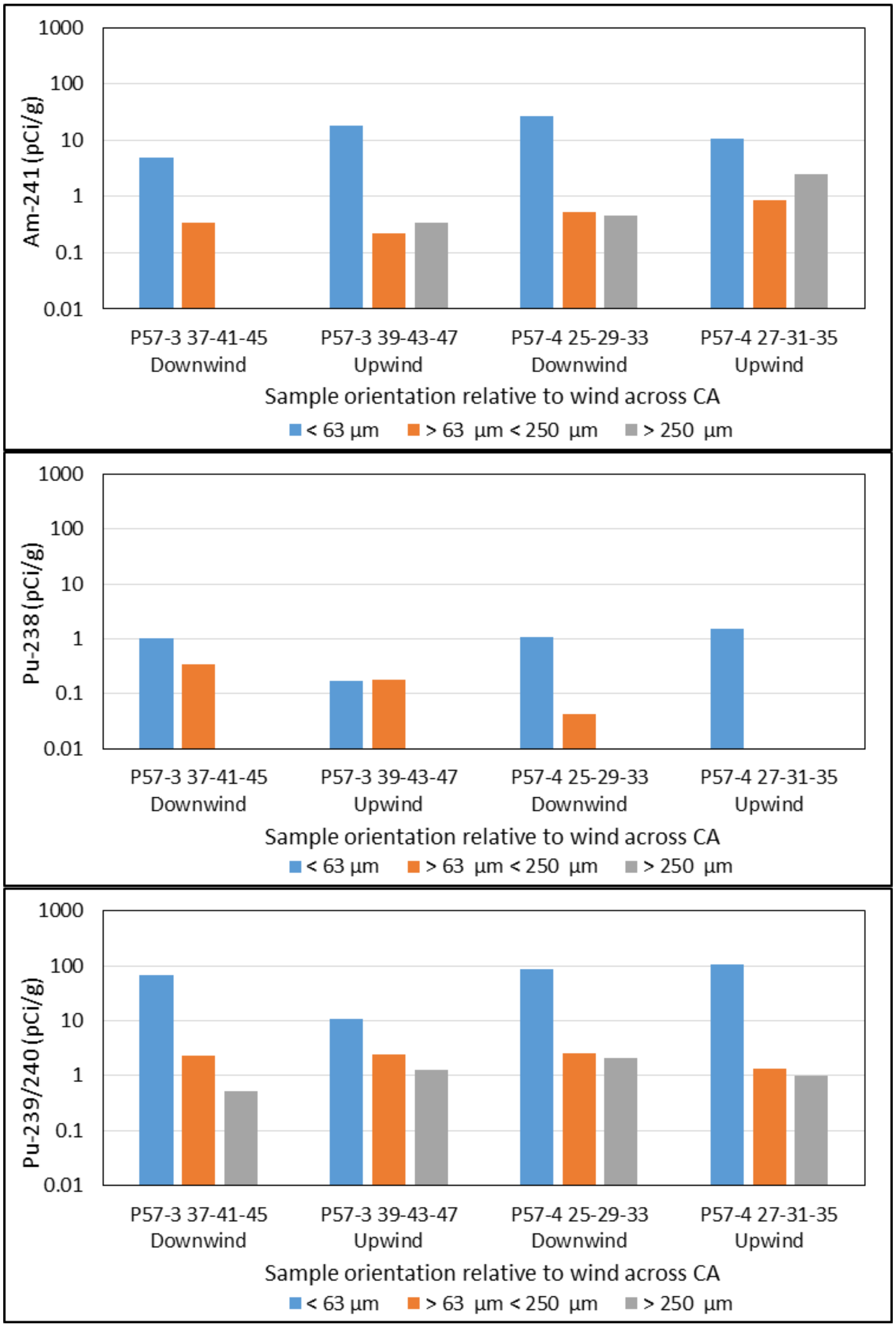

Figure 18. Am-241 (top), Pu-238 (middle), and Pu-239/240 (bottom) concentrations in saltation samples from Project 57 monitoring stations P57-3 and P57-4 collected on October 13, 2016. Note that the concentration is shown on a logarithmic scale.

In a comparison of the radionuclide concentrations in surface soils at off-site locations upwind and downwind of the NNSS, Turner *et al.* (2003) represented background using soil collected from an undisturbed alluvial fan near Searchlight, NV. The sample location was approximately 50 mi (80 km) south of Las Vegas, NV and 99 mi (160 km) southeast of the southern boundary of the NNSS. By analyzing the top 0.5 in (1.25 cm) of soil, Turner *et al.* (2003) determined that the background activities of Pu-238 and Pu-239/240 were 0.000405 pCi/g and 0.014056 pCi/g, respectively. The October 13, 2016, Project 57 saltation samples produced Pu-238 activity values that range between approximately 100 and 3,800 times this background concentration and Pu-239/240 activity values that are approximately 40 to 7,600 times the background concentration. This comparison suggests that soil material being redistributed by saltation at the Project 57 monitoring stations is contaminated.

DISCUSSION

Airborne dust collected at the monitoring stations was analyzed for gross alpha, gross beta, and gamma spectroscopy to determine if radiological contaminants were being transported from the Project 57 CA by wind. Some gross alpha and gross beta radioactivity is expected because of natural radioactivity associated with the geologic environment and cosmic radiation. Neither background nor baseline values representing gross alpha and gross beta conditions prior to the Project 57 safety experiment are available. The significance of gross alpha and gross beta concentrations for samples from Project 57 was determined by comparing them with values obtained from CEMP stations surrounding the northern ranges of the NTTR. Radiological data from the CEMP stations are assumed to represent areas in the region that are not influenced by surface soil contamination by plutonium distributed during safety tests of nuclear devices.

The mean gross alpha concentrations at P57-3 and P57-4 were approximately 1.5 times and approximately 2.3 times, respectively, the mean gross alpha concentrations at the surrounding CEMP stations. Minimum gross alpha concentrations reported for the Project 57 stations were in the range of minimum values observed at the CEMP stations. However, maximum gross alpha concentrations were greater than the maximum concentrations observed at the surrounding CEMP stations. These results suggest that the gross alpha concentrations associated with airborne particulate matter collected at the Project 57 monitoring stations are influenced by environmental conditions different from conditions that influence observations at the surrounding CEMP stations. The difference may result from differences in geologic materials in the area of each station and/or the influence of the Project 57 surface soil contamination. Mean gross beta concentrations at the Project 57 stations were within the range of mean gross beta values determined for the CEMP stations. Additionally, the range of gross beta concentrations for both P57-3 and P57-4 overlap the lower two-thirds of the range of values observed at the CEMP stations.

The gross alpha and gross beta values at Project 57 can also be compared with observations made on the NNSS during CY2015 (data for 2016 are not available). This comparison indicates that gross alpha concentrations observed at Project 57 fall within the range of values observed on the NNSS and that gross beta concentrations are below the range of values observed on the NNSS. This comparison also suggests that the gross alpha and gross beta observations from the Project 57 monitoring stations represent conditions that are similar to the conditions that influence these measurements at the NNSS.

Two samples were selected from the samples collected at each monitoring station each quarter in 2015 and 2016 for alpha spectrometery analysis. Three samples that were all collected in 2015 from P57-4 produced Pu-238 detections above the MDC. No sample collected in 2016 produced a Pu-238 detection. Pu-239/240 was detected in samples from both P57-3 and P57-4 during 2015, and from P57-4 in 2016.

Saltation samples were collected at P57-3 and P57-4 during 2016. The total mass of saltation material collected during southerly winds was 7.7 g and the total mass of saltation material collected during northerly winds was 6.6 g. This difference in mass suggests that southerly winds transported slightly more material by saltation than northerly winds. It also suggests that there may have been a net transport of saltation-size material from south to north during CY2016. However, the opposite was true in CY2015 (Mizell *et al.*, 2017), which indicates that the predominant direction of saltation transport depends on long-term average wind patterns. This contradiction indicates that short term sample collection is unlikely to include sufficient natural variability to fully characterize average saltation transport conditions.

Radiological analyses of the saltation samples show that the smaller particle size faction generally produced the highest activity levels of the Am-241, Pu-238, and Pu-239/241. In general, the isotope activity levels decreased as the particle size increased. These results support previous analyses that smaller particles have the greatest potential for transporting radiological contamination.

The CY2016 saltation data do not substantiate the expectation that higher isotope concentrations would be expected for winds blowing across the CA. The upwind and downwind samples produced high radionuclide concentrations with almost equal frequency for each particle size fraction. The difference between the radionuclide concentrations for upwind and downwind samples was small, which suggests that contaminated soil material may be moving back and forth over a limited area.

The radionuclide concentrations of saltation samples from Project 57 stations were significantly higher than those of soil samples identified as having background radionuclide concentrations by Turner *et al.* (2003). This indicates that the saltation samples include material transported from an area of contaminated soil. Comparing the Project 57 radionuclide concentrations with information on atmospheric fallout effects compiled and synthesized by Turner *et al.* (2003) shows that the Project 57 saltation samples reflect contamination by sources other than atmospheric fallout.

An analysis of the relationship between wind speed and saltation particle counts, $PM_{2.5}$ concentration, and PM_{10} concentration clearly indicates that dust concentration increases as wind speed increases. The wind/dust relationships show that dust concentrations remain generally low until wind speed exceeds 15 to 20 mph (24.1 to 32.2 km/hr) and that dust concentrations increase in conjunction with increasing wind speed. However, the wind observations also clearly show that the wind speeds needed to transport a significant amount of dust are infrequent and individual strong wind events are of short duration. Winds exceeding 20 mph (32.2 km/hr) occurred less than approximately three percent of the time.

Additionally, when winds at the P57-3 and P57-4 stations are separated into the dominant northerly and southerly patterns, the southerly winds produced the higher PM_{10} concentrations and tend to be the dominant influence on the overall average dust/wind relationship.

The combined results of the meteorological and particle monitoring at the Project 57 sites suggest that conditions for wind-borne contaminant migration exist but occur infrequently and for brief periods. It appears that radionuclide contaminants resulting from the Project 57 test may be transported by wind suspension and saltation but such transport occurs rather infrequently because the required wind conditions are rare.

CONCLUSIONS

The mean and maximum gross alpha concentrations at both stations P57-3 and P57-4 are higher than those for the surrounding CEMP stations. The mean gross beta concentrations at both Project 57 stations were in the range of concentrations determined for the surrounding CEMP stations. This comparison suggests that the Project 57 gross alpha observations reflect environmental conditions that are different from conditions surrounding the CEMP stations. These differences are likely to relate to the influence of contaminated soil at the Project 57 site and/or different geologic conditions.

Gamma spectrometry analyses of airborne particulate matter samples collected every other week at the Project 57 monitoring stations during CY2016 indicated only naturally occurring gamma-emitting radionuclides.

Alpha spectroscopy analysis of 16 selected suspended particulate matter samples produced three detections for Pu-238, which were all from P57-4. Pu-239/240 was reported in three samples from P57-3 in CY2015 and reported for most samples from P57-4 for both CY2015 and CY2016.

Observations of external radiation dose at the Project 57 monitoring stations indicate that the combined dose from natural sources and transport from the Project 57 CA was approximately half of the dose that the general public is expected to receive from natural sources alone. The external radiation dose exposure at the Project 57 monitoring stations is generally similar to that measured at surrounding CEMP stations.

Generally, saltation counts, PM_{10} concentrations, and $PM_{2.5}$ concentrations increase exponentially with increasing wind speed. The greatest increase in dust occurs for winds exceeding 20 mph (32.2 km/hr). When winds at the P57-3 and P57-4 stations were separated into the dominant northerly and southerly patterns, the southerly winds produced the higher PM_{10} concentrations and tend to be the dominant influence on the overall average dust/wind relationship.

Wind speeds exceed 15 mph (24.1 km/hr) approximately nine percent of the time and 20 mph (32.2 km/hr) approximately three percent of the time. Winds that were sufficient to generate significant dust were infrequent and generally of short duration. Therefore, significant dust events were also infrequent and short-lived. A preliminary review of the eight highest wind-speed events during the reporting period indicates that the PM_{10} concentration and the saltation count observations were highly variable.

The mass of saltation material collected in the southerly facing traps (downwind at P57-3 and upwind at P57-4) was slightly greater than the mass of material collected in the northerly facing traps. This suggests that although saltation material may be moving back and forth under the two dominant wind directions, there was a net trend for saltation material to be transported toward the north.

The concentrations of Am-241, Pu-238, and Pu-239/240 in saltation samples collected downwind of the Project 57 CA was similar to values determined for samples collected upwind of the CA. Additionally, the concentrations were sometimes greater in the upwind samples. This suggests that the opposing dominant wind directions are moving the saltation material back and forth in the vicinity of the saltation traps.

RECOMMENDATIONS

1. Size and radiological analyses of a representative sample of the soil material on the surface at each of the monitoring stations should be performed. This would facilitate characterization of the amount of PM_{10} and saltation material available at each site. This information would in turn be useful for interpreting the saltation and dust transport observations.
2. Establishing background/baseline conditions for the airborne particulate matter radionuclide concentrations is important for interpreting Project 57 data. Monitoring data from the surrounding CEMP stations are important for bracketing the results from the Project 57 monitoring stations. These locations should be evaluated to identify comparable and contrasting characteristics. There may also be information on uncontaminated soil sites at the NNSS that are comparable. Another alternative is to establish an additional monitoring/sample collection station near Project 57 that is environmentally similar but not subject to potential transport from the Project 57 CA. This site would provide control samples from an area that is presumably clean, which could be compared with samples collected adjacent to the CA.
3. Supplementing the BSNE saltation sand traps at P57-3 and P57-4 with additional traps farther downwind from the Project 57 ground zero point may provide radiological data that are useful for estimating the distance contaminated particles may be traveling.

REFERENCES

Clifford, M. J., in review. Vegetation assessment of the Project 57 air monitoring stations.

DeSilva, S., 2004. Extended Community: An Oral History of the Community Environmental Monitoring Program (CEMP), 1981 – 2003. Desert Research Institute report number 45209 prepared for the Nevada Field Office of the U.S. Department of Energy, pp. 467.

Friesen, H.N., 1992. Summary of the Nevada Applied Ecology Group and Correlative Programs. DOE/NV-357. Prepared for the U.S. Department of Energy, Nevada Operations Office. Las Vegas, NV.

HI-Q, 2016. -5624-WR Brushless, Automatic Flow Control DC Powered Low Volume Air Sampler for Continuous Use. HI-Q Environmental Products Co., San Diego, CA, p. 21.

Met One, 2007. Model 212 Profiler Operation Manual. Document No. 212-9800 Revision E. Met One Instruments, Inc. Grants Pass, OR, p. 23.

Misra, M., C. Neve, and A. Raichur, 1993. Characterization and Physical Separation of Radionuclides from Contaminated Soils. Proceedings of the Soil Decon ’93: Technology Targeting Radionuclides and Heavy Metals, Gatlinburg, TN, ORNL-6769, Oak Ridge National Laboratory, Oak Ridge, TN.

Mizell, S.A., G. Nikolich, G. McCurdy, C. Shadel, and J. Miller, 2016. Project 57 Air Monitoring Report: October 1, 2013 through December31, 2014. Desert Research Institute report number 45264 prepared for the Nevada field Office of the U.S. Department of Energy, p. 87.

Mizell, S.A., G. Nikolich, C. Shadel, G. McCurdy, and J.J. Miller, 2017. Project 57 Air Monitoring Report: January 1 through December 31, 2015. Desert Research Institute report number 45272 prepared for the Nevada Field Office of the U.S. Department of Energy, p. 114.

Murarik, T.M., T.K. Wenstrang, and L.A. Rogers, 1992. Characterization Studies and Indicated Remediation Methods for Plutonium Contaminated Soils at the Nevada Test Site. Spectrum 1992: Nuclear and Hazardous Waste Management, Boise, Idaho.

Nikolich, G., C. Shadel, J. Chapman, G. McCurdy, V. Etyemezian, J.J. Miller, and S Mizell, 2016. Tonopah Test Range Air Monitoring: CY2015 Meteorological, Radiological, and Airborne Particulate Observations. Desert Research Institute report number 45271 prepared for the Nevada Field Office of the U.S. Department of Energy, p. 95.

NRC, 2011. Fact Sheet: Biological Effects of Radiation. U.S. Nuclear Regulatory Commission, Office of Public Affairs, p. 4.

NSTec, 2011a. Nevada National Security Site Environmental Report 2010. DOE/NV/25946-1305, p. 298.

NSTec, 2011b. Nevada National Security Site Environmental Report 2010 Attachment A: Site Description. DOE/NV/25946-1305-ATT A, p. 80.

NSTec, 2016. Nevada National Security Site Environmental Report 2015. DOE/NV/25946-2950, p. 270.

Shreve, J.D., Jr., 1958. Operation Plumbbob Summary Report, Test Group 57. Extracted Version prepared by Sandia Corporation for Defense Nuclear Agency 4 June 1982, p. 85.

Tamura, T., 1985. Characterization of Plutonium in Surface Soils, Area 13 of the Nevada Test Site. *The Radioecology of Plutonium and Transuranics in Desert Environments*, HVO, 153, 1973.

Turner, M., M. Rudin, J. Cizdziel, and V. Hodge, 2003. Excess plutonium in soil near the Nevada Test Site, USA. Environmental Pollution 125, pp. 193-203.

APPENDIX A: METEOROLOGICAL OBSERVATIONS AT PROJECT 57 MONITORING STATIONS FOR THE REPORTING PERIOD (JANUARY 1, 2016, THROUGH DECEMBER 31, 2016)

Definitions

10-minute average = average of 200 instantaneous observations made every 3 seconds during each 10-minute time period

Daily maximum = maximum value from 144 10-minute averages of 3-second observations

Daily minimum = minimum value from 144 10-minute averages of 3-second observations

Daily average = average of 144 10-minute averages made during the 24-hour period

Daily period of record maximum = maximum of daily maximums for specific calendar date during the period of record

Daily period of record minimum = minimum of daily minimums for specific calendar date during period of record

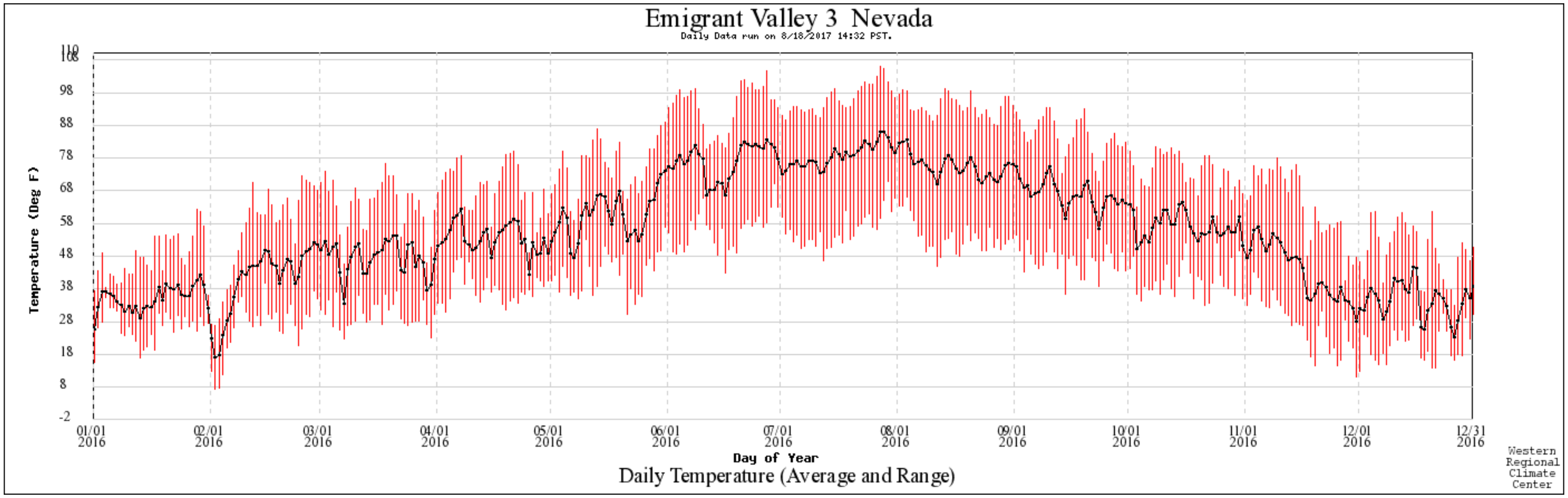

Figure A-1. Daily maximum, minimum, and average air temperature at P57-3 for the reporting period. The black line connects the daily average temperature. The bright red vertical lines connect the maximum and minimum temperature values for each day.

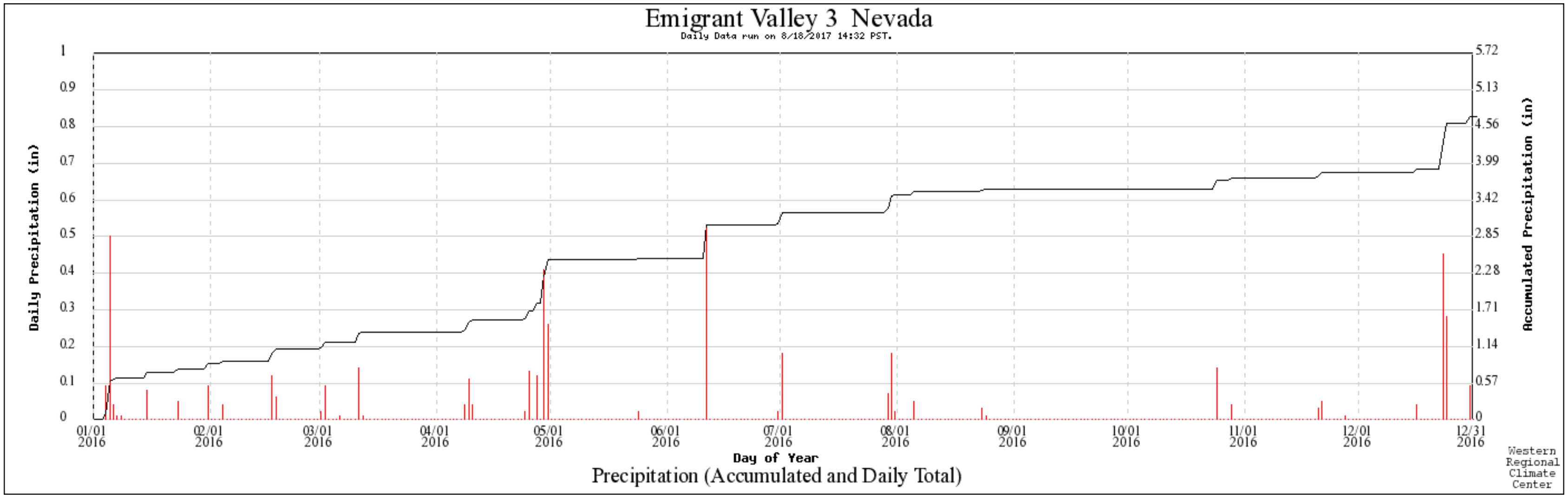

Figure A-2. Total daily precipitation (vertical red lines) and annual accumulated precipitation (black line) at P57-3 for the reporting period.

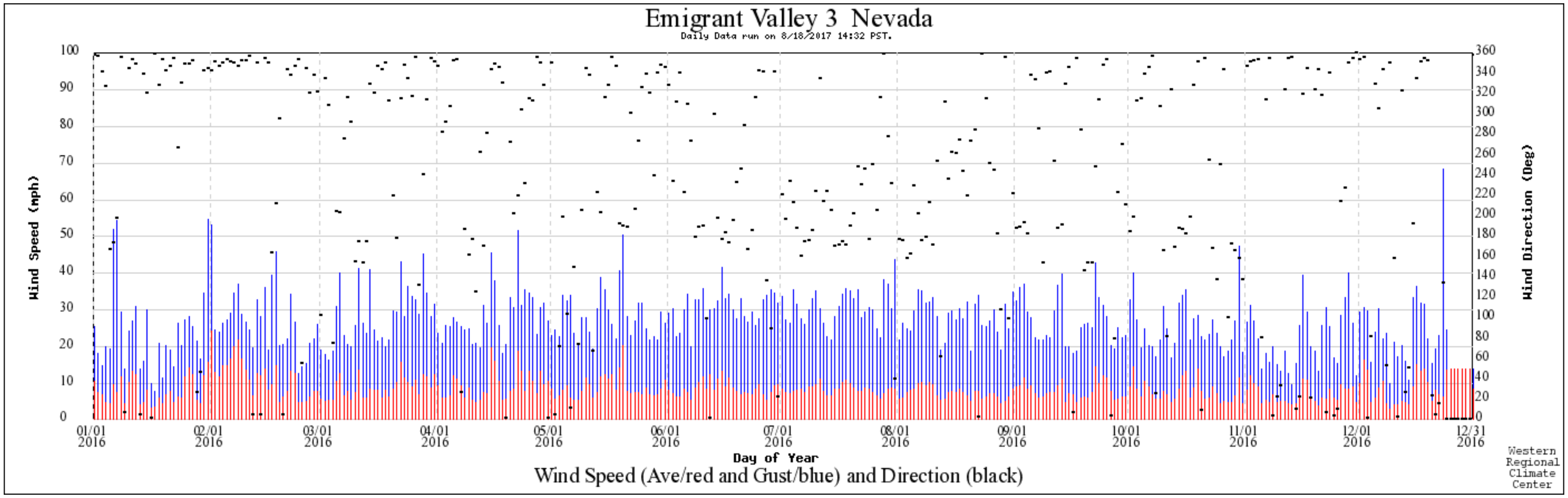

Figure A-3. Daily average (vertical red line) and maximum (vertical blue line) wind speed and daily average wind direction (black dot) at P57-3 for the reporting period.

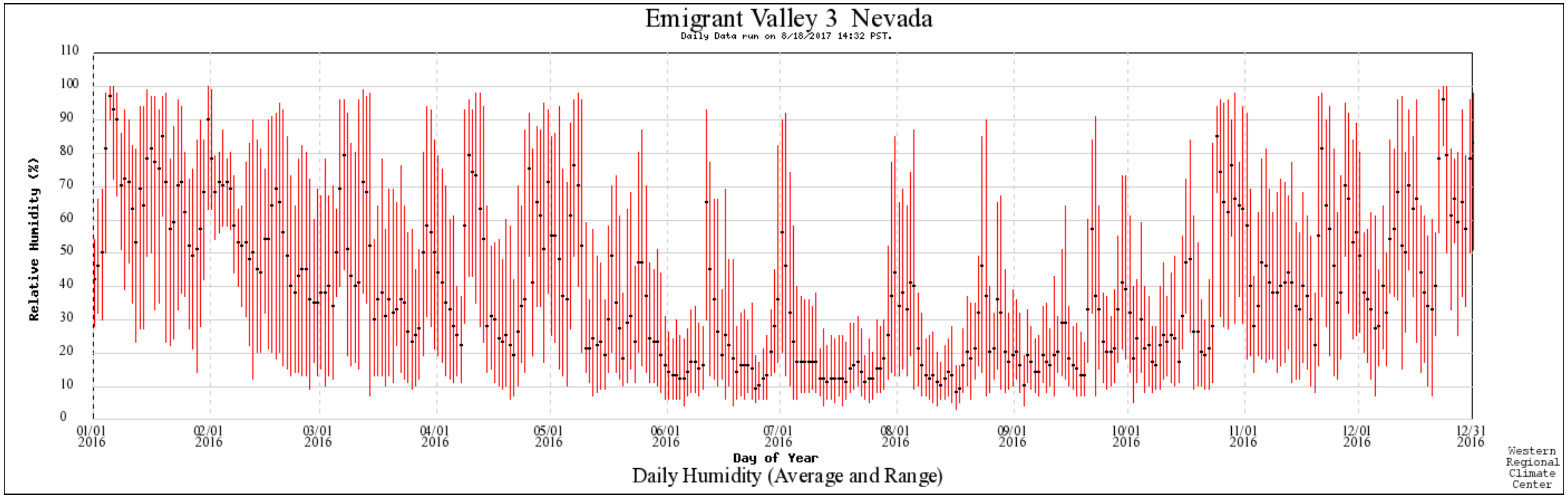

Figure A-4. Daily average relative humidity (black dots) and the daily range of relative humidity indicated by the red vertical lines that connect the daily maximum and minimum values at P57-3 for the reporting period.

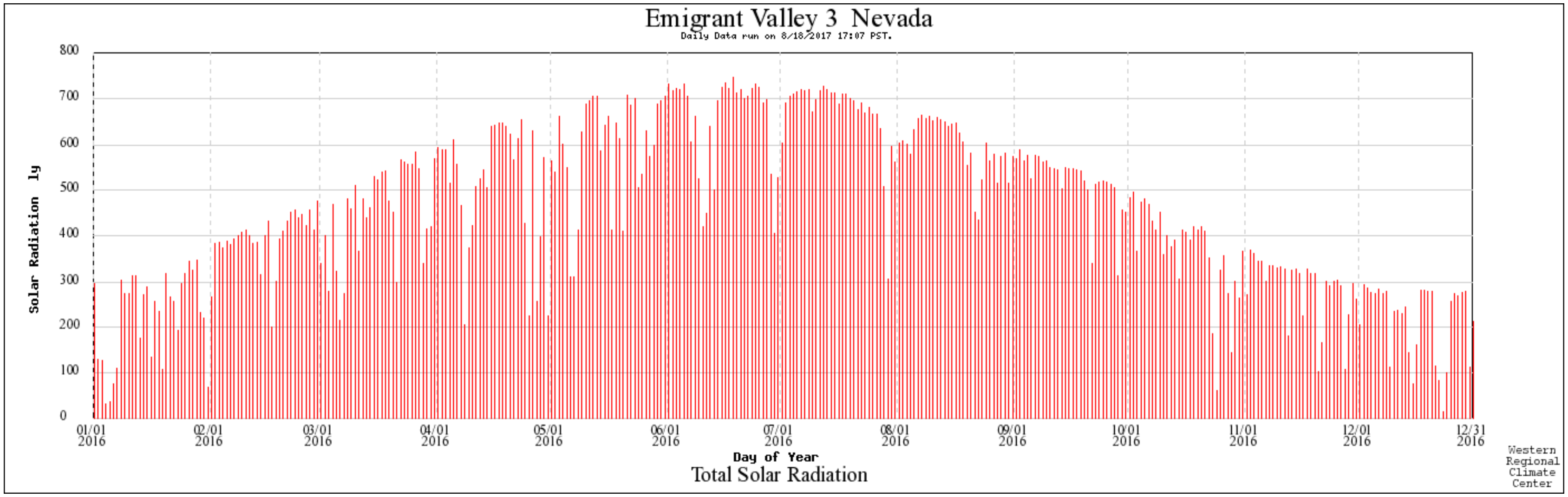

Figure A-5. Daily total solar radiation at P57-3 is indicated by vertical red lines.

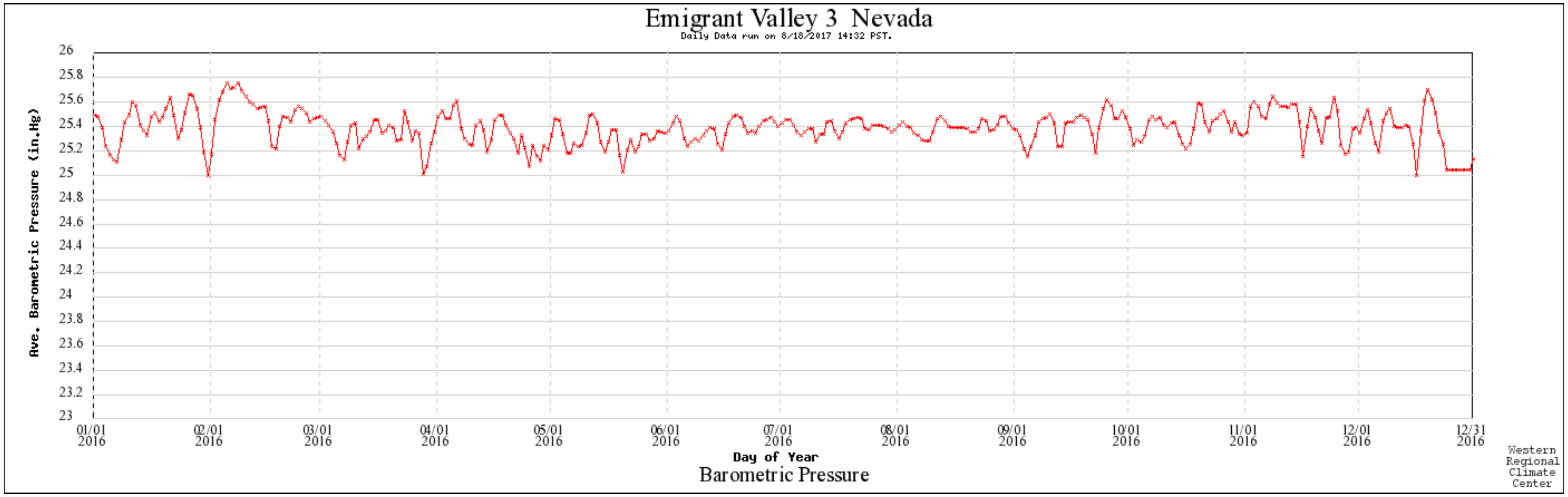

Figure A-6. Daily average barometric pressure at P57-3 for the reporting period.

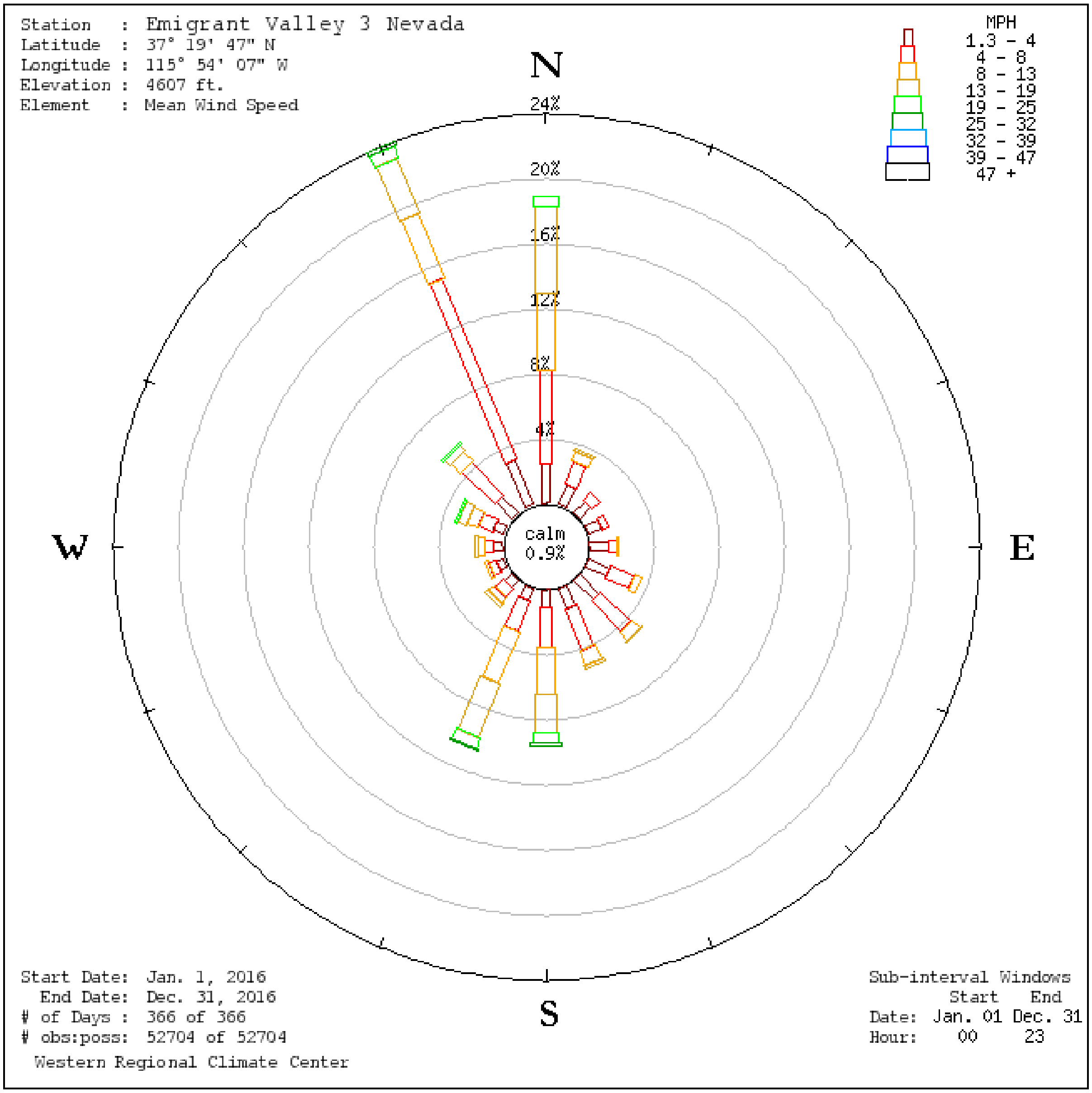

Figure A-7. P57-3 wind rose for the reporting period (January 1, 2016, through December 31, 2016).

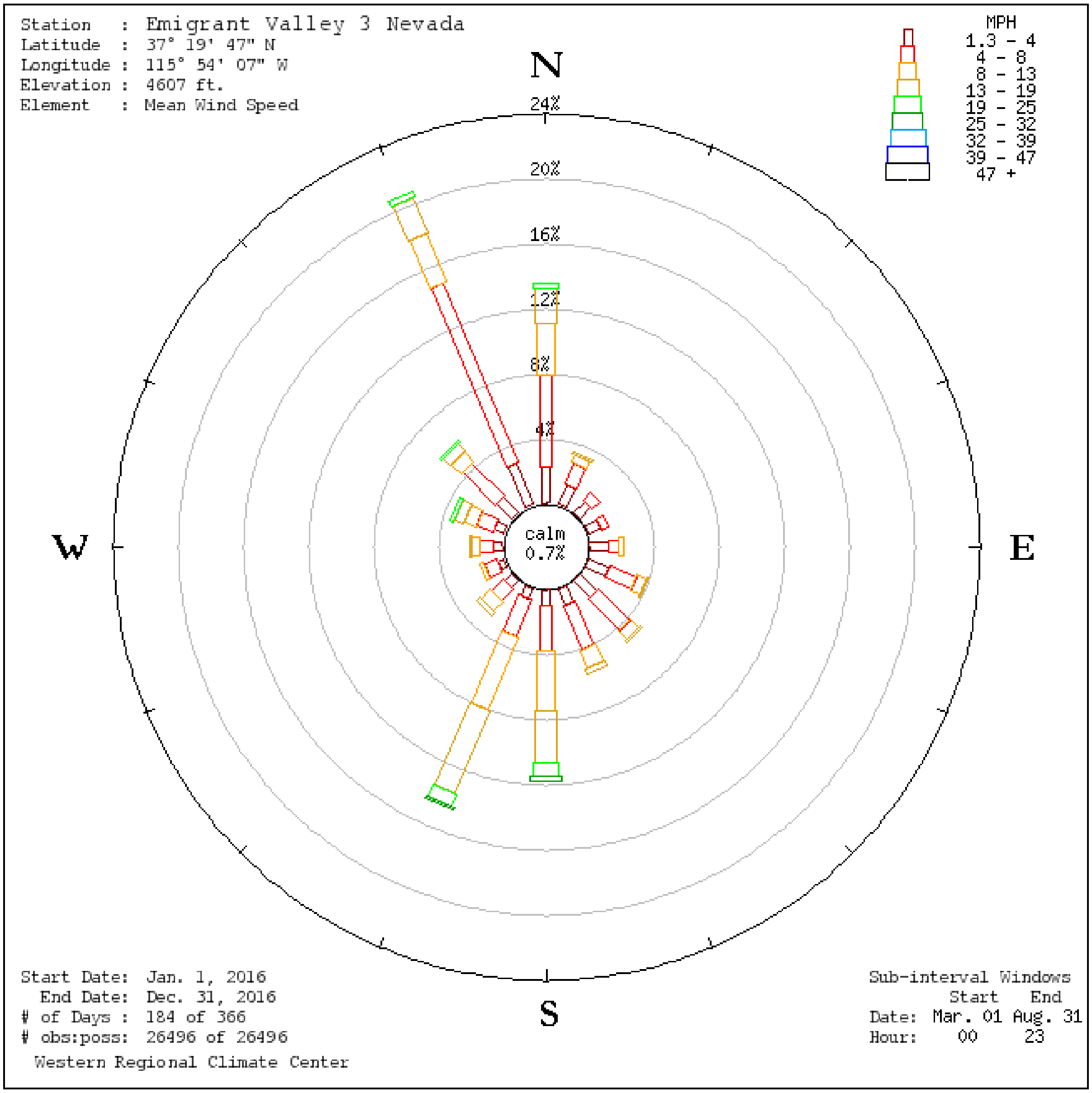

Figure A-8. P57-3 wind rose for the summer season (includes data collected between March 1, 2016, and August 31, 2016, during the reporting period).

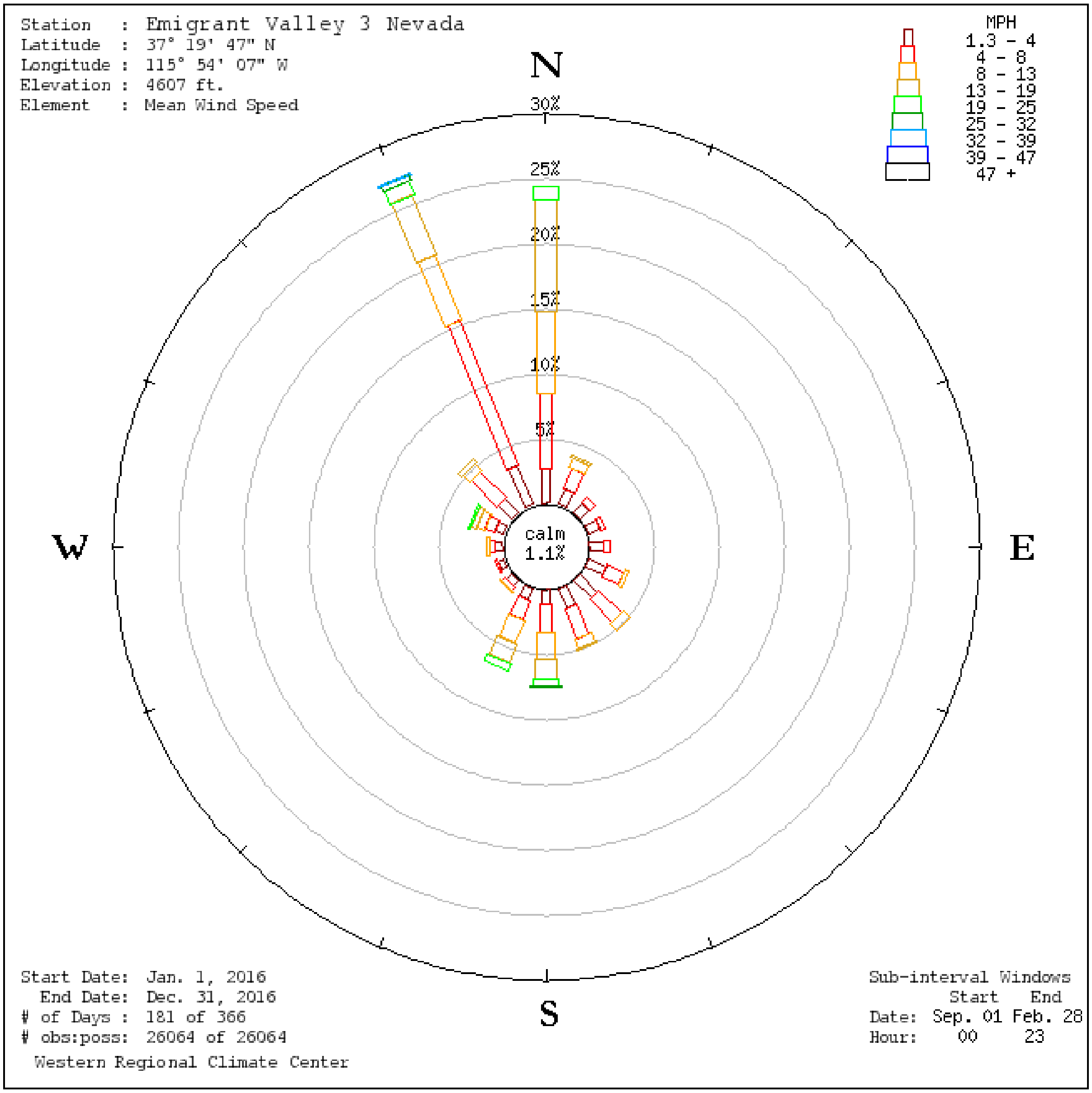

Figure A-9. P57-3 wind rose for the winter season (includes data collected between January 1, 2016, and February 28, 2016, and between September 1, 2016, and December 31, 2016, during the reporting period).

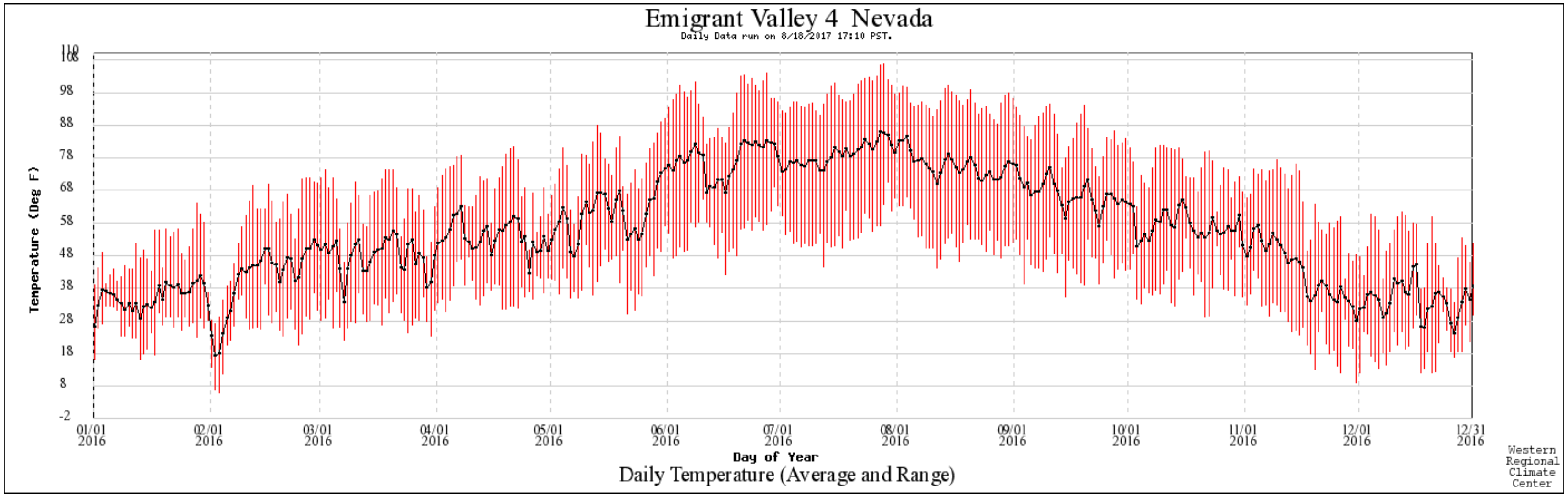

Figure A-10. Daily maximum, minimum, and average air temperature at P57-4 for the reporting period and for the period of record. The black line connects the daily average temperature. The bright red vertical lines connect the maximum and minimum temperature values for each day.

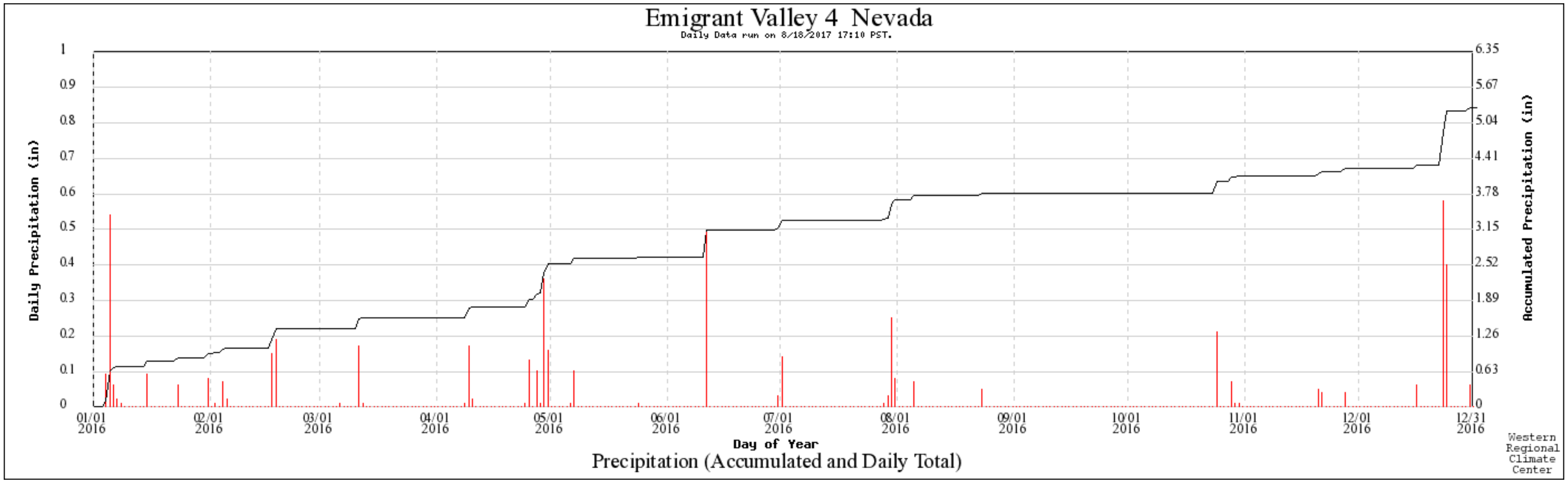

Figure A-11. Total daily precipitation (vertical red lines) and annual accumulated precipitation (black line) at P57-4 for the reporting period.

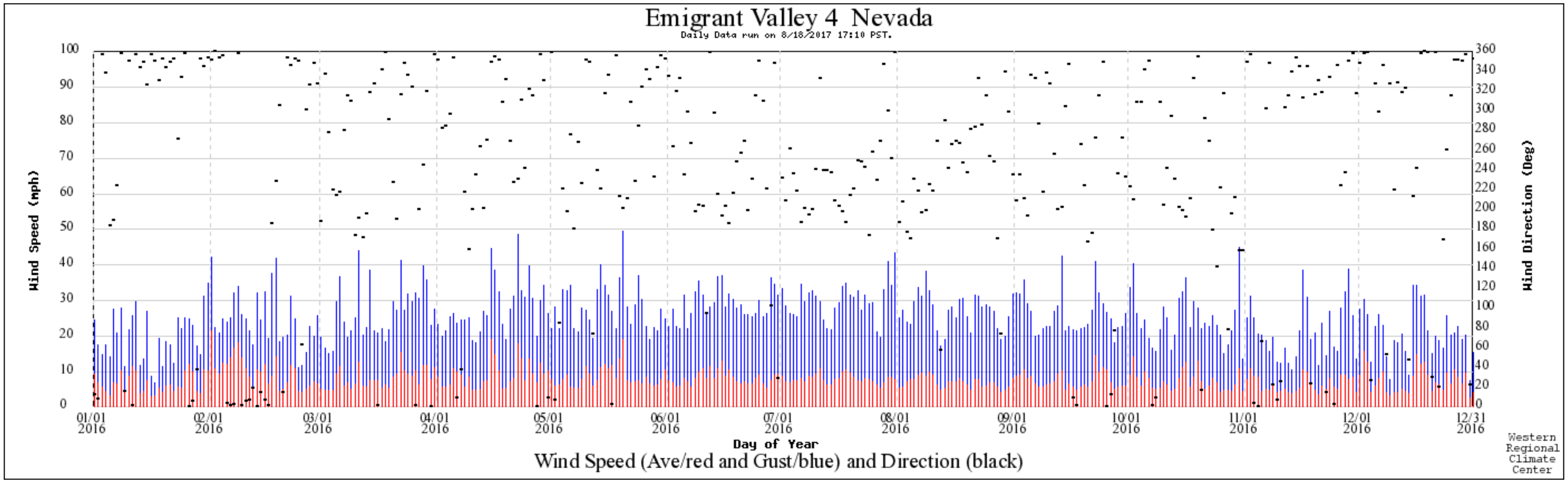

Figure A-12. Daily average (vertical red line) and maximum (vertical blue line) wind speed and daily average wind direction (black dot) at P57-4 for the reporting period.

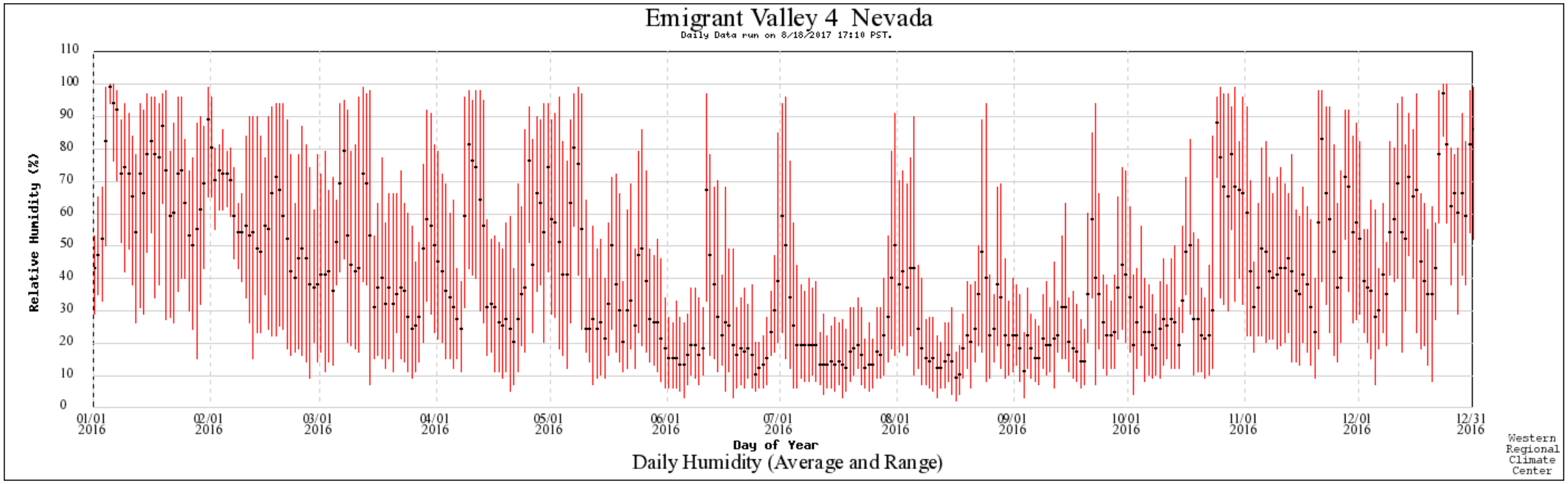

Figure A-13. Daily average relative humidity (black dots) and the daily range of relative humidity indicated by the red vertical lines that connect the daily maximum and minimum values at P57-4 for the reporting period.

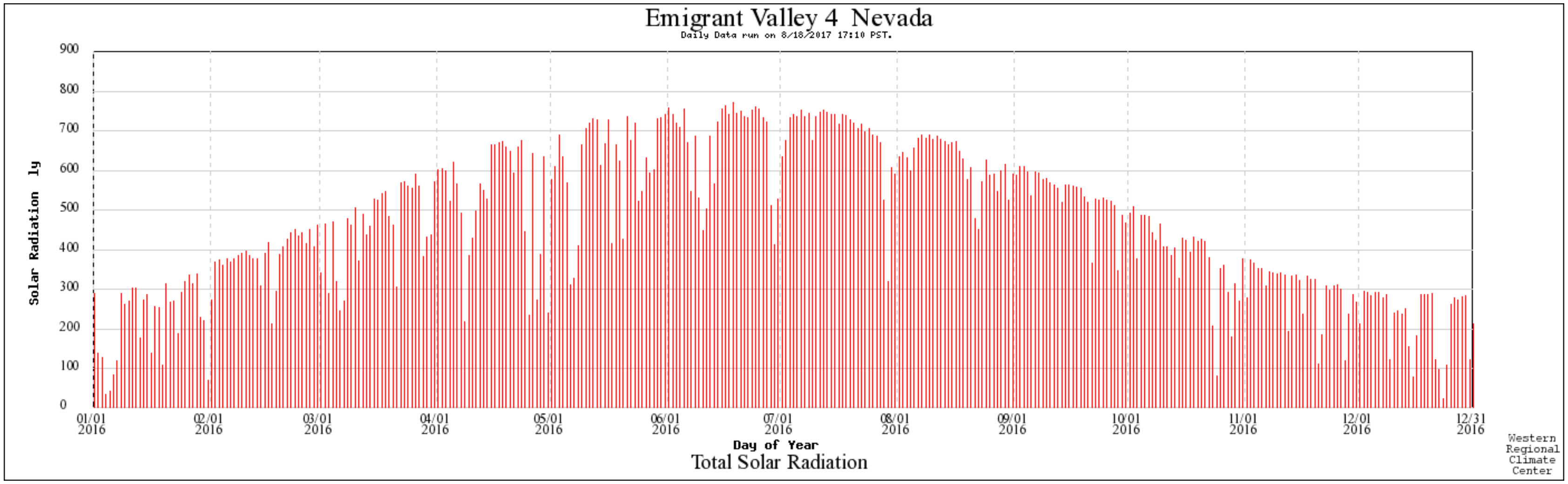

Figure A-14. Daily total solar radiation at P57-4 is indicated by vertical red lines.

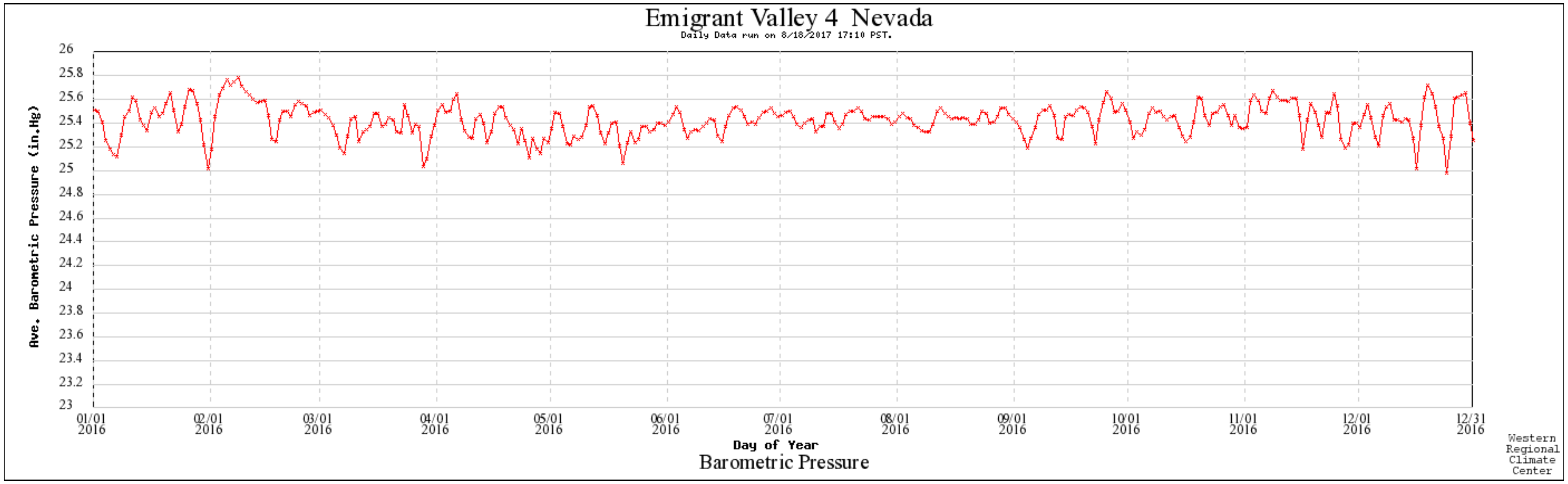

Figure A-15. Daily average barometric pressure at P57-4 for the reporting period.

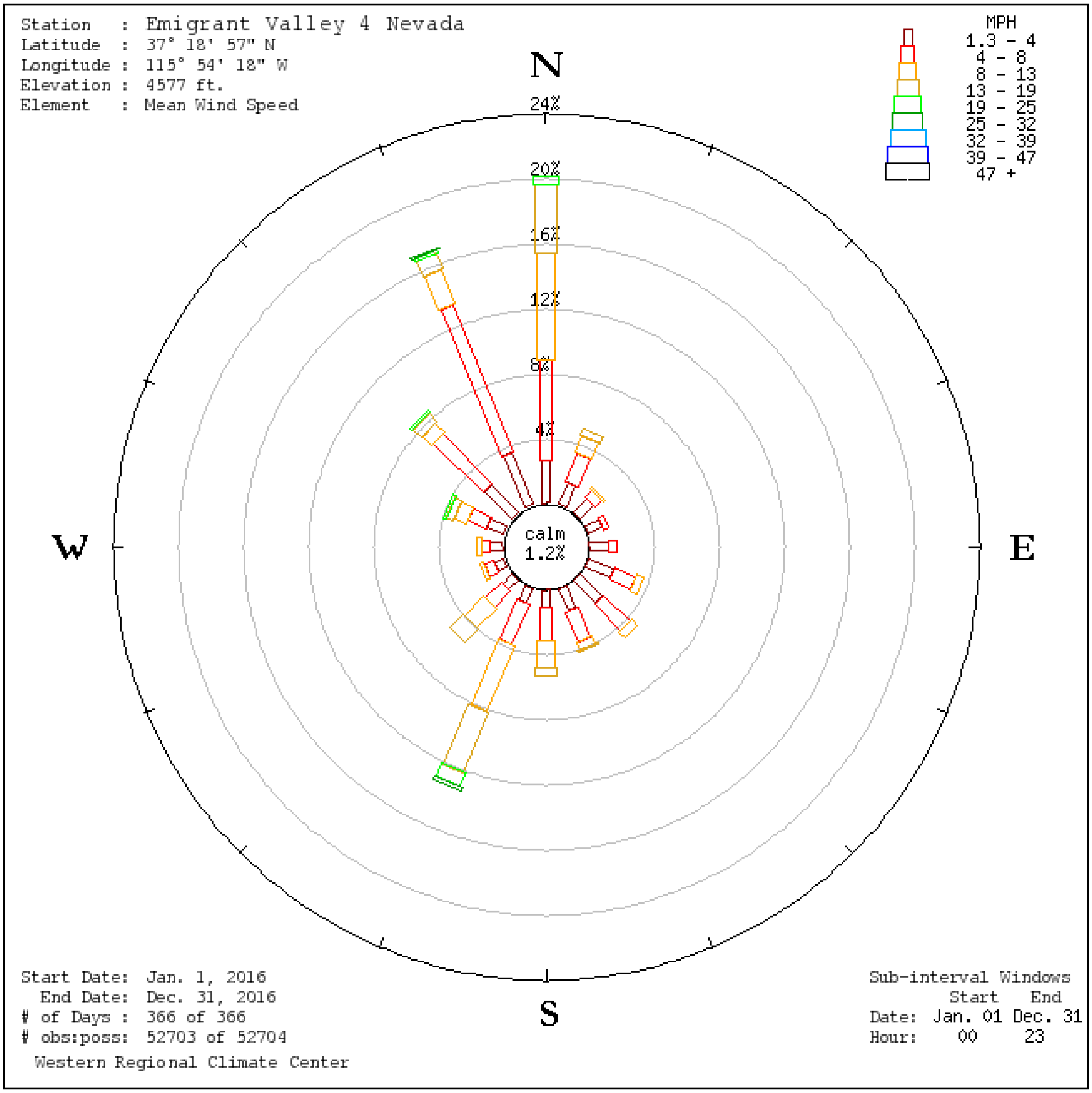

Figure A-16. P57-4 wind rose for the reporting period (January 1, 2016, through December 31, 2016).

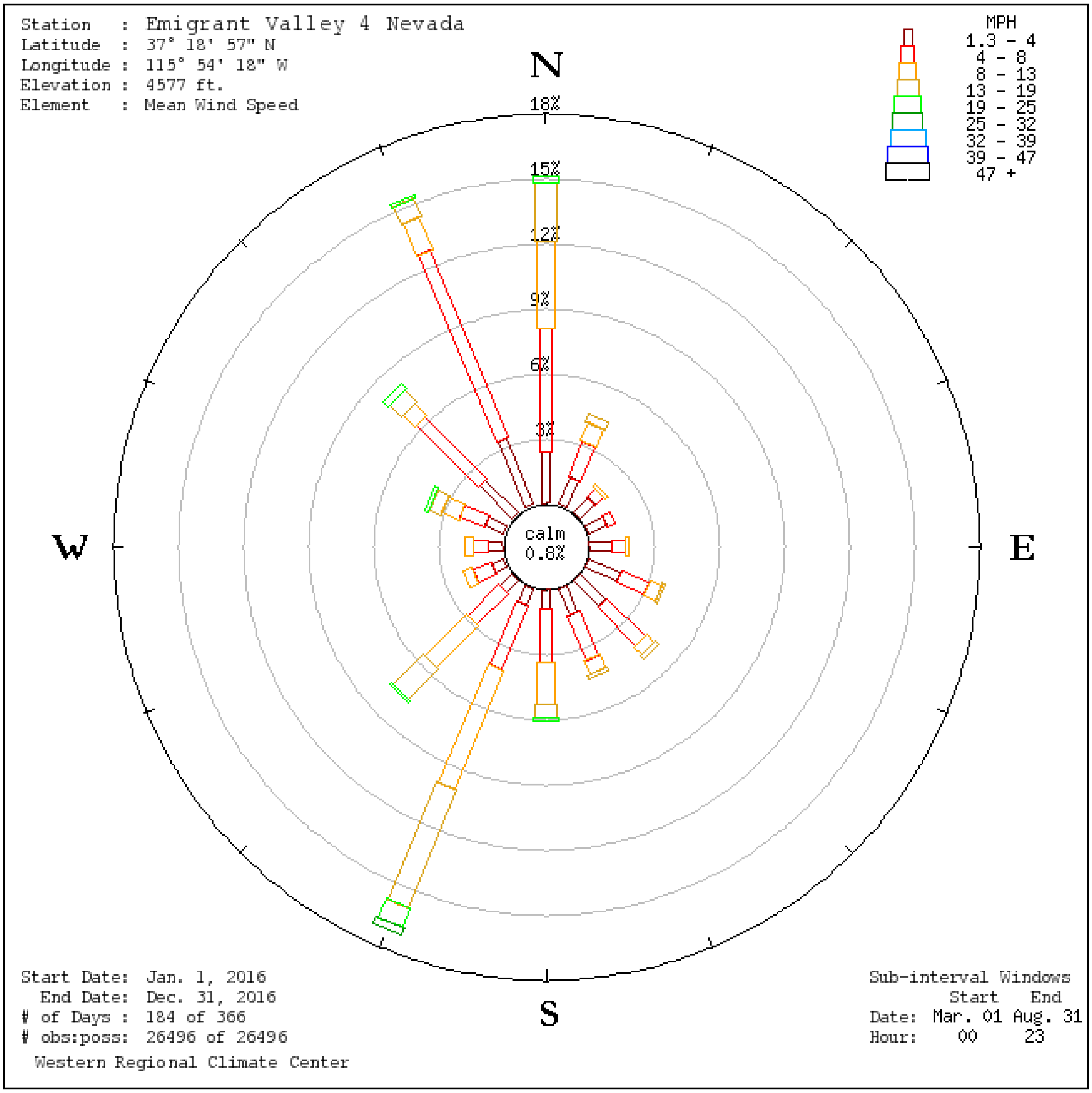

Figure A-17. P57-4 wind rose for the summer season (includes data collected between March 1, 2016, and August 31, 2016, during the reporting period).

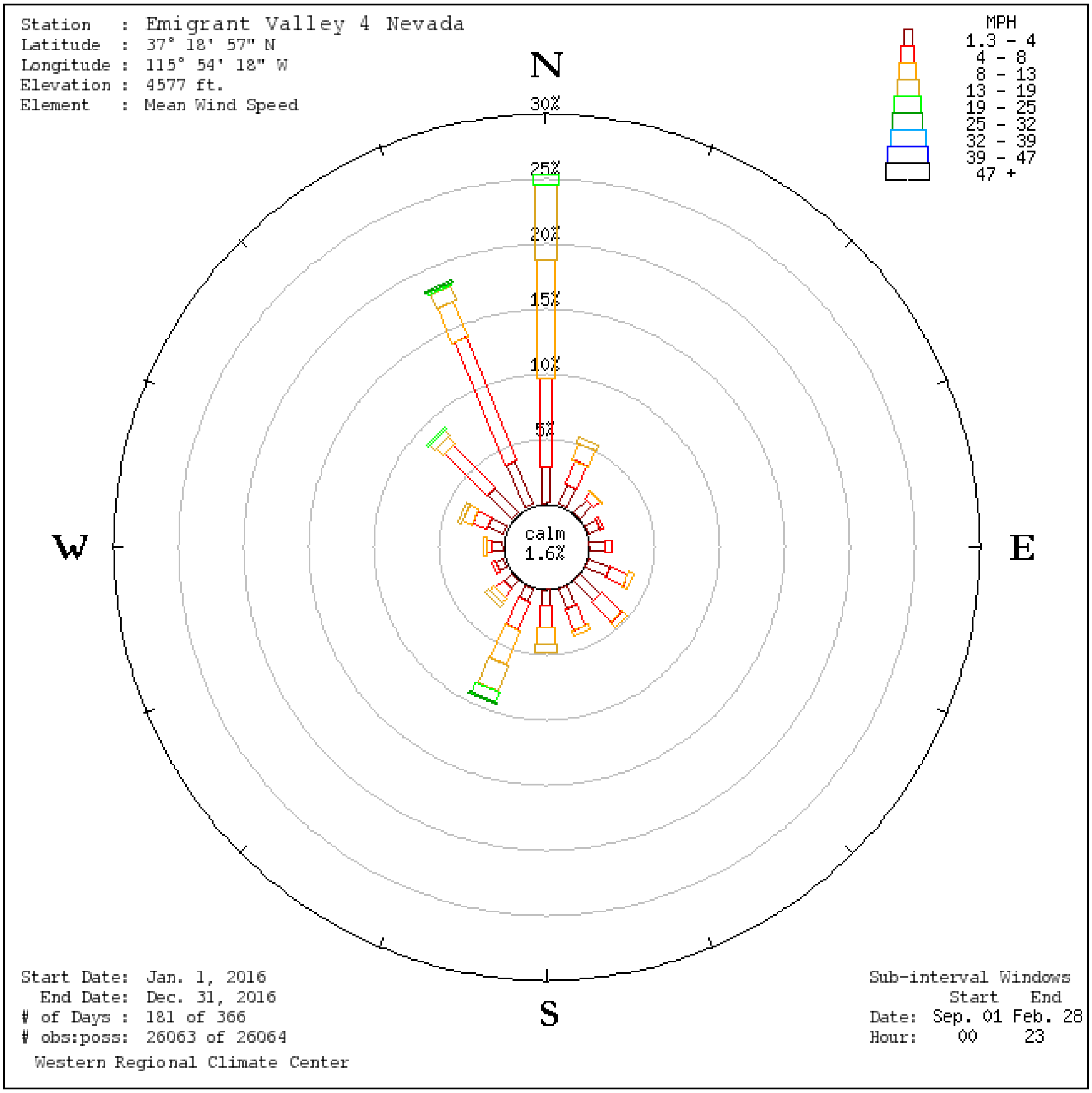

Figure A-18. P57-4 wind rose for the winter season (includes data collected between January 1, 2016, and February 28, 2016, and between September 1, 2016, and December 31, 2016, during the reporting period).

APPENDIX B: SOIL TEMPERATURE AND WATER CONTENT

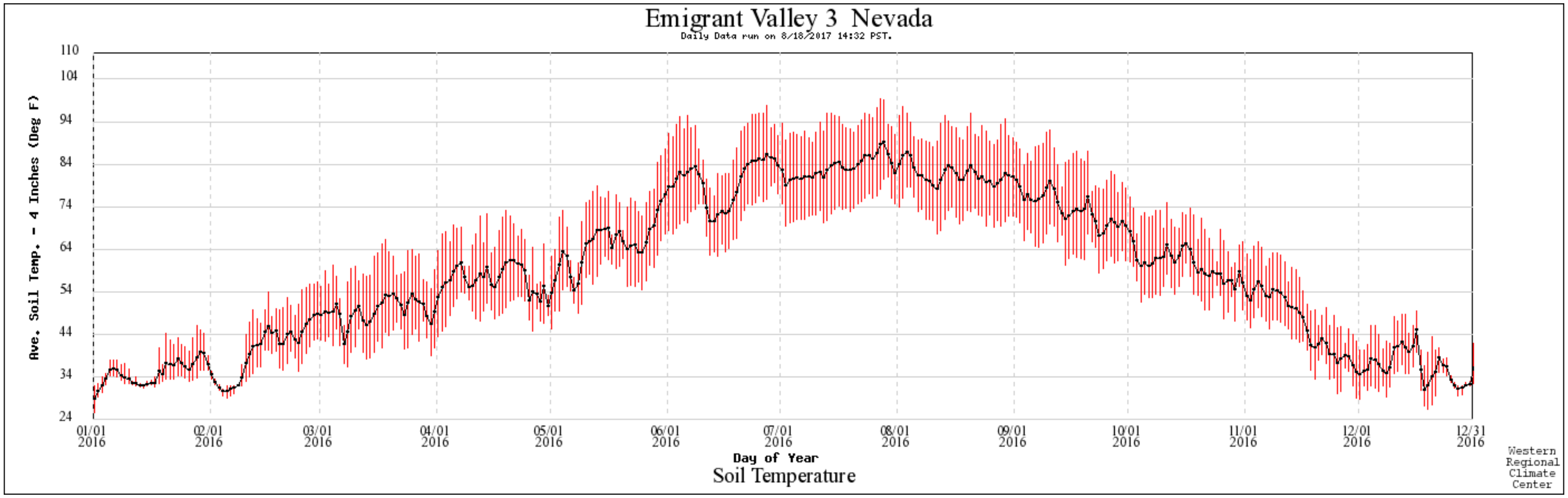

Figure B-1. Daily maximum, minimum, and average soil temperature at P57-3.

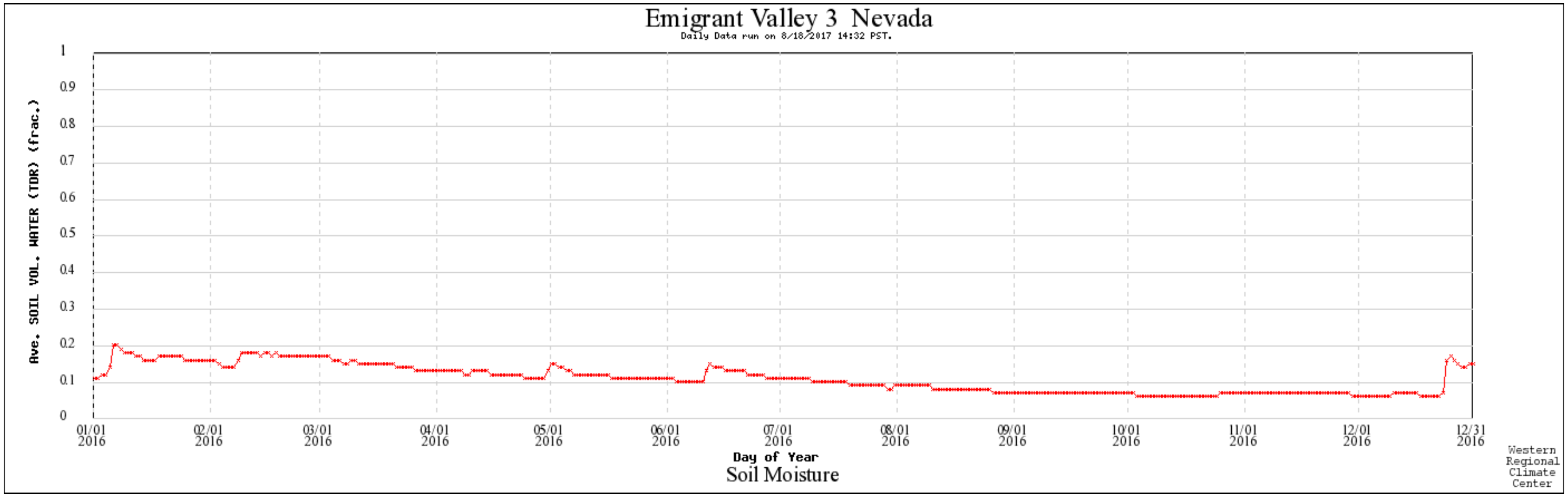

Figure B-2. Daily average soil moisture (volumetric water content [fraction]) at P57-3.

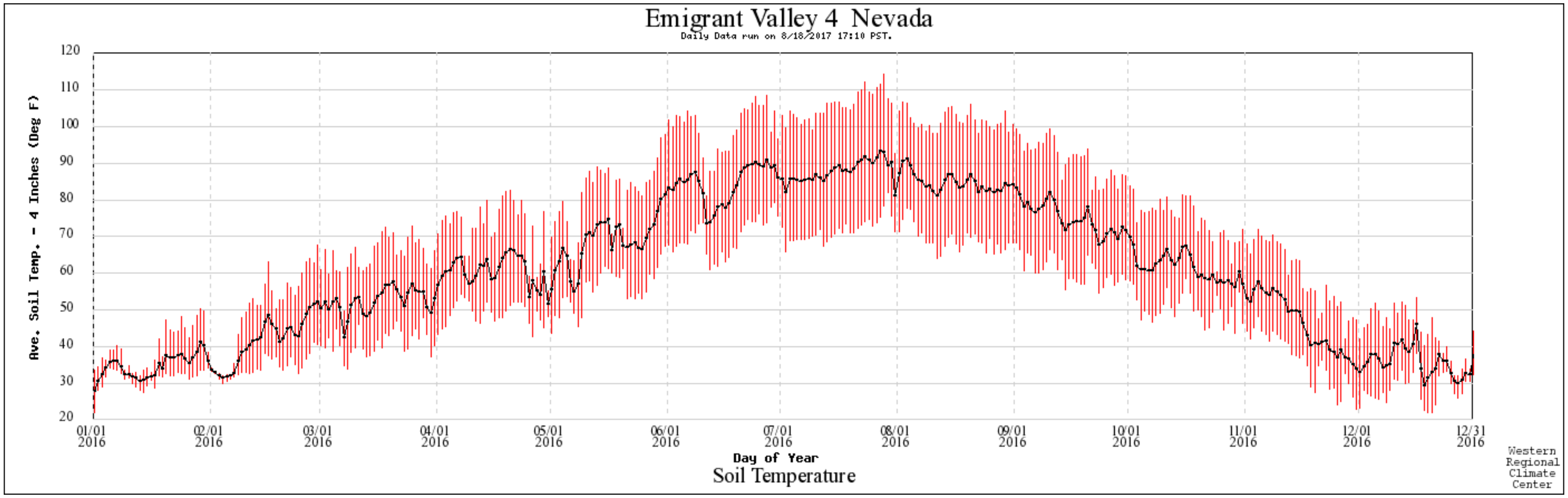

Figure B-3. Daily maximum, minimum, and average (black) soil temperature at P57-4.

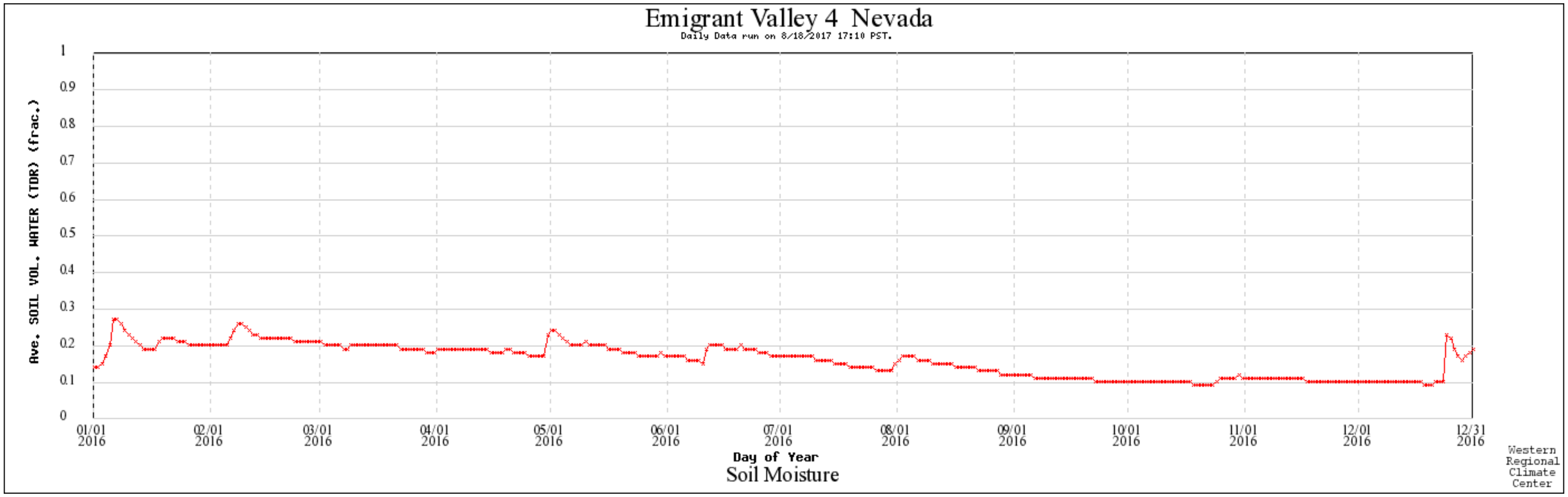

Figure B-4. Daily average soil moisture (volumetric water content [fraction]) at P57-4.

APPENDIX C: AIRBORNE AND SALTATION DUST PARTICLE OBSERVATIONS

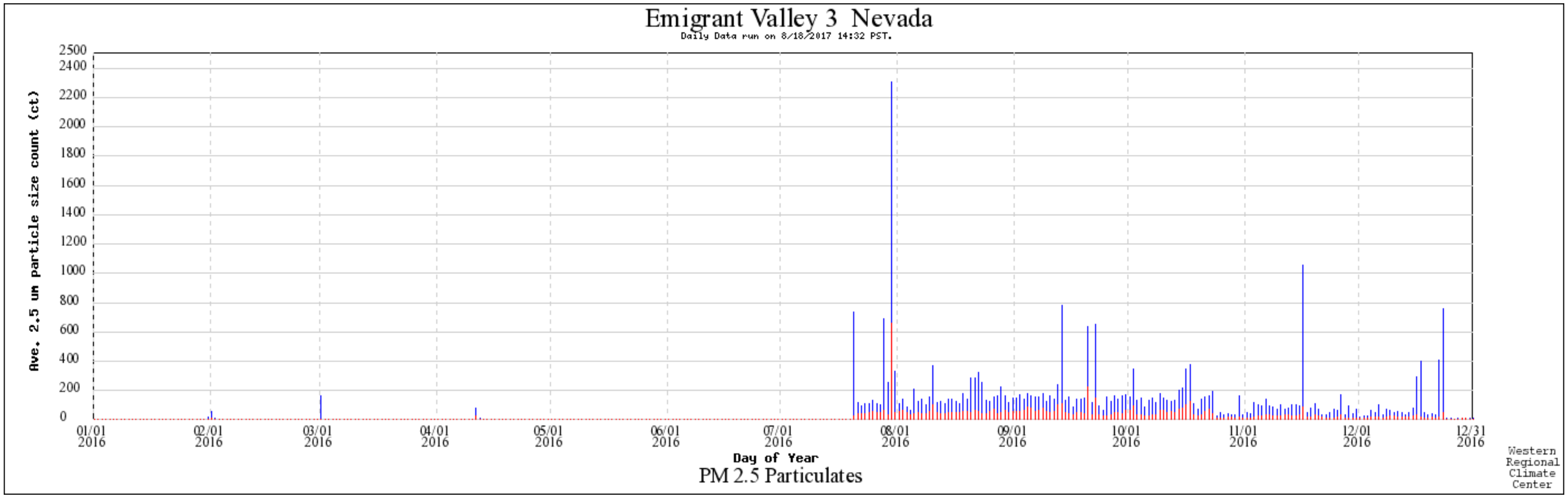

Figure C-1. Daily average (red) and maximum (blue) $PM_{2.5}$ counts at P57-3.

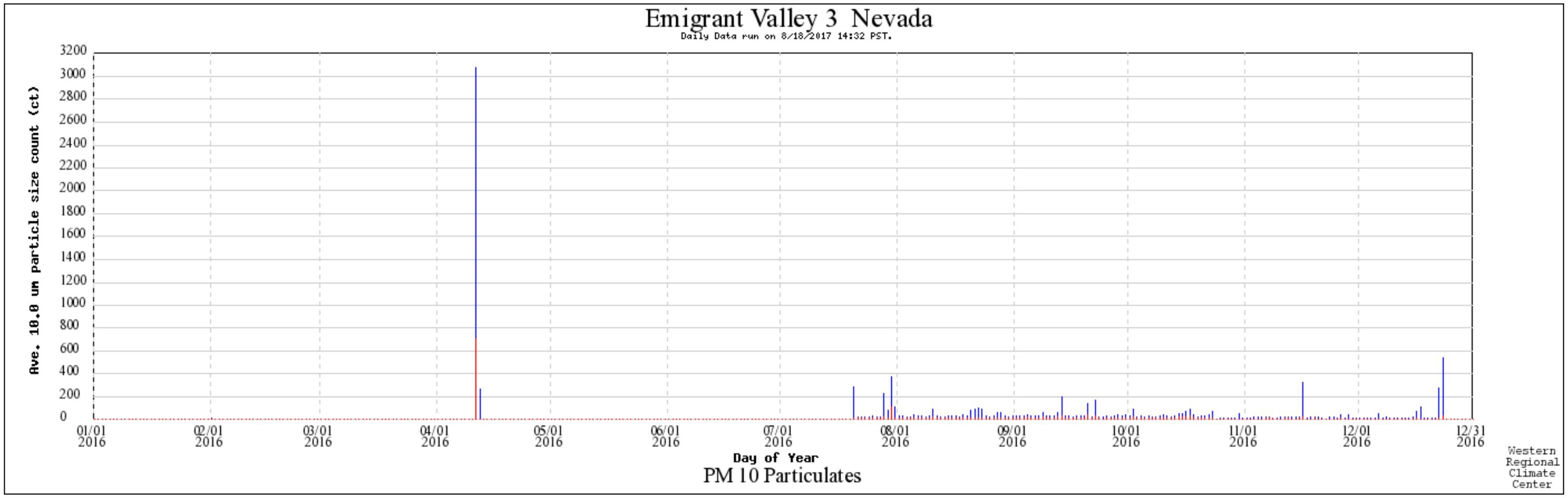

Figure C-2. Daily average (red) and maximum (blue) PM_{10} counts at P57-3.

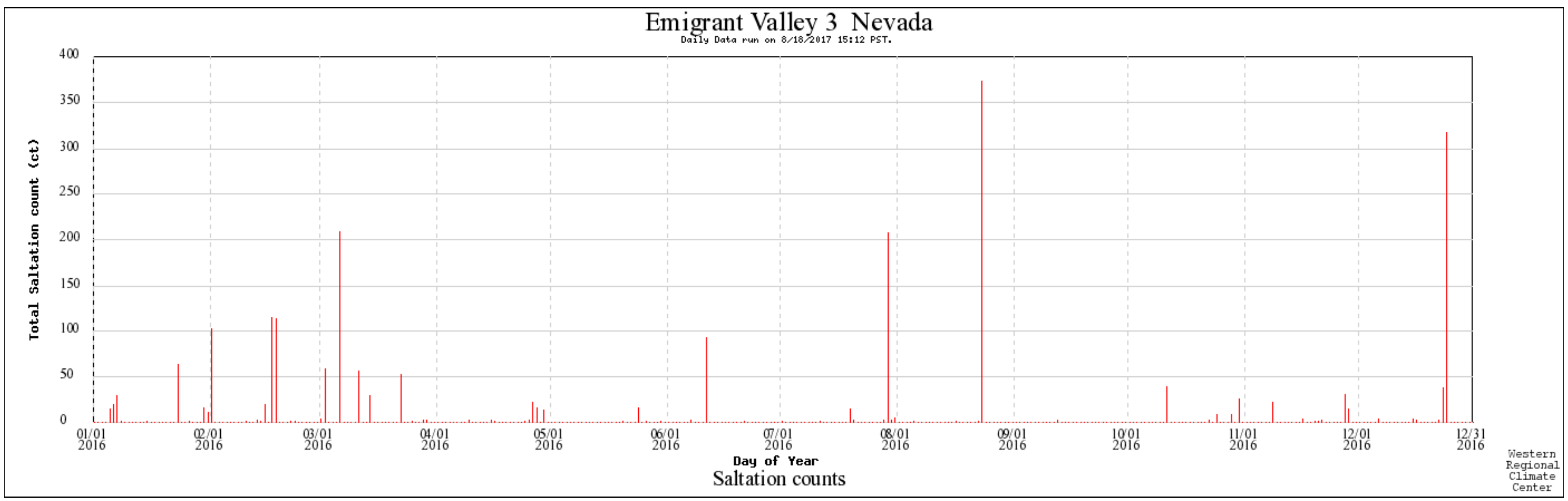

Figure C-3. Daily saltation counts at P57-3.

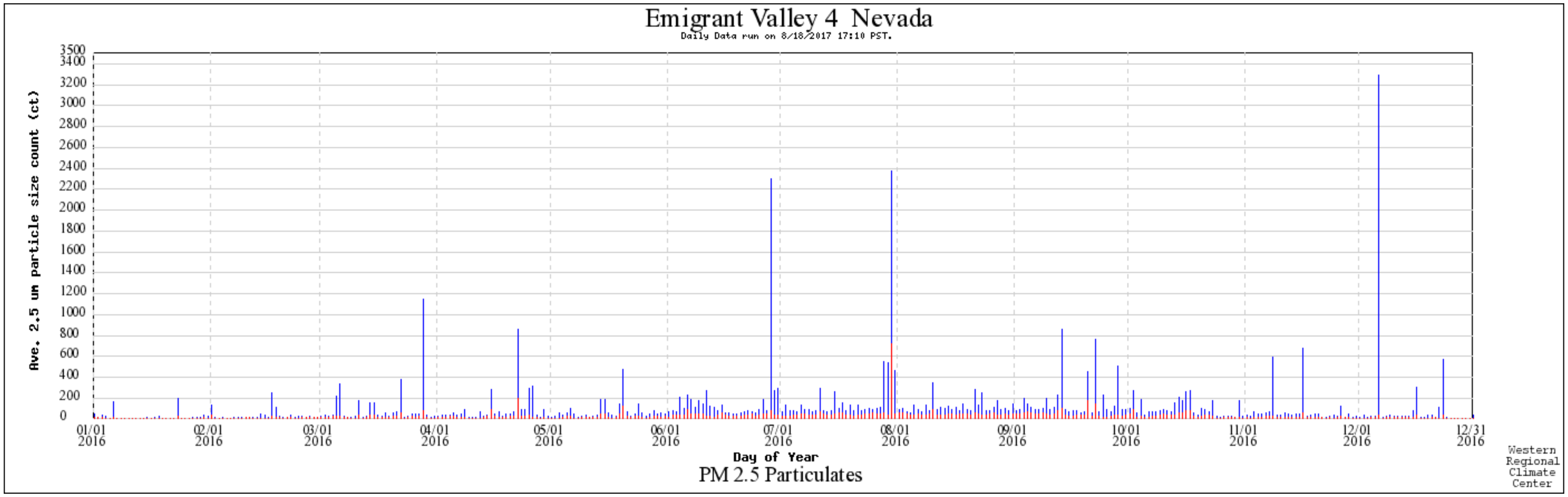

Figure C-4. Daily average (red) and maximum (blue) $PM_{2.5}$ counts at P57-4.

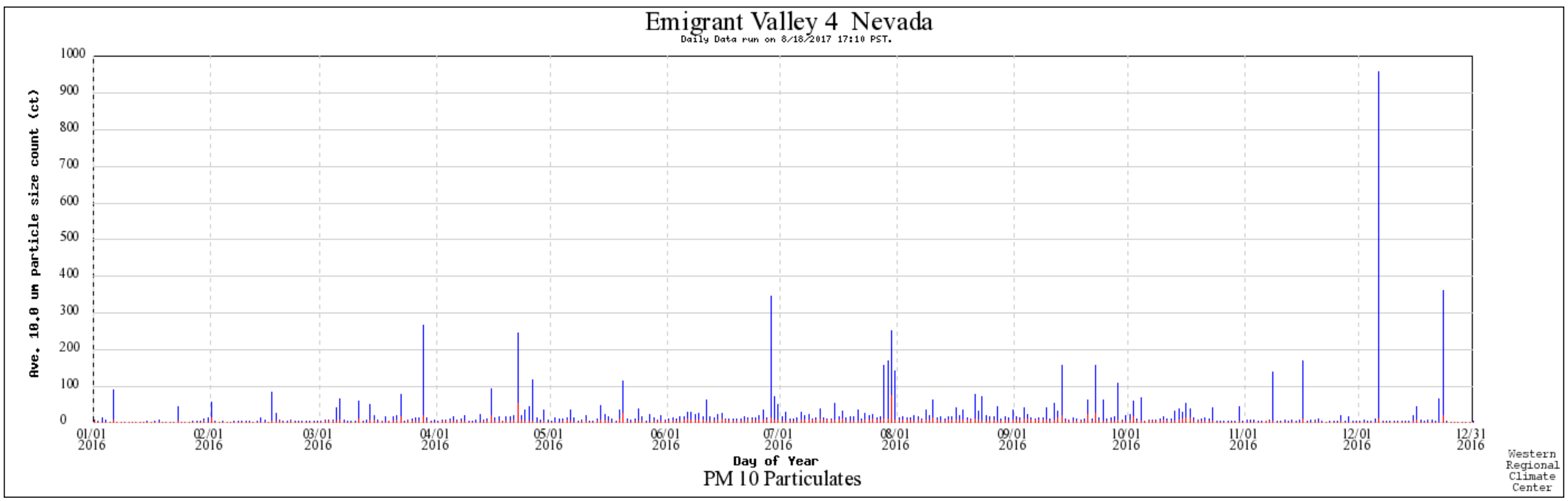

Figure C-5. Daily average (red) and maximum (blue) PM_{10} counts at P57-4.

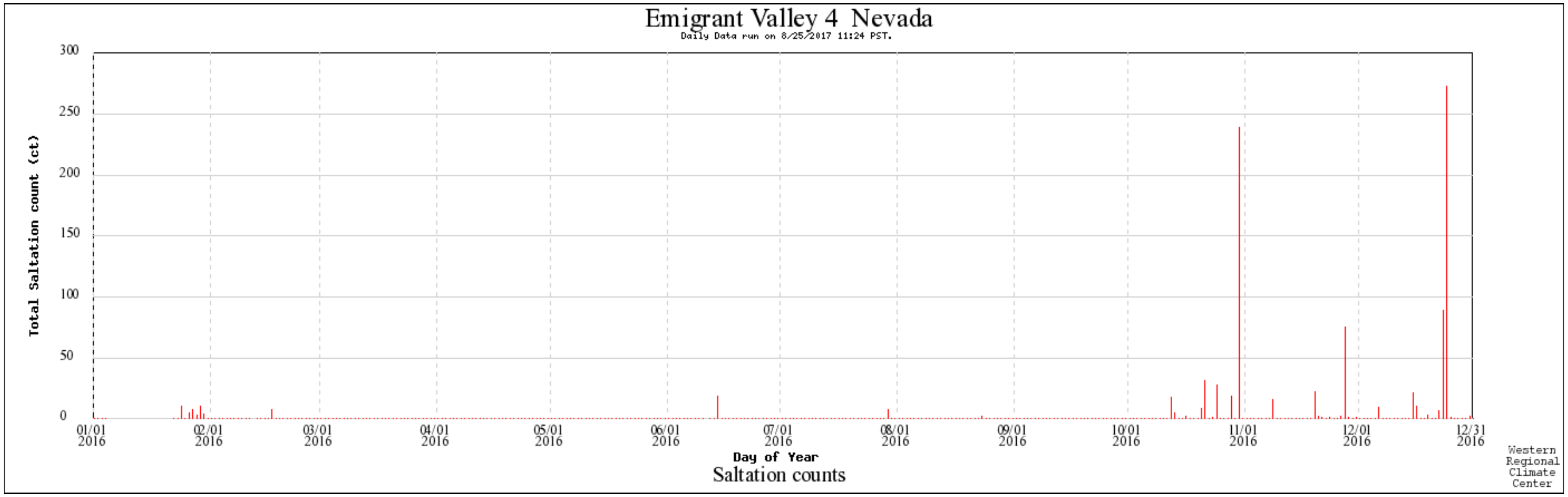

Figure C-6. Daily saltation counts at P57-4.

APPENDIX D: RADIOLOGICAL RESULTS FOR SALTATION SAMPLES

Table D-1. Mass (grams) of the three size fractions for saltation samples collected from Project 57 monitoring stations on March 3, 2015.

BSNE # Orientation	Retrieval Date	Size Fraction			Total
		<63 µm	63 µm to 250 µm	>250 µm	
P57-1 25-29-35 2 down 1 up	March 3, 2015	0.4882	3.7940	No measurement	> 4.2822
P57-1 27-31-33 1 down 2 up	March 3, 2015	0.7523	3.3696	No measurement	> 4.1619
P57-2 37-41-45 Downwind	March 3, 2015	0.4874	2.7840	No measurement	> 3.2714
P57-2 39-43-47 Upwind	March 3, 2015	0.2137	1.9527	No measurement	> 2.1664

Particle size separation and sample mass by Southwest Research Institute, San Antonio, Texas.

Table D-2. Radionuclide analysis results for saltation samples collected from Project 57 monitoring stations on March 3, 2015.

BSNE # Orientation	Date	Size Fraction	
		<63 µm	63 to 250 µm
Am-241 (pCi/g)			
P57-1 25-29-35 2 down 1 up	March 3, 2015	0.698	0.535
P57-1 27-31-33 1 down 2 up	March 3, 2015	0.735	0.303
P57-2 37-41-45 Downwind	March 3, 2015	0.414	0.0503
P57-2 39-43-47 Upwind	March 3, 2015	0.307	0.0962
Pu-238 (pCi/g)			
P57-1 25-29-35 2 down 1 up	March 3, 2015	0.115	0.324
P57-1 27-31-33 1 down 2 up	March 3, 2015	0.251	0.125
P57-2 37-41-45 Downwind	March 3, 2015	0.233	0.105
P57-2 39-43-47 Upwind	March 3, 2015	0.145	0.0426
Pu-239/240 (pCi/g)			
P57-1 25-29-35 2 down 1 up	March 3, 2015	3.74	1.94
P57-1 27-31-33 1 down 2 up	March 3, 2015	3.57	1.15
P57-2 37-41-45 Downwind	March 3, 2015	2.24	0.369
P57-2 39-43-47 Upwind	March 3, 2015	1.34	0.279

Radiological analyses by GEL Laboratories, Charleston, South Carolina.

Table D-3. Mass (grams) of the three size fractions for saltation samples collected from Project 57 monitoring stations on January 4, 2016.

BSNE # Orientation	Retrieval Date	Size Fraction			Total
		<63 µm	63 µm to 250 µm	>250 µm	
P57-3 38-42-46 Downwind	January 4, 2016	1.7193	10.4219	3.3458	15.4870
P57-3 40-44-48 Upwind	January 4, 2016	1.7989	12.8518	3.7701	18.4208
P57-4 26-30-34 Downwind	January 4, 2016	0.7844	3.0300	0.9374	4.7518
P57-4 28-32-36 Upwind	January 4, 2016	0.3708	1.9334	0.8523	3.1565

Particle size separation and sample mass by Southwest Research Institute, San Antonio, Texas.

Table D-4. Radionuclide analysis results for saltation samples collected from Project 57 monitoring stations on January 4, 2016.

BSNE # Orientation	Date	Size Fraction	
		<63	63 to 250 µm
Am-241 (pCi/g)			
P57-3 38-42-46 Downwind	January 4, 2016	6.58	0.203
P57-3 40-44-48 Upwind	January 4, 2016	4.21	0.152
P57-4 26-30-34 Downwind	January 4, 2016	16.6	0.167
P57-4 28-32-36 Upwind	January 4, 2016	14.4	0.188
Pu-238 (pCi/g)			
P57-3 38-42-46 Downwind	January 4, 2016	0.830	0.152
P57-3 40-44-48 Upwind	January 4, 2016	0.664	0.245
P57-4 26-30-34 Downwind	January 4, 2016	2.65	0.0519
P57-4 28-32-36 Upwind	January 4, 2016	1.48	0.0114
Pu-239/240 (pCi/g)			
P57-3 38-42-46 Downwind	January 4, 2016	73.1	0.843
P57-3 40-44-48 Upwind	January 4, 2016	40.3	0.834
P57-4 26-30-34 Downwind	January 4, 2016	338	1.60
P57-4 28-32-36 Upwind	January 4, 2016	247	0.946

Radiological analyses by GEL Laboratories, Charleston, South Carolina.

Table D-5. Mass (grams) of saltation trap samples collected from Project 57 monitoring stations on October 13, 2016.

BSNE # Orientation	Date	Size Fraction <63 µm	63 to 250 µm	>250 µm	Total
P57-3 37-41-45 Downwind	October 13, 2016	0.7127	3.4056	0.6579	4.7662
P57-3 39-43-47 Upwind	October 13, 2016	0.4621	2.2815	0.3470	3.0906
P57-4 25-29-33 Downwind	October 13, 2016	0.6194	1.9937	0.8700	3.4831
P57-4 27-31-35 Upwind	October 13, 2016	0.6588	1.8116	0.3901	2.8605

Mass determination by Southwest Research Institute, San Antonio, Texas.

Table D-6. Radionuclide analysis results for saltation samples collected from Project 57 monitoring stations on October 13, 2016.

BSNE # Orientation	Date	Size Fraction <63 µm	63 to 250 µm	>250 µm
Am-241 (pCi/g)				
P57-3 37-41-45 Downwind	October 13, 2016	4.96	0.35	0.181U
P57-3 39-43-47 Upwind	October 13, 2016	17.8	0.223	0.337
P57-4 25-29-33 Downwind	October 13, 2016	26.1	0.54	0.458
P57-4 27-31-35 Upwind	October 13, 2016	10.7	0.855	2.45
Pu-238 (pCi/g)				
P57-3 37-41-45 Downwind	October 13, 2016	1.05	0.346	0.0253U
P57-3 39-43-47 Upwind	October 13, 2016	0.17	0.179	-0.0205U
P57-4 25-29-33 Downwind	October 13, 2016	1.06	0.0423	0.0319U
P57-4 27-31-35 Upwind	October 13, 2016	1.53	0.0283U	0.0146U
Pu-239/240 (pCi/g)				
P57-3 37-41-45 Downwind	October 13, 2016	67.7	2.27	0.53
P57-3 39-43-47 Upwind	October 13, 2016	11.0	2.46	1.29
P57-4 25-29-33 Downwind	October 13, 2016	88.0	2.51	2.13
P57-4 27-31-35 Upwind	October 13, 2016	107.0	1.35	1.01

Radiological analyses by Southwest Research Institute, San Antonio, Texas.

U = reported value less than Minimum Detectable Activity.

Appendix D2: Saltation Trap Deployment Patterns and History

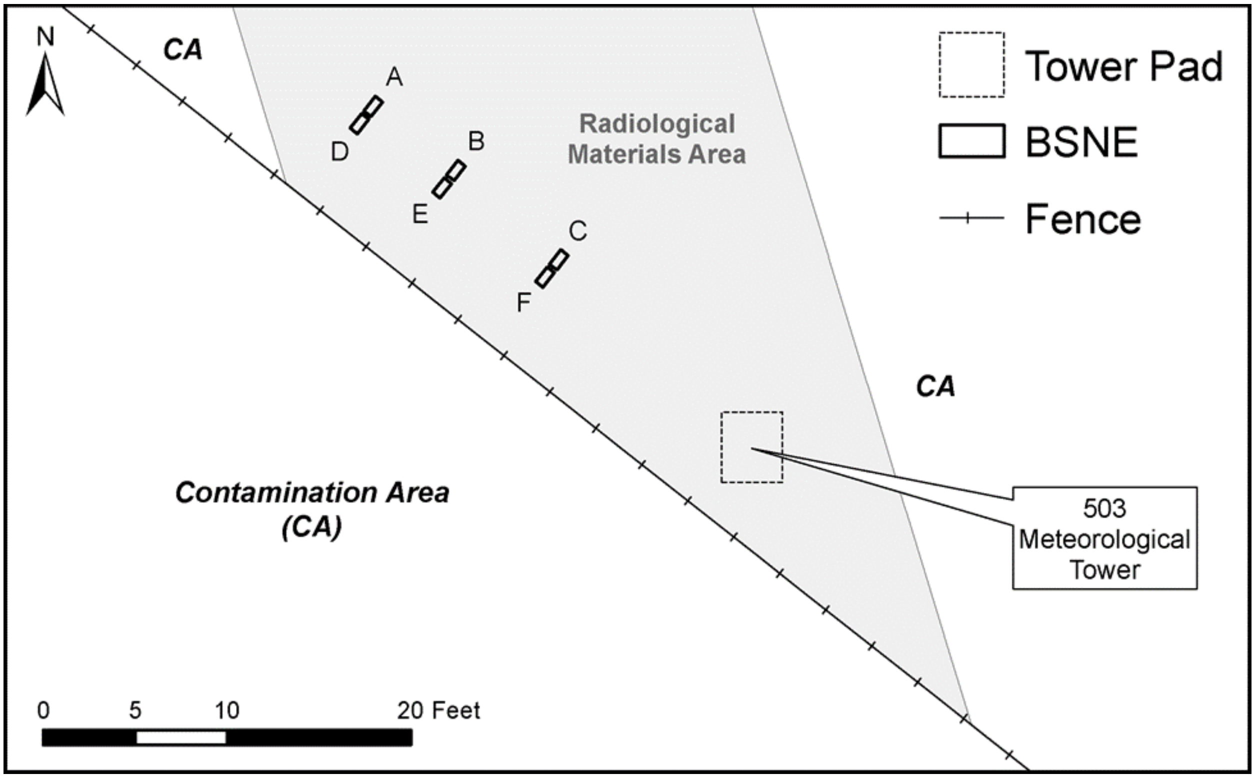

Figure D-1. Saltation trap deployment pattern at P57-3 (station 503). Traps A, B, and C are upwind of, face away from, the CA. Traps D, E, and F are downwind of and face toward the CA.

Table D-7. Distribution and deployment schedule for individual saltation traps at P57-3.

Date		Days Deployed	Saltation Trap identification						Combined sample	
Deployment	Retrieval		503A	503B	503C	503D	503E	503F	Upwind	Downwind
3/3/2015	1/4/2016	307	48	44	40	46	42	38	503-40, 44, 48	503-38, 42, 46
1/4/2016	10/13/2016	282	47	43	39	45	41	37	503-39, 43, 47	503-37, 41, 45
11/8/2016	5/16/2017	189	48	44	40	46	42	38	503-40, 44, 48	503-38, 42, 46
5/22/2017	deployed	--	47	43	39	45	41	37	503-39, 43, 47	503-37, 41, 45

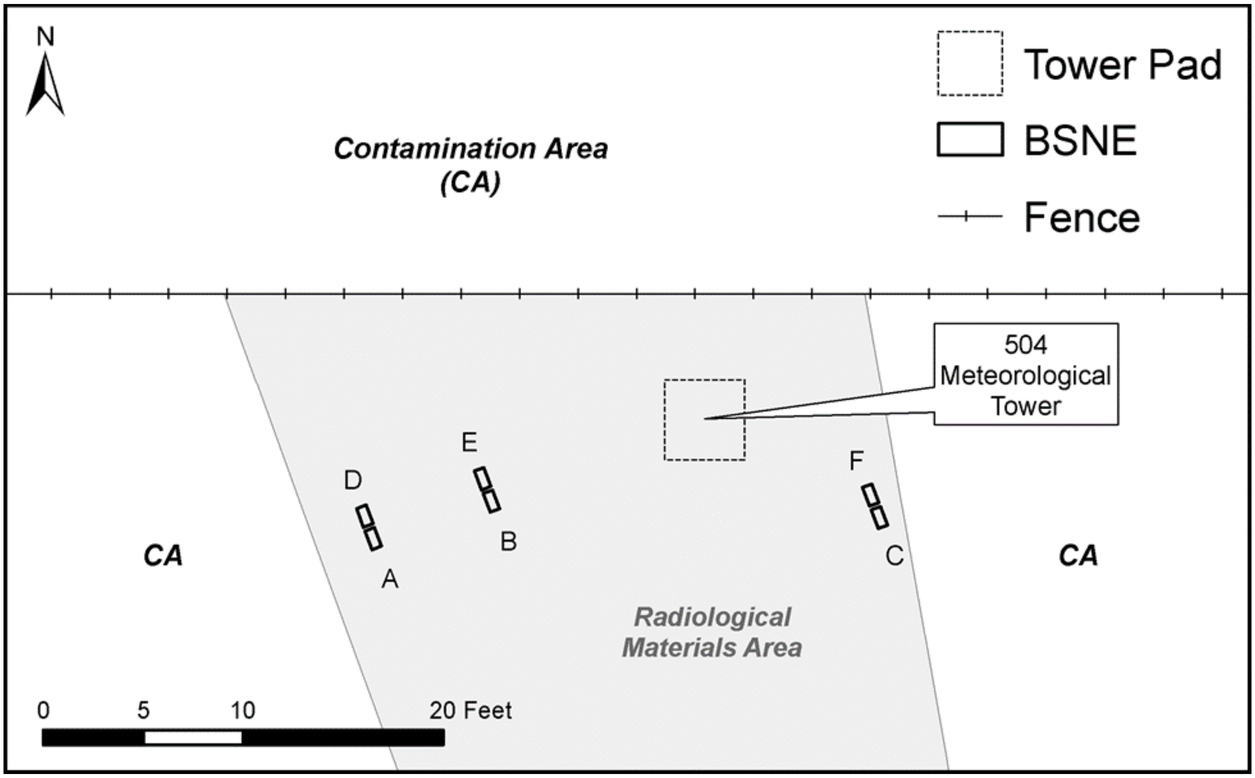

Figure D-2. Saltation trap deployment pattern at P57-4 (station 504). Traps A, B, and C are upwind of, face away from, the CA. Traps D, E, and F are downwind of and face toward the CA.

Table D-8. Distribution and deployment schedule for individual saltation traps at P57-4.

Date		Days Deployed	Saltation Trap Identification						Combined sample	
Deployment	Retrieval		504A	504B	504C	504D	504E	504F	Upwind	Downwind
3/3/2015	1/4/2016	307	28	32	36	26	30	34	504-28, 32, 36	504-26, 30, 34
1/4/2016	10/13/2016	282	27	31	35	25	29	33	504-27, 31, 35	504-25, 29, 33
11/8/2016	5/16/2017	189	28	32	36	26	30	34	504-28, 32, 36	504-26, 30, 34
5/22/2017	deployed	--	27	31	35	25	29	33	504-27, 31, 35	504-25, 29, 33

APPENDIX E: GRAPHICAL PRESENTATION OF WIND AND DUST CONDITIONS DURING MAJOR WIND EVENTS AT P57-NORTH AND SOUTH

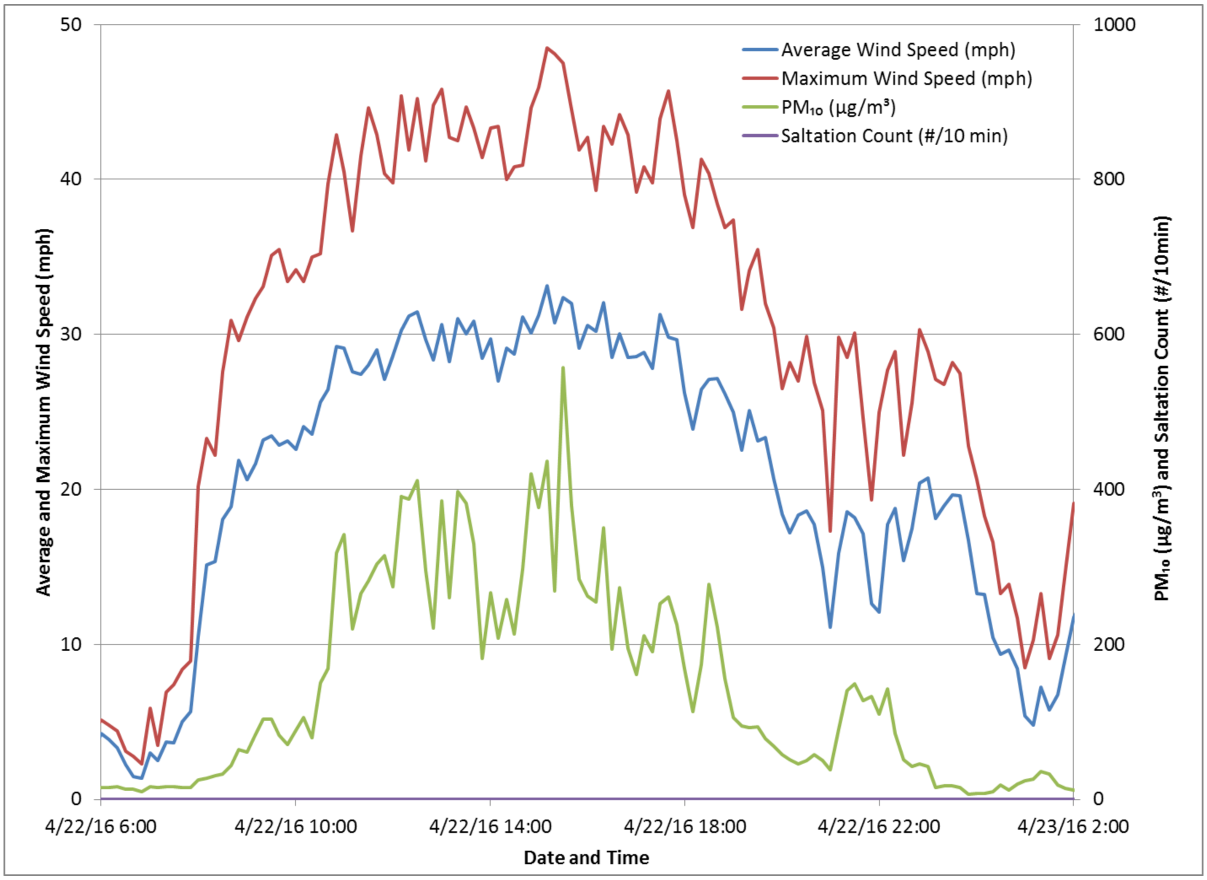

Figure E-1. Wind and dust episode April 22, 2016.

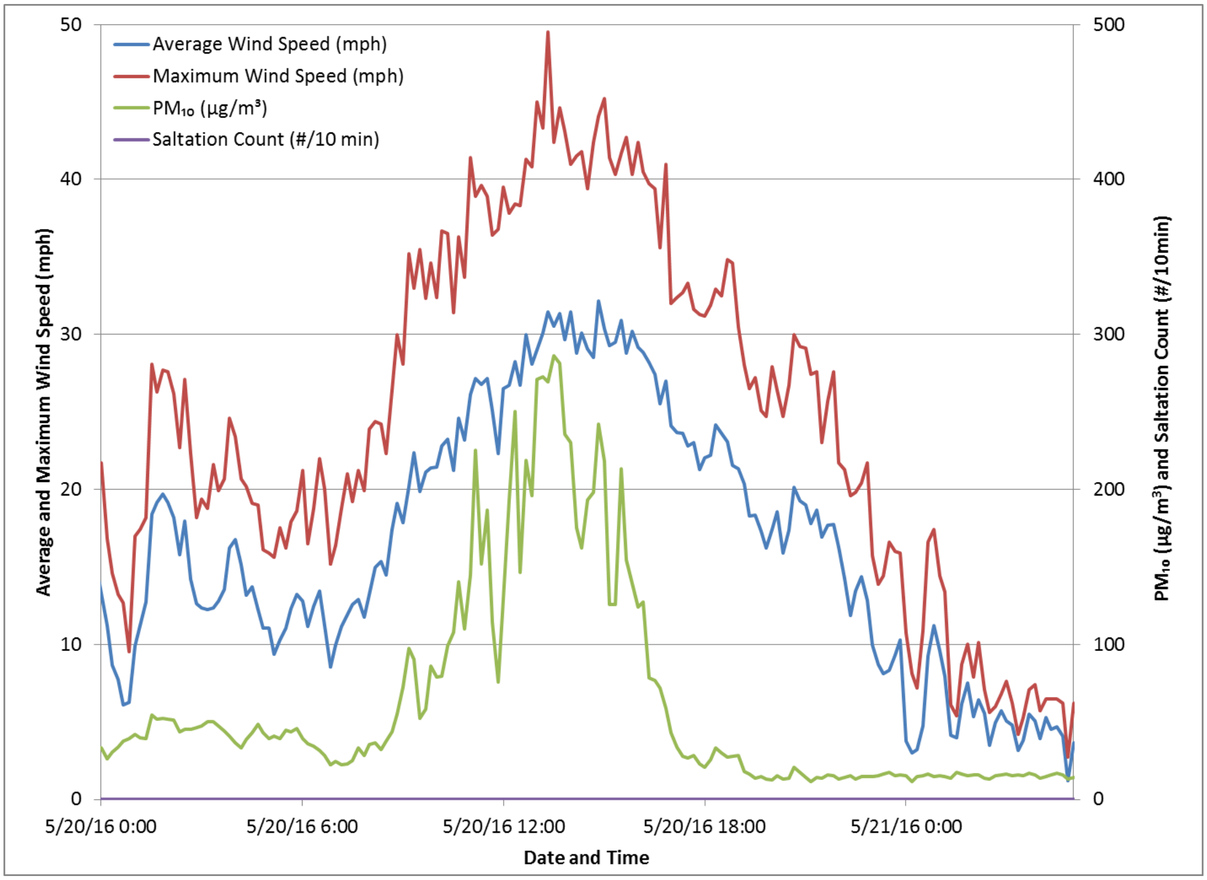

Figure E-2. Wind and dust episode May 20, 2016.

Figure E-3. Wind and dust episode June 28, 2016.

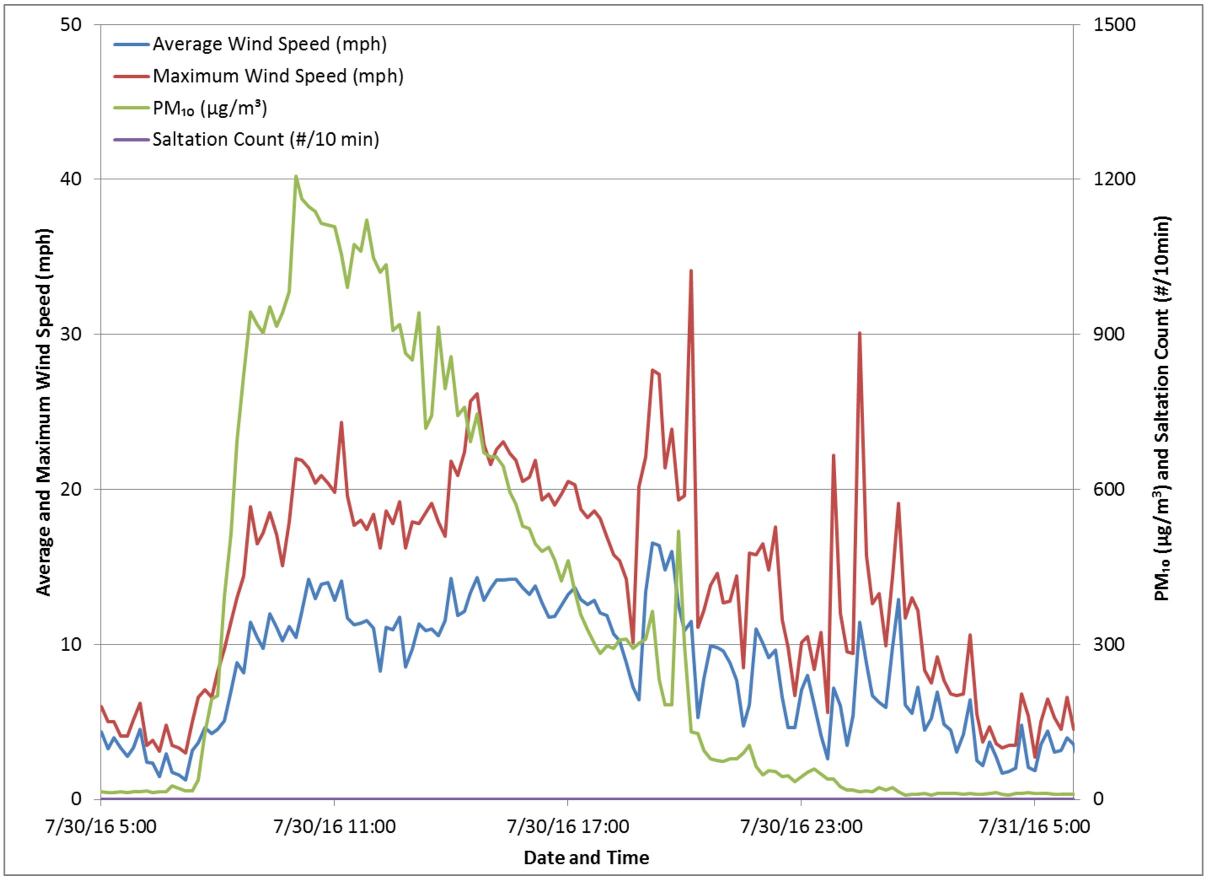

Figure E-4. Wind and dust episode July 30, 2016.

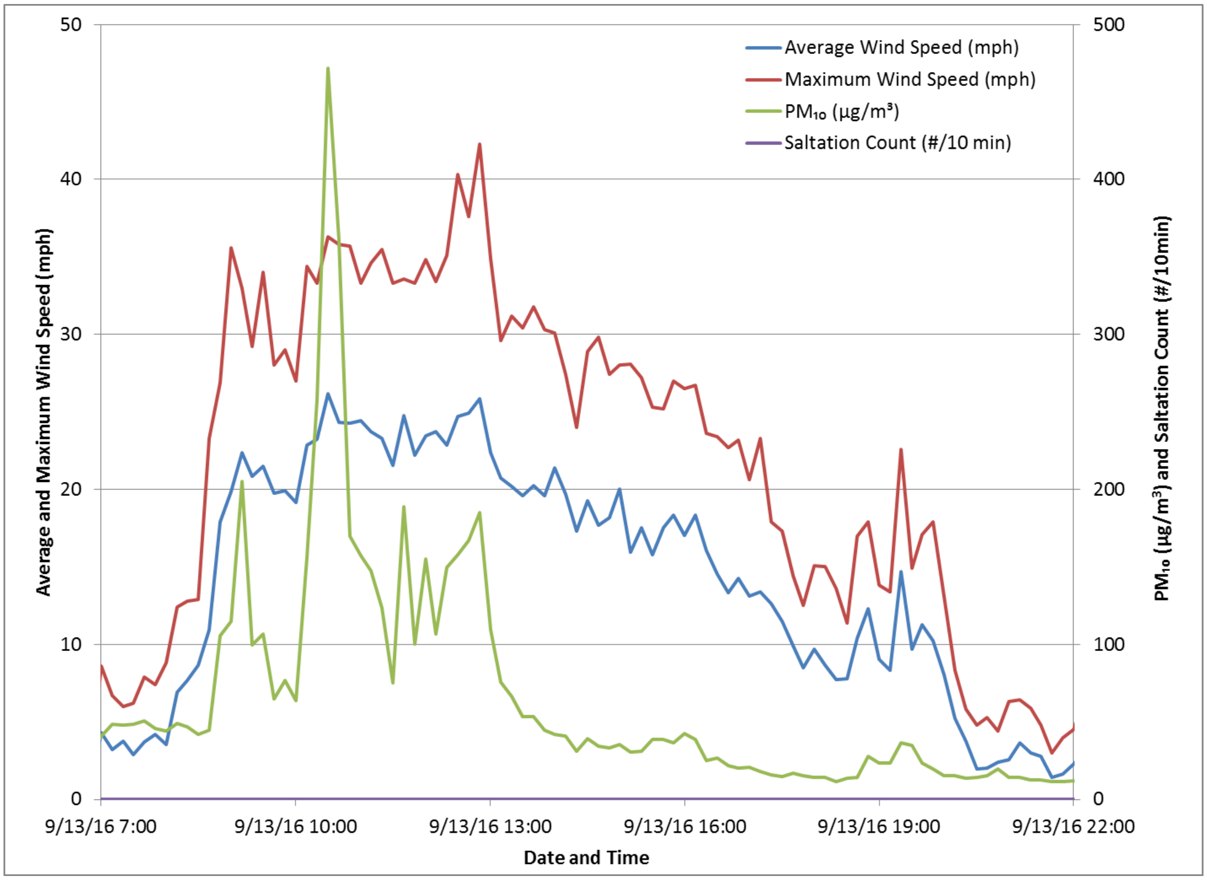

Figure E-5. Wind and dust episode September 13, 2016.

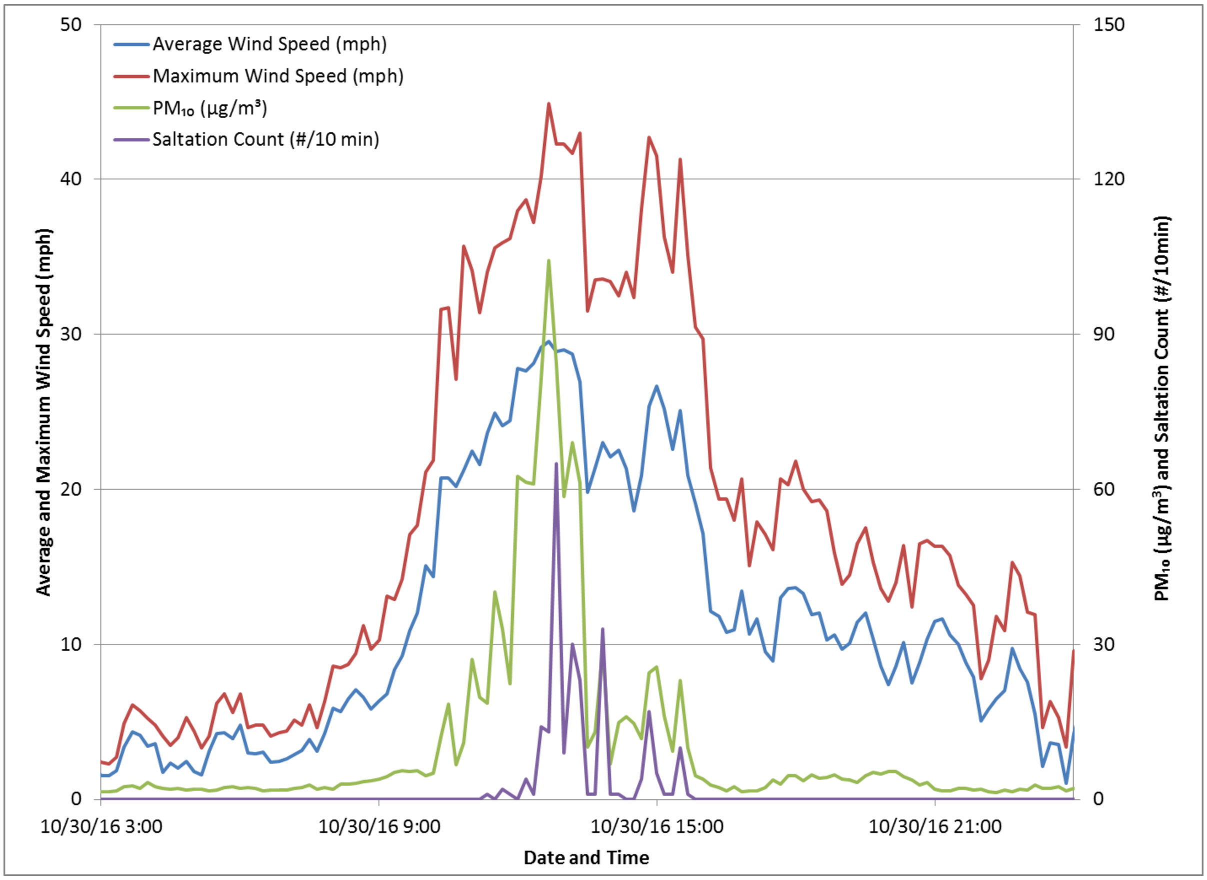

Figure E-6. Wind and dust episode October 30, 2016.

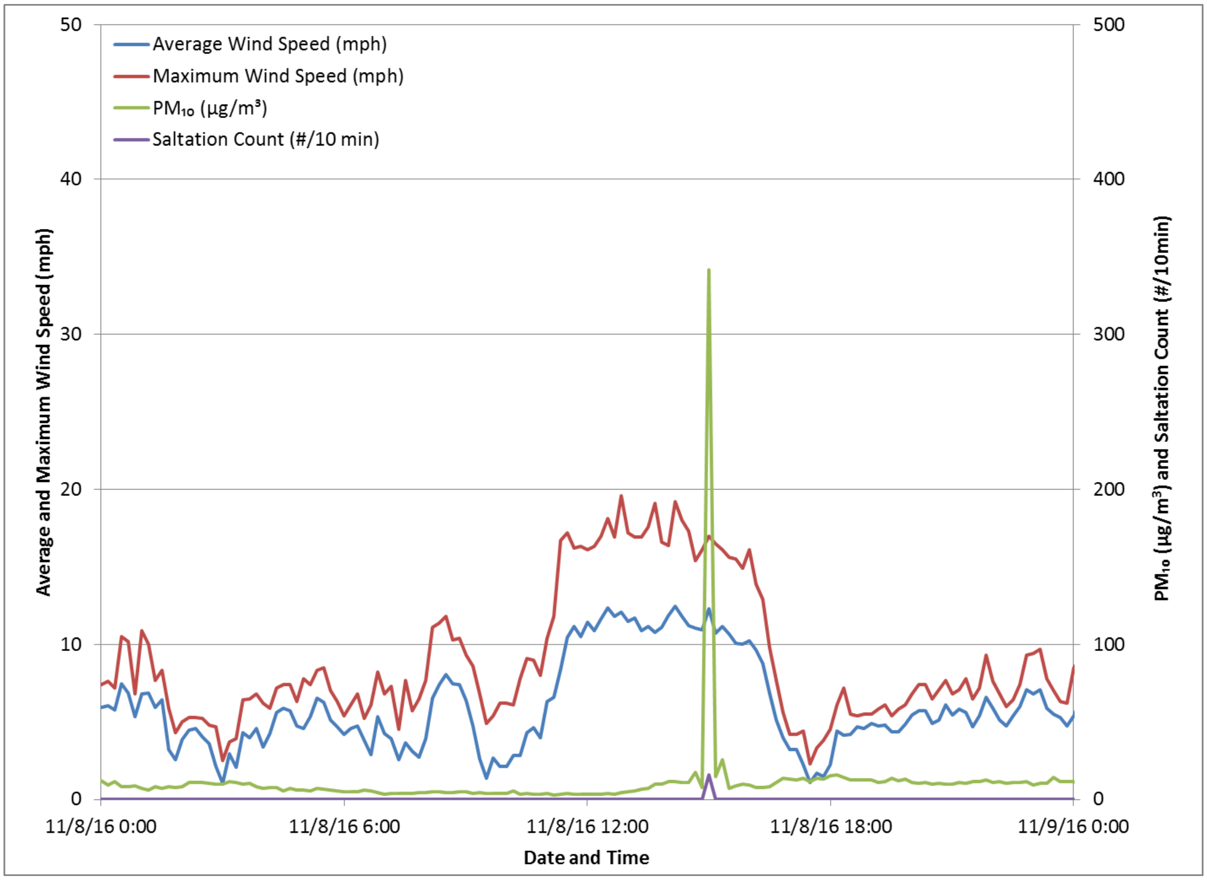

Figure E-7. Wind and dust episode November 8, 2016.

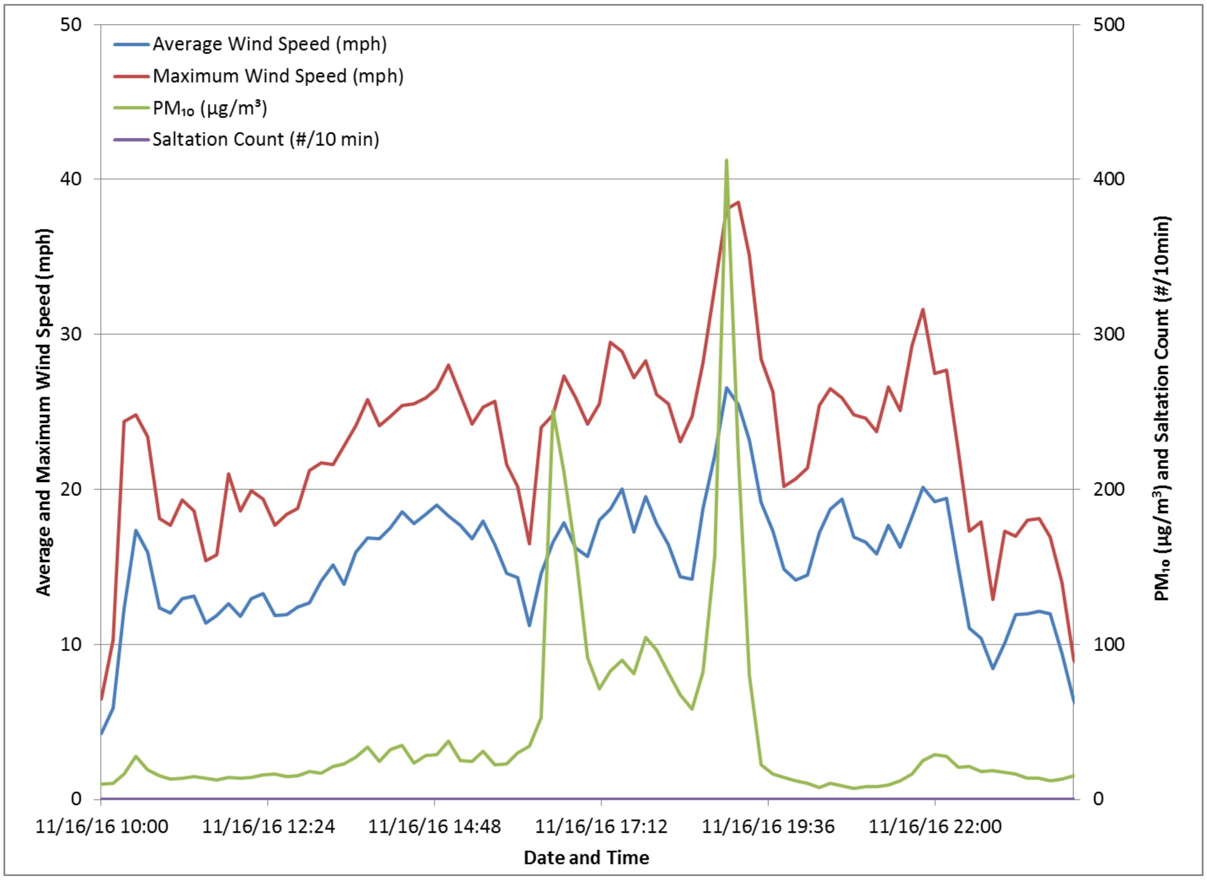

Figure E-8. Wind and dust episode November 16, 2016.

APPENDIX F: MAJOR OPERATIONAL AND OBSERVATIONAL EVENTS DURING DRI P57 MONITORING ACTIVITY

Table F-1. Project 57: October 2010 through September 2011.

FY2011 (Oct 2010 – Sept 2011)	
April 20, 2011*	P57-1 Temporary installation outside CA
May 2011[1]	NSTec RCTs downgraded corridors between the 1957 CA fence and 2007 CA signage to RMAs
July 27 through August 11, 2011*	P57-1 was dismantled and removed from field site at the request of the land management organization
August 11, 2011*	P57-1 was moved up to the 1957 CA fence in the northeast RMA
FY2012 (Oct 2011 – Sept 2012)	
November 18, 2011*	P57-2 was installed adjacent to the 1957 CA fence in the southeast RMA
November 2011	P57-1 and P57-2 Initial deployment of TLDs
December 13, 2011	P57-2 Saltation particle counter installed
January 9, 2012	P57-1 Saltation particle counter installed
January 9, 2012	P57-1 and P57-2 Begin quarterly exchange and analysis of TLDs
January 25, 2012	P57-2 tower was found blown over
April 3, 2012	P57-1 Replaced Met One™ because it was giving inaccurate values
May 29, 2012	Battery imbalance causing power outage, converter replaced
August 20, 2012	P57-1 Split 12v and 24v battery systems
September 17, 2012	P57-2 Split 12v and 24v battery systems

Table F-2. Project 57: October 2012 through September 2014

FY2013 (Oct 2012 – Sep 2013)	
February 11, 2013	P57-1 and P57-2 Hi-Q™ samplers were removed from the field for manufacturer calibration and maintenance
February 15, 2013	P57-1 and P57-2 Hi-Q™ samplers were re-installed after manufacturer calibration and maintenance
February 21, 2013	P57-1 Hi-Q™ blower failed due to fuse failure
March 5 2013	P57-1 Hi-Q™ returned to service
May 2, 2013	P57-2 Replaced fuse in Hi-Q™
May 14, 2013	P57-2 Replaced Hi-Q™ blower motor and Met One™
June 2013	P57-2 Hi-Q™ sampler fuse failed due to short in pump; parts were acquired, repairs made, and instrument returned to service
June 25, 2013	P57-2 tower leaning and Hi=Q air sampler laying on the ground
August 5, 213	P57-1 and P57-2 Saltation (Sensit™) sensors lowered to 2.5 in above ground
August 7, 2013	P57-2 Replaced Met One™ for annual calibration
FY2014 (Oct 2013 – Sep 2014)	
November 25, 2013	P57-2 Replaced WXT520 sensor
February 4, 2014	P57-1 and P57-2 Changed from cellulose to fiberglass filters in Hi-Q™ sampler
February 19, 2014	P57-2 Re-set wind speed output from m/s to MPH
April 14, 2014	P57-1 and P57-2 Initial deployment of BSNE Saltation Sand Traps installed
April 15, 2014	P57-2 Removed Sensit™ and swapped Met One™
August 18 2014	P57-2 Install new Sensit™
August 21, 2014	P57-1 Swapped Met One™

Table F-3. Project 57: October 2014 through July 2016

FY2015 (Oct 2014 – Sep 2015)	
January 7, 2015	P57-1 and P57-2 decommissioned and relocated P57-3 and P57-4 established
March 3, 2015	P57-1 and P57-2 BSNE saltation sand traps recovered P57-3 and P57-4 clean BSNE traps deployed
April 13, 2015	P57-3 and P57-4 installed new Hi-Q™ blower motors
April 15, 2015	P57-3 and P57-4 collected 2-day sample to evaluate impact of observed wind storm
May 11 2015	P57-3 Met One™ (K14481) recovered for annual manufacturer calibration (K13708) installed
June 23, 2015	P57-4 Hi-Q™ sample reported Am-241 detection, sample required additional analyses
July 30, 2015	P57-4 Data review indicates Sensit™ saltation sensor failed beginning in April or May
September 14, 2015	P57-3 Hi-Q™ not running, returned to manufacturer for repair
FY2016 (Oct 2015 – Sep 2016)	
October 13, 2015	P57-3 and P57-4 rain gage calibrated, P57-4 Sensit™ replaced
October 22, 2015	P57-3 Hi-Q™ reinstalled after repair
November 9, 2015	P57-3 Hi-Q™ tipped over on face, intake on the ground, discarded sample 10/27/15 – 11/9/15
November 23, 2015	P57-3 Hi-Q™ tipped over on back, intake on the ground, discarded sample 11/9/15 – 11/23/15
January 4, 2016	P57-3 and P57-4 BSNE Saltation Sand Traps recovered and clean traps deployed
March 2, 2016	P57-3 replaced station tower, transferred all equipment and sensors to new tower
May 10, 2016	P57-4 Met One™ (SN K14481) removed for annual calibration replaced with spare (SN M5276)
June 7, 2016	P57-4 Batteries in 24v system not holding adequate charge, Hi-Q™ shutting down overnight, Sensit™ failed
June 21, 2016	P57-4 batteries for 24v system replaced, Hi-Q™ operating 24/7
July 6, 2016	P57-3 Hi-Q™ not running blower/fuse may have failed
July 18, 2016	P57-3 Hi-Q™ removed from field for manufacturer repair; Met One™ (Sn K13708) removed for manufacturer calibration, Met One™ (Sn K14481) returned from calibration and installed

1 Historical notes for May 2011 through January 2012 were obtained from Miller 2012a.

2 Thermoluminescent dosimeters (TLDs) are retrieved and replaced quarterly beginning in January 2012.

APPENDIX G: QUALITY ASSURANCE PROGRAM

Although the current data collected for the Project 57 Air Monitoring study are considered for informational purposes to support conceptual models or guide investigations, the U.S. Department of Energy National Nuclear Security Administration Nevada Field Office (DOE/NNSA/NFO) Soils Activity Quality Assurance Plan (QAP) (2012) was used as a guideline for the collection and analysis of the airborne radiological data presented in the section of this report titled, "Radiological Assessment of Airborne Particulate Matter." This QAP as well as the Desert Research Institute Quality Assurance Program Manual for the DOE Program (2010) ensures compliance with U.S. Department of Energy (DOE) Order DOE O 414.1D, "Quality Assurance", which implements a quality management system to ensure the generation and use of quality data. The following items are addressed by the aforementioned QA documents:

- Data quality objectives (DQOs)
- Sampling plan development appropriate to satisfy the DQOs
- Environmental health and safety
- Sampling plan execution
- Sample analyses
- Data review
- Continuous improvement

Data Quality Objectives (DQOs)

The DQO process is a strategic planning approach that is used to plan data collection activities. It provides a systematic process for defining the criteria that a data collection design should satisfy. These criteria include when and where samples should be collected, how many samples to collect, and the tolerable level of decision errors for the study. The DQOs are unique to the specific data collection or monitoring activity and their defined level of use (in this case, for informational purposes).

Measurement Quality Objectives (MQOs)

The MQOs are basically equivalent to DQOs for analytical processes. The MQOs provide direction to the laboratory concerning performance objectives or requirements for specific method performance characteristics. Default MQOs are established in the subcontract with the laboratory but may be altered to satisfy changes in the DQOs. The MQOs for the Project 57 Air Monitoring study are described in terms of precision, accuracy, representativeness, completeness, and comparability requirements. These terms are defined and discussed in the DOE/NNSA/NFO (QAP).

Sampling Quality Assurance Program

Quality Assurance (QA) in field operations for the Project 57 Air Monitoring study includes sampling assessments, surveillances, and oversight of the following supporting elements:

- The sampling plan, DQOs, and field data sheets accompanying the sample package
- Database support for field and laboratory results, including systems for long-term storage and retrieval
- Qualified personnel who are available and able to perform required tasks
- Sample packages include the following items:
- Sample collectors field notes confirming all observable information pertinent to sample collection
- An Air Surveillance Network Sample Data Form that documents air sampler parameters, collection dates and times, and total sample volumes collected
- Chain-of-custody forms that also include some of the elements of the field notes

This managed approach to sampling ensures that the sampling is traceable and enhances the value of the final data available to the project manager. The sample package also ensures that the personnel responsible for sample collection have followed proper procedures for sample collection.

Data obtained in the course of executing field operations are entered in the documentation that accompany the sample package during sample collection and in the Project 57 Study database along with analytical results on their receipt and evaluation.

Completed sample packages are kept as hard copy in file archives. Analytical reports are kept as hard copy in file archives as well as in a dedicated and secure archival systems that are protected and maintained in accordance with the Desert Research Institute's Computer Protection Program.

Laboratory QA Oversight

Although the data for the Project 57 Air Monitoring study are for informational purposes, the main aspects of the DOE O 414.1D requirements are used as guidelines to evaluate laboratory services through review of the vendor laboratory policies formalized in a Laboratory Quality Assurance Plan (LQAP). The Project 57 study is assured of obtaining quality data from laboratory services through a multifaceted approach that involves specific procurement protocols, the conduct of quality assessments, and requirements for selected laboratories to have an acceptable QA Program. These elements are discussed below.

<u>Procurement</u>

Laboratory services are procured through subcontracts that establish the technical specifications required of the laboratory to provide the basis for determining compliance with those requirements and evaluating overall performance. A subcontract is usually awarded on a best-value basis as determined by pre-award audits, but because of the specific requirement requested for gamma spectroscopy analysis (24 hour count duration) for the Project 57 study, the laboratory was procured on a sole-proprietor basis. The laboratory was required to provide a review package that included the following items:

- All procedures pertinent to subcontract scope
- Environment, Safety, and Health Plan
- LQAP
- Example deliverables (hard copy and/or electronic)
- Proficiency testing (PT) results from the previous year from recognized PT programs
- Résumés
- Accreditations and certifications
- Licenses

Continuing Assessment

A continuing assessment of a selected laboratory involves the ongoing monitoring of a laboratory's performance against the contract terms and conditions, of which technical specifications are a part. The following tasks support continuing assessment:

- Tracking schedule compliance
- Reviewing analytical data deliverables
- Monitoring the laboratory's adherence to the LQAP
- Monitoring for continued successful participation in approved PT programs

Data Review

Essential components of process-based QA are data checks, verification, validation, and data quality assessment to evaluate data quality and usability.

Data Checks: Data checks are conducted to ensure accuracy and consistency of field data collection operations prior to and on data entry into Project 57 databases and data management systems.

Data Verification: Data verification is defined as a compliance and completeness review to ensure that all laboratory data and sample documentation are present and complete. Sample preservation, chain-of-custody, and other field sampling documentation shall be reviewed during the verification process. Data verification ensures that the reported results entered in Project 57 databases correctly represent the sampling and/or analyses performed and includes evaluation of quality control (QC) sample results.

Data Validation: Data validation is the process of reviewing a body of analytical data to determine if it meets the data quality criteria defined in operating instructions. Data validation ensures that the reported results correctly represent the sampling and/or analyses performed, determines the validity of the reported results, and assigns data qualifiers (or "flags") if required. The process of data validation consists of the following:

- Evaluating the quality of the data to ensure that all project requirements are met
- Determining the impact on data quality of those requirements if they are not met
- Verifying compliance with QA requirements
- Checking QC values against defined limits
- Applying qualifiers to analytical results in the Project 57 databases for the purposes of defining the limitations in the use of the reviewed data

Operating instructions, procedures, applicable project-specific work plans, field sampling plans, QA plans, analytical method references, and laboratory statements of work may all be used in the process of data validation. Documentation of data validation includes checklists, qualifier assignments, and summary forms.

Data Quality Assessment (DQA): The DQA is the scientific evaluation of data to determine if the data obtained from environmental data operations are of the right type, quality, and quantity to support their intended use. The DQA review is a systematic review against preestablished criteria to verify that the data are valid for their intended use.

2016 Sample QA Results

The QA assessments were performed by the Project 57 Air Monitoring study, including the laboratory responsible for sample analyses. These assessments ensure that sample collection procedures, analytical techniques, and data provided by the subcontracted laboratory comply with Project 57 study requirements. Data were provided by the University of Nevada, Las Vegas, Radiation Services Laboratory (gross alpha/beta and gamma spectroscopy data), TestAmerica Laboratories, Inc., (alpha spectroscopy), and Mirion Technologies (TLD data). A brief discussion of the 2016 results for laboratory duplicates, control samples, blank analyses, and interlaboratory comparison studies is provided along with summary tables within this section.

Laboratory Duplicates (Precision)

A laboratory duplicate is a sample that is handled and analyzed following the same procedures as the primary sample analysis. The relative percent difference (RPD) between the initial result and the corresponding duplicate result is a measure of the variability in the analytical process of the laboratory, mainly overall measurement uncertainty. The average absolute RPD, expressed as a percentage, was determined for the calendar year 2016 samples and is listed in Table G-1. An RPD of zero indicates a perfect duplication of results of the duplicate pair, whereas an RPD greater than 100 percent generally indicates that a duplicate pair falls beyond QA requirements and is not considered valid for use in data interpretation. These samples are further evaluated to determine the reason for QA failure and if any corrective actions are required. Overall, the RPD values for all analyses indicate very good results with no samples exceeding an RPD of 100 percent.

Table G-1. Summary of laboratory duplicate samples for the Project 57 Air Monitoring study in 2016.

Analysis	Matrix	Number of Samples Reported[(a)]	Number of Samples Reported above MDC[(b)]	Average Absolute RPD of those above MDC (%)[(c)]
Gross Alpha	Air	6	6	17.5
Gross Beta	Air	6	6	4.4
Gamma – Beryllium-7	Air	7	7	13.5
Gamma – Lead-210	Air	7	0	N/A
Alpha Spectroscopy	Air	2	2	2.1
TLDs	Ambient Radiation	8	NA	3.5

a) Represents the number of laboratory duplicates reported for the purpose of monitoring precision. If an associated field sample was not processed, the field duplicate was not included in this table.

b) Represents the number of laboratory duplicate sets reported above the minimum detectable concentration (MDC) (MDC is not applicable for TLDs). If either the original laboratory analysis or its duplicate was reported below the detection limit, the precision was not determined.

c) Reflects the average absolute RPD calculated for those field duplicates reported above the MDC.

The absolute RPD calculation is as follows:

$$Absolute\ RPD = \frac{|LD - LS|}{(LD + LS)/2}\ X\ 100\%$$

Where: LD = Laboratory duplicate result
LS = Laboratory sample result

Laboratory Control Samples (Accuracy)

Laboratory control samples (LCSs) (also known as matrix spikes) are performed by the subcontract laboratory to evaluate analytical accuracy, which is the degree of agreement of a measured value with the true or expected value. Samples of known concentration are analyzed using the same methods as employed for the project samples. The results are determined as the measured value divided by the true value, expressed as a percentage. To be considered valid, the results must fall within established control limits (or percentage ranges) for further analyses to be performed. The LCS results obtained for 2016 are summarized in Table G-2. The LCS results were satisfactory with all samples falling within control parameters for the air sample matrix.

Table G-2. Summary of laboratory control samples for the Project 57 Air Monitoring study in 2016.

Analysis	Matrix	Number of LCS Results Reported	Number Within Control Limits[(a)]
Gross Alpha	Air	8	8
Gross Beta	Air	8	8
Gamma	Air	8	8
Alpha Spectroscopy	Air	2	2

a) Control limits are as follows: 78 percent to 115 percent for gross alpha, 87 percent to 115 percent for gross beta, 90 percent to 115 percent for gamma (137Cs, 60Co, 241Am).

Laboratory Blank Analysis

Laboratory blank sample analyses are essentially the opposite of LCSs discussed above. These samples do not contain any of the analyte of interest. Results of these analyses are expected to be zero, or more accurately below the MDC of a specific procedure. Blank analysis and control samples are used to evaluate overall laboratory procedures, including sample preparation and instrument performance. The laboratory blank sample results obtained for 2016 are summarized in Table G-3. The laboratory blank results were satisfactory with all of the alpha and beta blank samples falling within control parameters for the air sample matrix.

Table G-3. Summary of laboratory blank samples for the Project 57 Air Monitoring study in 2016.

Analysis	Matrix	Number of Blank Results Reported	Number within Control Limits[(a)]
Gross Alpha	Air	8	8
Gross Beta	Air	8	8
Gamma	Air	8	8
Alpha Spectroscopy	Air	1	1

a) Control limit is less than the MDC.

Interlaboratory Comparison Studies

Interlaboratory comparison studies are conducted by the subcontracted laboratories to evaluate their performance relative to other laboratories providing the same service. These types of samples are commonly known as blind samples, in which the expected values are known only to the program conducting the study. The analyses are evaluated and if found satisfactory, the laboratory is certified that its procedures produce reliable results. The interlaboratory comparison sample results obtained for 2016 are summarized in Tables G-4 and G-5.

Table G-4 shows the summary of interlaboratory comparison sample results for the subcontract radiochemistry laboratory. The laboratory participated in the QA Program administered by Mixed Analyte Performance Evaluation Program (MAPEP) for gross alpha, gross beta, and gamma analyses, and the Environmental Research Associates (ERA) proficiency testing program for alpha spectroscopy. The subcontractors performed very well during the year by passing all of the parameters analyzed.

Table G-4. Summary of interlaboratory comparison samples of the radiochemistry laboratory for the Project 57 Air Monitoring study in 2016.

		MAPEP and ERA Results	
Analysis	**Matrix**	**Number of Results Reported**	**Number Within Control Limits[(a)]**
Gross Alpha	Air	2	2
Gross Beta	Air	2	2
Gamma	Air	2	2
Alpha Spectroscopy	Air	1	1

a) Control limits are determined by the individual inter-laboratory comparison study.

Table G-5 shows the summary of the in-house performance evaluation results conducted by the subcontract dosimetry group. This internal evaluation was based on National Voluntary Laboratory Accreditation Program (NVLAP) criteria and was performed biannually. The dosimetry group performed very well during the year by passing 12 out of 12 of the TLDs analyzed.

Table G-5. Summary of interlaboratory comparison TLD samples of the subcontract dosimetry group for the Project 57 Air Monitoring study in 2016.

Analysis	**Matrix**	**Number of Results Reported**	**Number Within Control Limits[(a)]**
TLDs	Ambient Radiation	12	12

a) Based upon NVLAP criteria; absolute value of the bias plus one standard deviation < 0.3.

References

Desert Research Institute, 2010. *Desert Research Institute Quality Assurance Program Manual for the DOE Program*, October 2010.

U.S. Department of Energy, 2011. DOE O 414.1D, *Quality Assurance*, April 2011.

U.S. Department of Energy, 2013. *Soils Activity Quality Assurance Plan*, May 2012.

APPENDIX H: INSTRUMENTATION MODELS AND MANUFACTURERS

Instrument/Measurement	Model	Manufacturer
Wind speed	WXT-510	Vaisala Louisville, CO
Wind direction	WXT-510	Vaisala Louisville, CO
Precipitation	TE-525	Texas Electronics Dallas, TX
Temperature	WXT-510	Vaisala Louisville, CO
Relative humidity	WXT-510	Vaisala Louisville, CO
Solar radiation	CS-300	Apogee Instruments Logan, UT
Barometric pressure	WXT-510	Vaisala Louisville, CO
Soil temperature	Type T thermocouple	Omega Norwalk, CT
Soil moisture content	CS-616	Campbell Scientific Logan, UT
Ambient Particulate Profiler	Model 212	Met One™ Instruments Grants Pass, OR
Sensit H11-LINTM™	--	Sensit, Inc. Redlands, CA
Datalogger	CR1000	Campbell Scientific Logan, UT
Airborne particle collector	--	Hi-Q San Diego, CA
Thermoluminescent dosimeters	--	
BSNE Saltation Sand Traps	Big Spring Number Eight	Custom Products and Consulting LLC Big Spring, Texas

STANDING DISTRIBUTION LIST

Robert Boehlecke
EM NV Program Manager
Nevada Field Office
National Nuclear Security Administration
U.S. Department of Energy
P.O. Box 98518
Las Vegas, NV 89193-8518
Robert.Boehlecke@nnsa.doe.gov

Acting, EM NV Deputy Program Manager, Operations
Nevada Field Office
National Nuclear Security Administration
U.S. Department of Energy
P.O. Box 98518
Las Vegas, NV 89193-8518

Kevin Cabble
Soils Activity Lead
Nevada Field Office
National Nuclear Security Administration
U.S. Department of Energy
P.O. Box 98518
Las Vegas, NV 89193-8518
Kevin.Cabble@nnsa.doe.gov

Tiffany Lantow
Long-Term Monitoring Activity Lead
Nevada Field Office
National Nuclear Security Administration
U.S. Department of Energy
P.O. Box 98518
Las Vegas, NV 89193-8518
Tiffany.Lantow@nnsa.doe.gov

Peter Sanders
Nevada Field Office
National Nuclear Security Administration
U.S. Department of Energy
P.O. Box 98518
Las Vegas, NV 89193-8518
Peter.Sanders@nnsa.doe.gov

Sarah Hammond, Contracting Officer
Office of Acquisition Management
NNSA Service Center
Pennsylvania and H Street, Bldg. 20388
P.O. Box 5400
Albuquerque, NM 87185-5400
Sarah.Hammond@nnsa.doe.gov

Jenny Chapman
DOE Program Manager
Division of Hydrologic Sciences
Desert Research Institute
755 E. Flamingo Road
Las Vegas, NV 89119-7363
Jenny.Chapman@dri.edu

Julianne Miller
DOE Soils Activity Manager
Division of Hydrologic Sciences
Desert Research Institute
755 E. Flamingo Road
Las Vegas, NV 89119-7363
Julie.Miller@dri.edu

Pat Matthews
Navarro, LLC
P.O. Box 98952
M/S NSF167
Las Vegas, NV 89193-8952
Patrick.Matthews@nv.doe.gov

Reed Poderis
National Security Technologies, LLC
P.O. Box 98521
M/S NLV082
Las Vegas, NV 89193-8521
poderirj@nv.doe.gov

*****Nevada State Library and Archives
State Publications
100 North Stewart Street
Carson City, NV 89701-4285

Archives Getchell Library
University of Nevada, Reno
1664 N. Virginia St.
Reno, NV 89557
tradniecki@unr.edu

DeLaMare Library 262
University of Nevada, Reno
1664 N. Virginia St.
Reno, NV 89557
tradniecki@unr.edu

Document Section, Library
University of Nevada, Las Vegas
4505 Maryland Parkway
Las Vegas, NV 89154
sue.wainscott@unlv.edu

†Library
Southern Nevada Science Center
Desert Research Institute
755 E. Flamingo Road
Las Vegas, NV 89119-7363

‡Nuclear Testing Archive
ATTN: Martha DeMarre
National Security Technologies, LLC
Mail Stop 400
PO Box 98521
Las Vegas, NV 89193-8521
demarrme@nv.doe.gov
(2 CDs)

§Office of Scientific and Technical Information
U.S. Department of Energy
P.O. Box 62
Oak Ridge, TN 37831-9939

All on distribution list receive one electronic PDF copy, unless otherwise noted.

***** 12 paper copies
† 3 paper copies; CD with pdf (from which to print)
‡ compact disc only
§ electronic copy (pdf) only